Quantum Transport in Floquet Formalism

Daniela Filipa Carradas Gonçalves
Master's in Physics
Department of Physics and Astronomy
Faculty of Sciences of the University of Porto
2024

Quantum Transport in Floquet Formalism

Daniela Filipa Carradas Gonçalves
Dissertation carried out as part of the Master's in Physics
Department of Physics and Astronomy
2024

Supervisor
João Manuel Parente Viana Lopes, Professor Auxiliar, Faculty of Sciences of the University of Porto

Co-supervisor
João Manuel Borregana Lopes dos Santos, Professor Catedrático Convidado, Faculty of Sciences of the University of Porto

"– Sim, à beira do vazio compreendeu o mais importante – miou Zorbas.
– Ah sim? E o que é que ela compreendeu? – perguntou o humano.
– Que só voa quem se atreve a fazê-lo – miou Zorbas."

Luis Sepúlveda,

História de uma gaivota e do gato que a ensinou a voar

Acknowledgments

First of all, I would like to thank my supervisor, Prof. João Viana Lopes, for suggesting this project to me and for all his help and support in making this work possible even with all the deadlines that appeared along the way. To my co-supervisor, Prof. João Lopes dos Santos, for the guidance and discussions that were crucial to my understanding of this topic.

To my colleague Duarte, for all the useful scientific discussions in CFP, and the ultimate competition, which gave me extra motivation to appear in the days that would not be so easy.

Since this thesis is the sum of all the knowledge that I have acquired during my undergraduate and graduate studies, I would also like to thank Rita and Carolina for their mutual support in carrying out the TPCs and during the hard times of preparing for the exams.

To all the friends who helped me keep it together, those I have met here and those from my home town. You were always ready to listen to my complaints and give me your words of support.

Especially to Francisca, whom I couldn't mention in any of the above paragraphs, because you were there in different parts of this way to talk about everything from science to existential crises.

To my family, especially my parents and my little sister, who have supported, believed in and encouraged me all these years and without whom my education wouldn't have been possible.

Last but not least, to Carlos, who could not have been more patient and who has been there for me in every moment, from the happiest to the most desperate. No words would be enough.

Resumo

Surgem diferentes fenómenos, geralmente não lineares na intensidade do campo, quando um campo eletromagnético perturba um sistema cristalino. É possível utilizar uma abordagem microscópica para descrever a resposta ótica não linear em termos da densidade de corrente, calculada através da matriz de densidade (DM), que descreve completamente o estado do sistema e evolui no tempo sob o campo de radiação externo. Um método analítico frequentemente utilizado para calcular a evolução temporal da DM para um campo eletromagnético fraco é a teoria de perturbações dependentes do tempo. Quando a perturbação se torna suficientemente forte, a eficácia da expansão em potências do campo diminui, obrigando ao desenvolvimento de técnicas alternativas. Como alternativa à teoria de perturbações, usaremos o formalismo de Floquet para estudar a resposta ótica não-linear. A premissa é tirar proveito da periodicidade temporal da perturbação com o formalismo de Floquet. Como prova de conceito, considerámos a resposta de um modelo semicondutor com duas bandas 1D à temperatura zero sob a influência de uma perturbação electromagnética periódica, com diferentes intensidade de campo. O problema foi definido em *velocity gauge*, em que o campo elétrico é introduzido por um vetor potencial uniforme e dependente do tempo. Neste caso as equações de evolução da DM são desacopladas para cada momento k. Depois de resolver as equações de evolução temporal para cada k, somámos sobre a primeira zona de Brillouin para obter a resposta temporal em corrente. Ao longo da tese, mostraremos como conseguimos calcular a corrente para cada k e a corrente total no espaço de frequências, usando o formalismo de Floquet. Estudámos o comportamento da corrente para cada k no regime perturbativo, e encontrámos uma limitação da dinâmica semiclássica. No que diz respeito à corrente total, vimos que as únicas frequências que aparecem na resposta são múltiplos da frequência do campo e relacionadas com os extremos do *gap* de Floquet. Como o formalismo de Floquet não se limita a campos fracos, calculamos as amplitudes das componentes da corrente nos três primeiros múltiplos da frequência do campo até observarmos a quebra do comportamento perturbativo.

Palavras-chave: Hamiltoniano periódico no tempo; Formalismo de Floquet; Ótica não-linear; Cristais unidimensionais

Abstract

Different phenomena appear, generally nonlinear with the field intensity, when an electromagnetic field perturbs a crystalline system. It is possible to use a microscopic approach to describe the nonlinear optical response in terms of the current density compute via the density matrix (DM), which fully describes the state of the system and evolves in time under the external radiation field. A frequently used analytical method to compute the time evolution of DM for weak electromagnetic field is time-dependent perturbation theory. When the perturbation become strong enough, the efficacy of the expansion in powers of the field diminishes, necessitating the development of alternative techniques. For the cases where the perturbation is time periodic, an alternative to perturbation theory is Floquet formalism to study the nonlinear optical response. The premise is to take advantage of the time periodicity of the perturbation to compute the time evolution of the system with Floquet formalism. As a proof of concept, we considered the response of a semiconductor model with two 1D bands at zero temperature under the influence of a periodic electromagnetic perturbation, with different field intensities. The problem was defined in velocity gauge, where the electric field is introduced by a time-dependent and uniform vector potential. In this case the time evolution equations of the DM are decoupled for each momentum k. After solving the time evolution equations for each k, we summed over the first Brillouin zone to obtain the total current. Through this thesis, we will show how we were able to compute the current for each k and the total current in frequency space, using the Floquet formalism. We studied the behaviour of the current for each k in the perturbative regime, and we found a limitation of the semiclassical dynamics. Concerning the total current, we saw that the only frequencies that appear in the response are multiples of the field frequency and related to the extremes of the Floquet gap. Because the Floquet formalism is not limited to weak fields, we compute the amplitudes of the current components at the first three multiples of the field frequency until we observe the breakdown of the perturbative behaviour.

Keywords: Time periodic Hamiltonian; Floquet formalism; Non-linear Optics; One dimensional crystals

Contents

List of Figures

List of Acronyms

- 1D: One-dimensional
- 2D: Two-dimensional
- DM: Density matrix
- EFH: Extended Floquet Hamiltonian
- FBZ: First Brillouin zone
- RK4: Fourth-order Runge-Kutta

Introduction

In 1875, Reverend John Kerr demonstrated that the refractive index of various solids and liquids is slightly changed by applying a strong DC field [1]. This is known as the DC Kerr effect and was the first nonlinear optical response observed. Later, in 1882, a similar effect, known as the Pockels effect, was observed in crystalline materials with a lack of inversion symmetry by Friedrich Pockels at the University of Göttingen [2]. Further progress had to wait for the availability of lasers, a source of strong optical fields (1960), that allowed the discovery of the second harmonic generation [3]. The authors propagated a ruby laser beam at 6942 Å through a quartz crystal and observed ultraviolet radiation from the crystal at 3471 Å, as represented in Fig. 1. This is considered by several authors [4, 5] to be the beginning of the field of nonlinear optics.

Nonlinear optics focuses on phenomena that occur when the optical response of matter depends nonlinearly on the optical field's strength. For sufficiently weak electromagnetic fields, not only is the optical current response expected to behave linearly with the amplitude of the field, but it also displays the same frequency. With increasing field intensity, more complex phenomena emerge [6–8]. One such phenomenon is harmonic generation, which pertains to the current response displaying frequencies corresponding to multiples of the frequency of the electromagnetic field. The second and third harmonic generation are examples of these phenomena corresponding to a response with twice and three times the original frequency. When the perturbations become sufficiently intense, the material shows other responses, such as the stimulated Raman effect, self-induced transparency, and electromagnetically-induced transparency [9].

The current density $\overrightarrow{\mathbf{J}}$, for example, is a typical quantity through which non-linear effects manifest themselves. A common way to describe the current density evolution is to use the density matrix (DM) formalism [10, 11]. The DM is a powerful tool for describing the quantum state of the system as well as its observable quantities. The current density is given by the trace of the product of the current density with the density matrix [12].

According to the Liouville equation, the DM evolves in time under the external radiation field. There are several analytical and numerical methods capable of solving the time evolution of the DM. A commonly used analytical method is the time-dependent perturbation theory. It consists of finding an approximate solution by expanding the Hamiltonian and other operators around a known solution, usually the equilibrium, as a function of powers of the perturbation [13]. To ensure the accuracy of the result, this method is usually applied to small perturbations. In the context of optical responses, the results of the time-dependent perturbation theory are limited to weak electromagnetic fields. When the perturbations become sufficiently intense, the effectiveness of field power expansion diminishes, necessitating the development of alternative techniques.

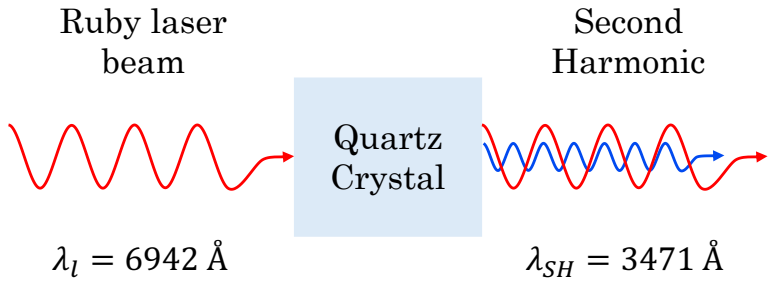

Figure 1.: Schematic of the second harmonic generation of the experiment described in [3]: propagation of a ruby laser beam at $\lambda_l = 6942\,\text{Å}$ through a quartz crystal and observation of light from the crystal at $\lambda_{\text{SH}} = 3471\,\text{Å}$.

Whether within the perturbation theory regime or not, numerical approaches are very useful for computing the exact solution of the Liouville equation. Several numerical methods, such as the Euler or the Runge Kutta methods, serve this purpose. In the remainder of this thesis, we will use the fourth-order Runge-Kutta (RK4) method to evolve the density matrix, an ordinary differential equation solver with an accuracy of fourth order in the integration step and an error of fifth order [14].

Some problems in physics concern a system under time-periodic perturbations, which means that the Hamiltonian is periodic in time. Since the 1930's, several authors [15–17] have applied a method using a rotating coordinate system to solve magnetic resonance problems. Later, a method to solve the Schrödinger equation with a Hamiltonian that is periodic in time was implemented [18]. This method is essentially the Floquet formalism, initially developed by Achille Floquet [19] to solve linear differential equations with periodic coefficients. It consists of transforming the time-dependent Hamiltonian into a time-independent one and solving the eigenvalue problem to construct the time evolution operator and perform the complete time evolution of the system from the application of this operator to an initial state.

In the last decades, the Floquet formalism has been used to describe the non-equilibrium steady state of a system under periodic driving perturbations. Under these perturbations, the materials exhibit new characteristics. There are studies concerned with the topological features of materials under these perturbations [20], exploring gapped Dirac and Weyl materials [21], as the example of graphene [22]. New non-equilibrium topological states, called Floquet isolators, were also discovered [23, 24]. Other studies focused more on the optical properties of these lighted-induced electronic Floquet states [25–28], in particular, experiments with ultracold quantum gases in periodically driven optical lattices [29].

In nonlinear optical problems, the Floquet formalism can solve the Schrödinger equation of a system perturbed by a time-periodic electromagnetic field. This leads to the construction of the DM from the states of the system computed with Floquet formalism, and then the current density can be calculated using the DM formalism. As mentioned above, the evolution computed using the Floquet formalism implies the choice of an initial state from which we evolve the system. This is equivalent to a sudden switching of the perturbation,

as opposed to the usual conditions in which the time-dependent perturbation theory is applied, where the perturbation is switched on adiabatically. This work aims to study the use of the Floquet Formalism to directly solve the problem of a one-dimensional (1D) two-band semiconductor model at zero temperature suddenly perturbed by a monochromatic electromagnetic field suddenly switched and obtain its nonlinear optical current response. This method has already been applied to solve the time evolution of atomic and nuclear problems [30, 31]. However, as far as we know, it has not been applied previously in the context of nonlinear optics of crystals.

In Chapter 1, we review important concepts of Nonlinear Optics that are crucial to solve the problem at hand. We discuss the difference between the length and the velocity gauges and motivate our choice of the velocity gauge. Then, we briefly describe the time perturbation theory as a tool used to compute the optical response of the system for weak fields and then compare it to the Floquet results. In Chapter 2 we review the details of the Floquet Formalism and apply it to two preliminary problems. In Chapter 3, we finally approach the 1D two-band semiconductor model with the monochromatic electromagnetic perturbation. We start by describing the system and compute the linear response using time perturbation theory. After that, we define the Floquet Hamiltonian and compute the system's time evolution, comparing the results with the linear response for weak fields and with RK4 for stronger fields. In Chapter 4, we present some numerical results that follow the analysis of Chapter 3, searching for perturbative regimes by varying the frequency and the intensity of the field. Finally, in Chapter 5, we present a summary of the work and a reflection on future work.

1. Nonlinear Optics

In the universe of the nonlinear response in crystalline materials, a quantum description of the time response of a crystal by an electromagnetic perturbation can be done in terms of the current density, computed via density matrix formalism:

$$\mathbf{J}(t) = \mathrm{Tr}\left[\hat{\mathbf{J}}\,\hat{\rho}(t)\right], \tag{1.1}$$

where $\hat{\rho}(t)$ is the density matrix of the system at time t and $\hat{\mathbf{J}} = -N/\Omega\,|e|\,\hat{\mathbf{v}}$ is the current operator, where N is the number of particles, Ω is the volume and $\hat{\mathbf{v}}$ is the velocity operator. The density matrix evolves adiabatically in time through the Liouville equation

$$i\hbar\frac{\partial\hat{\rho}}{\partial t} = \left[\hat{H}(t), \hat{\rho}\right], \tag{1.2}$$

where $\hat{H}(t)$ is the system's Hamiltonian at time t. Starting with a crystalline material in equilibrium, with Hamiltonian $\hat{H}_0$, we need a gauge to describe an electromagnetic perturbation. Among several possibilities, the analysis is usually done in the length or the velocity gauges.

In this chapter, we have put together some concepts that will be useful in the analysis of the problem proposed in the thesis. We start by motivating the choice of the gauge that will be used to describe the electromagnetic perturbation, Section 1.1, and then we present the equations and start point of the expansion in perturbation theory that will be used to analyse the first order current of the system, Section 3.2.

1.1. Gauge choices

In length gauge, the Hamiltonian of the system in the presence of the perturbation is written as

$$\hat{H}(t) = \hat{H}_0 + |e|\,\hat{\mathbf{r}}\cdot\overrightarrow{\mathbf{E}}(t), \tag{1.3}$$

where $\hat{\mathbf{r}}$ is the position operator, e is the electron charge and $\overrightarrow{\mathbf{E}}(t)$ is the electric field. The velocity operator $\hat{\mathbf{v}}$ is given by

$$\hat{\mathbf{v}} = \frac{1}{i\hbar}\left[\hat{\mathbf{r}}, \hat{H}(t)\right], \tag{1.4}$$

which is equivalent to

$$\hat{\mathbf{v}} = \frac{1}{i\hbar}\left[\hat{\mathbf{r}}, \hat{H}_0\right] \tag{1.5}$$

once the position operator commutes with itself, the velocity operator is time independent in this gauge even in the presence of the $\overrightarrow{\mathbf{E}}(t)$.

This gauge is incompatible with periodic boundary conditions. Setting periodic conditions is equivalent to define $\hat{\mathbf{r}}_N = \hat{\mathbf{r}}_0$, as we see in Fig. 1.1 for a 1D lattice with one atom per cell in this boundary conditions. In the figure, we see that the position of each atom is defined such that the position variation between consecutive cells is $\Delta x = ((n+1) - n)\, a = a$. However, the difference in the positions of the first and the last atom does not correspond to the actual distance. The position operator is not well defined.

We can, however, proceed with this gauge if we consider the infinite-crystal limit of a d-dimensional crystal. Using the periodicity of the lattice, we write the operators in the Bloch vectors basis, $\left|\overrightarrow{\mathbf{k}}\right\rangle$ [32]

$$\hat{\mathcal{H}}^E(t) = \sum_{ss'} \int \frac{d^d\mathbf{k}}{(2\pi)^d} c^\dagger_{\mathbf{k}s} \left[\delta_{ss'}\epsilon_{\mathbf{k}s} + i|e|\mathbf{E}(t)\cdot\mathbf{D}_{\mathbf{k}ss'}\right] c_{\mathbf{k}s'}, \tag{1.6}$$

$$\hat{\mathbf{v}}^E = \frac{1}{\hbar}\left[\hat{\mathbf{D}}, \hat{\mathcal{H}}^E(t)\right], \tag{1.7}$$

where $c^\dagger_{\mathbf{k}s}$and $c_{\mathbf{k}s}$ are the creation and annihilation operators and the indices s, s' are the indices for the system's bands. The nonperturbed Hamiltonian is diagonal by blocks in the reciprocal lattice. For this reason, we can describe the system by its block matrices $\hat{\mathcal{H}}(\mathbf{k})$, such that the total Hamiltonian is given by

$$\hat{\mathcal{H}}_0 = \sum_{\mathbf{k}} \hat{\mathcal{H}}(\mathbf{k}) \tag{1.8}$$

and the band indices mentioned above correspond to the eigenbasis of those blocks with the eigenvalue equation given by

$$\hat{\mathcal{H}}(\mathbf{k})\left|u_{\mathbf{k}s}\right\rangle = \epsilon_{\mathbf{k}s}\left|u_{\mathbf{k}s}\right\rangle, \tag{1.9}$$

where $|u_{\mathbf{k}s}\rangle$ and $\epsilon_{\mathbf{k}s}$ are the eigenstates and eigenenergies of the nonperturbed system, respectively. The $\hat{\mathbf{D}}_{\mathbf{k}}$ operator that appears in the previous equation is the covariant derivative operator

$$\mathbf{D}_{\mathbf{k}ss'} \coloneqq \delta_{ss'}\nabla_{\mathbf{k}} - i\xi_{\mathbf{k}ss'}, \tag{1.10}$$

where $\xi_{\mathbf{k}ss'}$ is the Berry connection defined by

$$\xi_{\mathbf{k}ss'} \coloneqq i\left\langle u_{\mathbf{k}s}|\nabla_{\mathbf{k}}u_{\mathbf{k}s'}\right\rangle = i\int_{uc} d^d\mathbf{r}\, u^*_{\mathbf{k}s}(\mathbf{r})\nabla_{\mathbf{k}}u_{\mathbf{k}s'}(\mathbf{r}) \tag{1.11}$$

with the integral over the real space unit cell (uc). This operator is the representation of the position operator in $\mathbf{k}$ basis, $\hat{\mathbf{r}} \to i\hat{\mathbf{D}}_{\mathbf{k}}$:

$$\left\langle\psi_{\mathbf{k}s}\right|\hat{\mathbf{r}}\left|\Psi\right\rangle = \sum_{s'} i\mathbf{D}_{\mathbf{k}ss'}\Phi_{s'}(\mathbf{k}). \tag{1.12}$$

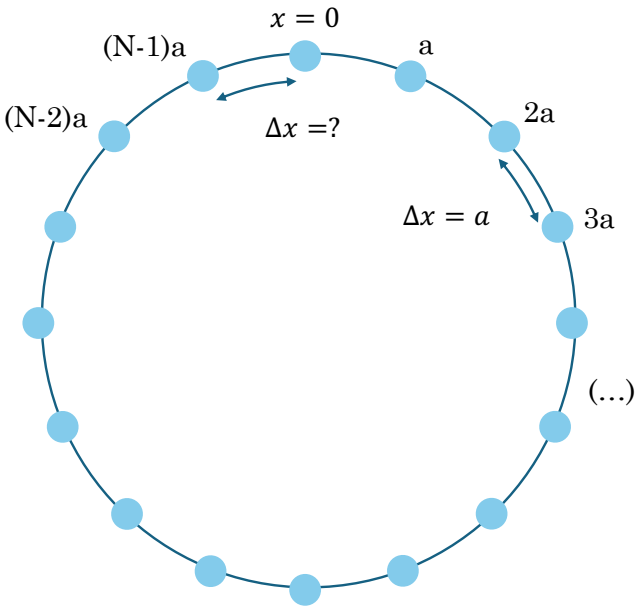

Figure 1.1.: Representation of a 1D lattice with periodic boundary conditions with the evidence of a ill definition of the position in the lattice. Scheme adapted from [32].

where $|\psi_{\mathbf{k}s}\rangle$ is the Bloch state and $|\Psi\rangle$ a general single particle state that can be expressed as a linear combination of the Bloch functions with coefficients $\Phi_s(\mathbf{k}) = \langle\psi_{\mathbf{k}s}|\Psi\rangle$. As a result, the density matrix evolution equation can be derived by writing Eq. (1.2) in the eigenbasis $|u_{ks}\rangle$ and entering Eq. (1.3) for the Hamiltonian [32]

$$\left[i\hbar\frac{\partial}{\partial t} - \Delta\epsilon_{\mathbf{k}ss'}\right]\rho^E_{\mathbf{k}ss'}(\mathbf{k},t) = i\,|e|\,\mathbf{E}(t)\cdot\left[\hat{\mathbf{D}}_{\mathbf{k}},\hat{\rho}^E(\mathbf{k},t)\right]_{ss'}, \tag{1.13}$$

with $\Delta\epsilon_{\mathbf{k}ss'} = \epsilon_{\mathbf{k}s} - \epsilon_{\mathbf{k}s'}$ and $\hat{\rho}^E(\mathbf{k},t)$ is the density matrix operator in the length gauge. This is a partial derivative equation in quasi-momentum $\mathbf{k}$. We cannot solve it for each quasi-momentum $\mathbf{k}$ independently.

Another possibility is the velocity gauge. In this gauge, there is no problem with periodic boundary conditions. The electric field is introduced through a vector potential $\mathbf{A}(t)$ which, following the Maxwell equations, satisfies $\mathbf{E}(t) = -\partial_t\mathbf{A}(t)$. In this gauge, the perturbed Hamiltonian is also block diagonal in the Bloch's basis, where the blocks are given by $\hat{\mathcal{H}}^A(\mathbf{k},t)$. Consequence of the gauge invariance of the electromagnetic field, the Hamiltonian constructed this will be also gauge invariance. According to Noether's theorem, a generic current is always associated with the system's symmetry. In this case, associated to the gauge invariance is the current density given by

$$\hat{\mathbf{J}}^A(t) = -\frac{1}{L}\frac{\partial\hat{\mathcal{H}}^A(t)}{\partial\mathbf{A}(t)}, \tag{1.14}$$

with L the size of the system. Since the Hamiltonian is block diagonal in k the density current will be, too, such that it can be written as

$$\hat{\mathbf{J}}^A(t) = \sum_{\mathbf{k}}\hat{\mathbf{J}}^A(\mathbf{k},t), \tag{1.15}$$

where

$$\hat{\mathbf{J}}^A(\mathbf{k},t) = \sum_{s,s'} \mathbf{J}^A_{ss'}(\mathbf{k},t)\,|u_{\mathbf{k}s}\rangle\,\langle u_{\mathbf{k}s'}|\,. \tag{1.16}$$

The velocity operator related to the current by

$$\hat{\mathbf{J}}^A(\mathbf{k},t) = -|e|\,\hat{\mathbf{v}}^A(\mathbf{k},t) \tag{1.17}$$

that is now time dependent, in contrast to the length gauge.

In this gauge, the density matrix equation evolves via the following equation [32]

$$\left[i\hbar\frac{\partial}{\partial t} - \Delta\epsilon_{\mathbf{k}ss'}\right]\rho^A_{\mathbf{k}ss'}(t) = \left[\hat{V}(t), \rho^A(\mathbf{k},t)\right]_{ss'}, \tag{1.18}$$

with

$$\hat{V}(t) = \hat{\mathcal{H}}^A(\mathbf{k},t) - \hat{\mathcal{H}}^A(\mathbf{k},0)\,. \tag{1.19}$$

As a result of the fact that the Hamiltonian of the perturbed system is block diagonal in base k and if the initial condition of the system is also block diagonal in k, Eq.(1.18) corresponds to a system of ordinary differential equations in t, decoupled in quasi-momenta $\mathbf{k}$, so it can be solved for each $\mathbf{k}$ individually. Throughout this thesis, we will define the main problem in the velocity gauge to take advantage of the block diagonalization in k-basis, despite the time dependency of the velocity and density current operator.

1.2. Perturbation theory

To compute the optical response as discussed before, we can either apply numerical methods such as Runge-Kutta or analytical approaches to address the problem. We can address the problem using time-dependent perturbation theory in a weak electromagnetic perturbation. In this condition, the conventional expansion in powers of the electromagnetic field is applicable. Therefore, one can expand the current density $\mathbf{J}(t)$ in a power series of $\mathbf{E}(t)$

$$\mathbf{J}(t) = \mathbf{J}^{(1)}(t) + \mathbf{J}^{(2)}(t) + \ldots + \mathbf{J}^{(n)} + \ldots, \tag{1.20}$$

where, considering causality, the n-th term is given by [13]

$$J^{(n)}(t) = \int_{-\infty}^{t} dt_1 \cdots \int_{-\infty}^{t} dt_n \sigma^{(n)}(t-t_1,\ldots,t-t_n)\,E(t_1)\ldots E(t_n)\,, \tag{1.21}$$

with $\sigma^{(n)}(t-t_1,\ldots,t-t_n)$ is the n-th order conductivity.

The result of Eq. (1.20) is a consequence of the expansion of the density matrix solution of Eq.(1.18), which uses the expanded Hamiltonian, and thus the operator $\hat{V}$, in powers of the electric field.

The analysis of perturbative response can account for optical phenomena such as the generation of harmonics. Still, outside the perturbation theory regime, new effects appear that require other techniques to be described.

In the specific case where the perturbation is periodic in time, the time evolution of the DM can be computed using the Floquet formalism. The main focus is to present an alternative to the time-dependent perturbation theory for computing a crystal's optical response. In the title of proof of concept, we will analyse a 1D two-band semiconductor perturbed with a monochromatic electromagnetic field at zero temperature.

2. Floquet formalism

In this chapter, we provide a detailed review of the Floquet formalism. We start by exploring the main concepts of the formalism. We present a modification to the basic formalism to solve more complex problems, and finally, we analyse two preliminary cases that help gaining some intuition. The exposition follows closely the references [33, 34][1].

2.1. Fundamental concepts

The Floquet formalism addresses systems described by a time-dependent periodic Hamiltonian

$$i\hbar\frac{\partial\left|\psi(t)\right\rangle}{\partial t}=\hat{H}(t)\left|\psi(t)\right\rangle, \quad \hat{H}(t+T)=\hat{H}(t), \tag{2.1}$$

where $\hat{H}(t)$ is the Hamiltonian that describes the system in study, $|\psi(t)\rangle$ is a state of the system and $T=2\pi/\Omega$ is the period of the Hamiltonian. Instead of choosing a basis of stationary states, as would be the case if the system was independent of time, we can choose a basis of states that can be seen, in analogy with spatial periodicity, as Bloch states in time:

$$\left|\psi_n(t)\right\rangle=e^{-i\epsilon_n t/\hbar}\left|u_n(t)\right\rangle, \quad \text{with } \left|u_n(t)\right\rangle=\left|u_n(t+T)\right\rangle, \tag{2.2}$$

and the evolution over one period from any other time is given by multiplying by the exponential $e^{-i\epsilon_n T/\hbar}$, a result of the time periodicity of the $|u_n(t)\rangle$

$$\left|\psi_n(t+T)\right\rangle=e^{-i\epsilon_n(t+T)/\hbar}\left|u_n(t+T)\right\rangle, \tag{2.3}$$

$$=e^{-i\epsilon_n T/\hbar}\left|\psi_n(t)\right\rangle. \tag{2.4}$$

In the Floquet picture, the states $|\psi_n(t)\rangle$ and the real value energies ϵ_n are called Floquet states and quasienergies, respectively, with $|u_n(t)\rangle$ referred to as Floquet modes. A generic state at a time t is therefore expanded in terms of the Floquet states in the following way

$$\left|\psi(t)\right\rangle=\sum_n c_n\left|\psi_n(t)\right\rangle=\sum_n c_n e^{-i\epsilon_n t/\hbar}\left|u_n(t)\right\rangle. \tag{2.5}$$

[1] There are other references with interesting approaches to the formalism, which have not been followed in detail in this exposition [30, 31, 35–38]

Note that the coefficients c_n are time-independent since the periodic time-dependence is already incorporated into the basis of Floquet states $|\psi_n(t)\rangle$. This means that each Floquet state has a preserved occupation probability $|c_n|^2$, despite the time evolution. Consequently, various concepts and techniques employed in time-independent quantum systems can be analogously applied to periodically driven systems.

Setting $t = 0$ in Eq.(2.4) we obtain

$$|\psi_n(T)\rangle = e^{-i\epsilon_n T/\hbar} |\psi_n(0)\rangle , \tag{2.6}$$

which is equivalent to the application of the time evolution operator over one period

$$\hat{U}(T,0) |\psi_n(0)\rangle = e^{-i\epsilon_n T/\hbar} |\psi_n(0)\rangle = e^{-i\epsilon_n T/\hbar} |u_n(0)\rangle . \tag{2.7}$$

This leads to the conclusion that $\exp(-i\epsilon_n T/\hbar)$ are the eigenvalues of $\hat{U}(T) \equiv \hat{U}(T,0)$, and the eigenvectors are $|u_n\rangle \equiv |u_n(0)\rangle$. Now we can define an effective Hamiltonian, the Floquet Hamiltonian $\hat{H}_F$, that governs the evolution of the system over one period

$$\hat{U}(T) = e^{-i\hat{H}_F T/\hbar}, \tag{2.8}$$

which is also diagonal in the $|u_n\rangle$ basis with the eigenvalues equal to ϵ_n

$$\hat{H}_F |u_n\rangle = \epsilon_n |u_n\rangle . \tag{2.9}$$

To compute the system state $|\psi(t)\rangle$ from an initial state $|\psi(0)\rangle$, it is always possible to construct a time evolution operator, $\hat{U}(t,0)$, that obeys the Schrödinger equation with an initial condition $\hat{U}(0) = \hat{\mathbb{1}}$. It is useful to define the time evolution operator, $\hat{U}(t)$, for any time t with an auxiliary operator $\hat{P}(t)$ and the Floquet Hamiltonian as:

$$\hat{U}(t) = \hat{P}(t) e^{-i\hat{H}_F t/\hbar}, \tag{2.10}$$

where $\hat{P}(t)$ is unitary. Applying this operator to $|\psi(0)\rangle$

$$\hat{U}(t) |\psi(0)\rangle = \hat{P}(t) e^{-i\hat{H}_F t/\hbar} \sum_n c_n |u_n\rangle = \sum_n c_n e^{-i\epsilon_n t/\hbar} \hat{P}(t) |u_n\rangle . \tag{2.11}$$

Comparing this equation with Eq.(2.5), we conclude that

$$|u_n(t)\rangle = \hat{P}(t) |u_n\rangle , \tag{2.12}$$

which means that the auxiliary operator has the same periodicity of the Hamiltonian

$$\hat{P}(t+T) = \hat{P}(t), \tag{2.13}$$

since the Floquet mode is periodic $|u_n(t+T)\rangle = |u_n(t)\rangle$. Once we know the operator $\hat{P}(t)$, we only need to construct the Floquet Hamiltonian to compute the system's evolution.

To compute the time evolution, we start by applying the unitary transformation that freezes the $\hat{P}(t)$ part of time evolution

$$|\tilde{\psi}(t)\rangle = \hat{P}^\dagger(t) |\psi(t)\rangle, \tag{2.14}$$

such that the evolution of the transformed state is then given by

$$|\tilde{\psi}(t)\rangle = e^{-i\hat{H}_F t/\hbar}|\tilde{\psi}(0)\rangle. \tag{2.15}$$

From Schrödinger's equation for $|\tilde{\psi}(t)\rangle$:

$$\mathrm{i}\hbar\frac{d\left|\tilde{\psi}(t)\right\rangle}{dt} = \left[-i\hbar\hat{P}^\dagger(t)\frac{d\hat{P}(t)}{dt} + \hat{P}^\dagger(t)\hat{H}(t)\hat{P}(t)\right]\left|\tilde{\psi}(t)\right\rangle, \tag{2.16}$$

appears the definition of the Floquet Hamiltonian

$$\hat{H}_F = \hat{P}^\dagger(t)\left[\hat{H}(t) - i\hbar\frac{d}{dt}\right]\hat{P}(t), \tag{2.17}$$

which maybe shown to be time independent with a proper choice of $\hat{P}(t)$. After diagonalizing the Floquet Hamiltonian, the time evolution of the system is totally determined by

$$|\psi(t)\rangle = \sum_n \hat{P}(t)\,|u_n\rangle\, e^{-i\epsilon_n t/\hbar}\,\langle u_n|\psi(0)\rangle\,, \tag{2.18}$$

where the index n takes values between 1 and d, the dimension of the original Hilbert space, since the $|u_n\rangle$ is the eigenbasis of $\hat{U}(T)$. Choosing any basis of the Hilbert space $\{|\varphi_\alpha\rangle\,, \alpha = 1, ..., d\}$:

$$|\psi(t)\rangle = \sum_n \sum_{\alpha,\beta,\gamma} |\varphi_\alpha\rangle\,\langle\varphi_\alpha|\,\hat{P}(t)\,|\varphi_\beta\rangle\,\langle\varphi_\beta|u_n\rangle\, e^{-i\epsilon_n t/\hbar}\,\langle u_n|\varphi_\gamma\rangle\,\langle\varphi_\gamma|\psi(0)\rangle \tag{2.19}$$

we can write the expression in matrix form as

$$\overrightarrow{\mathbf{\Psi}}(t) = \mathbf{P}(t)\cdot\mathbf{U}_F\cdot\begin{bmatrix} e^{-i\epsilon_1 t/\hbar} & 0 & \cdots \\ 0 & \ddots & 0 \\ \cdots & 0 & e^{-i\epsilon_d t/\hbar}\end{bmatrix}\cdot\mathbf{U}_F^\dagger\cdot\overrightarrow{\mathbf{\Psi}}(0), \tag{2.20}$$

where

$$\Psi_\alpha(t) = \langle\varphi_\alpha|\psi(t)\rangle\,, \tag{2.21}$$

$$P_{\alpha\beta}(t) = \langle\varphi_\alpha|\,\hat{P}(t)\,|\varphi_\beta\rangle\,, \tag{2.22}$$

and

$$U_{F\alpha n} = \langle\varphi_\beta|u_n\rangle\,. \tag{2.23}$$

In a few happy cases, we can, using a proper ansatz, guess an operator $\hat{P}(t)$, that yields a time-independent Floquet Hamiltonian via Eq.(2.17). This approach, however, is not always possible without computing the time evolution operator itself because of the difficulty of guessing $\hat{P}(t)$ by physical arguments.

2.2. Extended Floquet Hamiltonian

An alternative approach exploits the properties of Floquet states. Note that the Floquet Hamiltonian, given by Eq. (2.8), is not uniquely defined. Its eigenvalues, the quasienergies ϵ_n, are defined modulo $\hbar 2\pi/T = \hbar\Omega$, because of the invariance of the evolution operator $\hat{U}(T)$, Eq. (2.7), under the transformation

$$\epsilon_n \to \epsilon'_n = \epsilon_n + m\hbar\Omega\,, \qquad m \in \mathbb{Z}. \tag{2.24}$$

So, we can write a more general form of the Floquet Hamiltonian as

$$\hat{H'}_F = \sum_n |u_n\rangle \left(\epsilon_n + m\hbar\Omega\right) \langle u_n| \tag{2.25}$$

which, from Eq. (2.10), requires us to transform the operator $\hat{P}(t)$ as

$$\hat{P}'(t) = \hat{P}(t) e^{i\Omega t \sum_n |u_n\rangle m \langle u_n|} \tag{2.26}$$

to capture the correct dynamic of the system with the evolution operator $\hat{U}(t)$. The consequence of guessing the operator $\hat{P}(t)$ is to fix the factor m and consequently to fix the Floquet Hamiltonian. As mentioned before, it is not always possible to choose $\hat{P}(t)$, so the Extended Floquet Hamiltonian is a method of constructing both $\hat{P}(t)$ and $\hat{H}_F$.

Another property used in this approach is the time periodicity of the Floquet modes $|u_n(t)\rangle$. To explore that, we write a simplified equation for their evolution. By incorporating the expansion of a system's state, given by Eq. (2.5), into Eq. (2.1), we get:

$$i\hbar \frac{\partial \left(e^{-i\epsilon_n t/\hbar} |u_n(t)\rangle\right)}{\partial t} = \hat{H}(t) e^{-i\epsilon_n t/\hbar} |u_n(t)\rangle\,. \tag{2.27}$$

If we expand the derivative of the product and then divide both sides of the equation by the exponential, we arrive at the simplified equation:

$$\left(\hat{H}(t) - i\hbar\frac{\partial}{\partial t}\right) |u_n(t)\rangle = \epsilon_n |u_n(t)\rangle\,, \tag{2.28}$$

which is an eigenvalue equation for the Floquet modes. Using the time periodicity, we can write the Floquet modes on any basis $\{|\varphi_\alpha\rangle\,, \alpha = 1, ..., d\}$ of the original Hilbert space and expand the resulting components in a Fourier series in t

$$|u_n(t)\rangle = \frac{1}{\sqrt{T}} \sum_{\beta=1}^{d} \sum_{p\in\mathbb{Z}} a_{\beta p}^{(n)} e^{ip\Omega t} |\varphi_\beta\rangle. \tag{2.29}$$

By introducing the Fourier expansion in Eq. (2.28) and multiplying on the left by $\langle\varphi_\alpha|$, we obtain

$$\sum_{\beta=1}^{d} \left[\sum_{p\in\mathbb{Z}} \left(\langle\varphi_\alpha| \hat{H}(t) |\varphi_\beta\rangle + p\hbar\Omega\delta_{\alpha\beta}\right) e^{ip\Omega t} a_{\beta p}^{(n)}\right] = \epsilon_n \left[\sum_{p\in\mathbb{Z}} e^{ip\Omega t} a_{\alpha p}^{(n)}\right], \tag{2.30}$$

and by multiplying both sides by $\exp(-iq\Omega t)/T$ and integrating over a period we get

$$\sum_{\beta,p}\left(\hat{\mathcal{H}}_{\alpha q;\beta p}+\hbar p\Omega\delta_{q,p}\delta_{\alpha,\beta}\right)a_{\beta p}^{(n)}=\epsilon_n a_{\alpha q}^{(n)}, \tag{2.31}$$

with

$$\hat{\mathcal{H}}_{\alpha q;\beta p}=\frac{1}{T}\int_0^T dt\,\langle\varphi_\alpha|\,\hat{H}(t)\,|\varphi_\beta\rangle\,e^{-i(q-p)\Omega t}, \tag{2.32}$$

where the α, β indices refer to the original Hilbert space and p, q run over $\mathbb{Z}$. In Eq. (2.31), we arrived at a stationary eigenvalue equation where the Fourier coefficients are the coefficients of the eigenvectors of a time independent operator formally named the Extended Floquet Hamiltonian (EFH):

$$\hat{H}_{\text{Ext}}=\sum_{\alpha,\beta}\sum_{q,p}|\varphi_{\alpha q}\rangle\left(\hat{\mathcal{H}}_{\alpha q;\beta p}+\hbar p\Omega\delta_{q,p}\delta_{\alpha,\beta}\right)\langle\varphi_{\beta p}|, \tag{2.33}$$

in a Hilbert space of the form $\{|\varphi_\alpha\rangle\otimes|q\rangle\,,\alpha=1,...,d;q\in\mathbb{Z}\}$. Its eigenvalues can be categorised into sets of the form $\{\epsilon_n+m\Omega,m\in\mathbb{Z}\}$ and the eigenvectors with eigenvalues within the same set are equivalent to each other.

The proof of this conclusion starts by noting that the $\hat{\mathcal{H}}_{\alpha q;\beta p}$ depends only on the difference $p-q$, hence (2.31) is equivalent to

$$\sum_{\beta,p}\left(\hat{\mathcal{H}}_{\alpha q+r;\beta p+r}+\hbar p\Omega\delta_{q,p}\delta_{\alpha,\beta}\right)a_{\beta p+r}^{(n)}=(\epsilon_n-\hbar r\Omega)\,a_{\alpha q+r}^{(n)}. \tag{2.34}$$

where $q\to q+r$ and $p\to p+r$. Since $\hat{\mathcal{H}}_{\alpha q;\beta p}=\hat{\mathcal{H}}_{\alpha q+r;\beta p+r}$, just as the coefficient $a_{\alpha q}^{(n)}$ is a solution with eigenvalue ϵ_n, the coefficient $a_{\alpha q+r}^{(n)}$ is also a solution of the same equation with eigenvalue $\epsilon_n-\hbar r\Omega$. Looking at two different eigenvectors of the same set, $m=0$ and $m=r$, the resulting Floquet modes are:

$$\left|u_n^{(m=0)}(t)\right\rangle=\frac{1}{\sqrt{T}}\sum_{\beta=1}^{d}\sum_{p\in\mathbb{Z}}a_{\beta p}^{(n)}e^{ip\Omega t}\,|\varphi_\beta\rangle \tag{2.35}$$

and

$$\left|u_n^{(m=r)}(t)\right\rangle=\frac{1}{\sqrt{T}}\sum_{\beta=1}^{d}\sum_{p\in\mathbb{Z}}a_{\beta p+r}^{(n)}e^{ip\Omega t}\,|\varphi_\beta\rangle. \tag{2.36}$$

They are related to each other by

$$\left|u_n^{(m=r)}(t)\right\rangle=\frac{1}{\sqrt{T}}\sum_{\beta=1}^{d}\sum_{p\in\mathbb{Z}}a_{\beta p}^{(n)}e^{i(p-r)\Omega t}\,|\varphi_\beta\rangle=e^{-ir\Omega t}\left|u_n^{(m=0)}(t)\right\rangle \tag{2.37}$$

where in the first equality, we take Eq. (2.36) and apply the transformation $p\to p-r$.

Since the two Floquet modes, $m = 0$ and $m = r$, with their respective energies producing the same Floquet state $|\psi_n(t)\rangle$:

$$|\psi_n(t)\rangle = e^{-i\epsilon_n t/\hbar} \left|u_n^{(m=0)}(t)\right\rangle, \tag{2.38}$$

$$= e^{-i(\epsilon_n - r\hbar\Omega)t/\hbar} \cdot e^{-ir\Omega t} \left|u_n^{(m=0)}(t)\right\rangle = e^{-i(\epsilon_n - r\hbar\Omega)t/\hbar} \left|u_n^{(m=r)}(t)\right\rangle, \tag{2.39}$$

which is responsible for the system dynamics, Eq. (2.5), the two modes are redundant. This shows that the dynamics remains unchanged when choosing of any the vector from a set.

Therefore, all states of the system in the Floquet representation can be constructed using the Floquet modes with quasienergies confined within the same interval of width $\hbar\Omega$, often called the Brillouin zone [18, 36].

In conclusion, the EFH's diagonalization completely solves the system dynamics. Choosing any eigenvector from each set and the respective quasienergies, the solution for the evolution of the states of the system follows naturally from Eq. (2.18):

$$|\psi(t)\rangle = \sum_{n,\alpha,\beta} |\varphi_\alpha\rangle \langle\varphi_\alpha|u_n(t)\rangle e^{-i\epsilon_n t/\hbar} \langle u_n|\varphi_\beta\rangle \langle\varphi_\beta|\psi(0)\rangle, \tag{2.40}$$

where

$$\langle\varphi_\alpha|\, u_n(t)\rangle = \left[\hat{U}_F(t)\right]_{\alpha n} = \frac{1}{\sqrt{T}} \sum_p a_{\alpha p}^{(n)} e^{ip\Omega t}, \tag{2.41}$$

$$\langle u_n|\, \varphi_\beta\rangle = \left[\hat{U}_F^\dagger(0)\right]_{\beta n}, \tag{2.42}$$

$\{|\varphi_\alpha\rangle, \alpha = 1, ..., d\}$ is a basis in the original Hilbert space and the $a_{\alpha p}^{(n)}$ coefficients are obtained by diagonalization of EFH, Eq.(2.33). We can identify the equivalence between this equation and Eq. (2.20) by

$$\left[\hat{U}_F(0)\right]_{\alpha n} = [\mathbf{U}_F]_{\alpha n} \tag{2.43}$$

and

$$\left[\hat{U}_F(t)\right]_{\alpha n} = [\mathbf{P}(t) \cdot \mathbf{U}_F]_{\alpha n} \tag{2.44}$$

Although this concept works, it requires the diagonalization of an infinite matrix, an impractical proposition. Therefore, to implement a practical approach to solving the dynamics, we need to truncate the values of p in Eq. (2.41) to a finite set.

The method presented here for the computation of time evolution has also been used for atomic and nuclear methods, which we became aware of after we formulated the method [30, 31]. As far as we know it has not been used before in the context of nonlinear optics of crystals, which is the subject of Chapters 3 and 4.

2.3. Preliminary examples

To illustrate the concepts described before, we present two examples of two-level systems perturbed by a periodic field that will be solved using the Floquet formalism, one by fixing $\hat{P}(t)$ based on physical arguments and the other using the extended Floquet formalism [33].

2.3.1. Two-level system pumped with a circularly polarized field

A solvable example, where we can guess $\hat{P}(t)$ on physical grounds, is a two-level system pumped with a circularly polarized field

$$\hat{H} = \frac{\Delta}{2}\hat{\sigma}^z + e\frac{F}{2}\left(\hat{\sigma}^x \cos(\Omega t) + \hat{\sigma}^y \sin(\Omega t)\right), \tag{2.45}$$

where $\hat{\sigma}^i$, $i = x, y, z$ are the usual 2D Pauli matrices [39], Δ denotes the energy gap between the two states of the undriven system, and the parameters F and Ω specify the strength and the frequency of the driving field, respectively. The numerical results below will be shown in natural units ($e = \hbar = 1$) and Δ as energy unit.

In this case, the operator $\hat{P}(t)$ is built as

$$\hat{P}(t) = e^{i\Omega(\hat{\mathbb{1}} - \hat{\sigma}^z)t/2}, \tag{2.46}$$

to transition to a frame of reference that co-rotates with the circularly polarized field with the same period, where the field appears time-independent. The Floquet Hamiltonian is computed from Eq. (2.17) as

$$\hat{H}_F = e^{-i\Omega(\hat{\mathbb{1}} - \hat{\sigma}^z)t/2}\left[\frac{\Delta}{2}\hat{\sigma}^z + e\frac{F}{2}\left(\hat{\sigma}^x \cos(\Omega t) + \hat{\sigma}^y \sin(\Omega t)\right) - i\hbar\frac{d}{dt}\right] e^{i\Omega(\hat{\mathbb{1}} - \hat{\sigma}^z)t/2}. \tag{2.47}$$

If we choose the eigenbasis of $\sigma^z, |\sigma\rangle = \{|-1\rangle, |+1\rangle\}$, to write the operators, the terms of the previous expression can be written as

$$\hat{\sigma}^x \cos(\Omega t) + \hat{\sigma}^y \sin(\Omega t) = \begin{bmatrix} 0 & e^{-i\Omega t} \\ e^{i\Omega t} & 0 \end{bmatrix} \tag{2.48}$$

and

$$e^{i\Omega(\hat{\mathbb{1}} - \hat{\sigma}^z)t/2} = \begin{bmatrix} e^{i\Omega t} & 0 \\ 0 & 1 \end{bmatrix}. \tag{2.49}$$

The Floquet Hamiltonian then turns out to be

$$\hat{H}_F = \begin{bmatrix} \frac{\Delta}{2} & e\frac{F}{2} \\ e\frac{F}{2} & -\frac{\Delta}{2} + \hbar\Omega \end{bmatrix}. \tag{2.50}$$

From its diagonalization, the eigenvalues are obtained as

$$\epsilon_{\pm} = \frac{\hbar\Omega}{2} \pm \frac{\hbar\omega_R}{2}, \tag{2.51}$$

where ω_R is known as Rabi frequency

$$\omega_R = \sqrt{\left(\frac{\Delta}{\hbar} - \Omega\right)^2 + \frac{e^2F^2}{\hbar^2}}, \tag{2.52}$$

and the eigenvectors, the Floquet modes at $t = 0$,

$$|u_{\pm}\rangle = \chi_{\pm}\left(\left(\hbar\Omega - \Delta \pm \hbar\omega_R\right)|-1\rangle + eF\,|+1\rangle\right), \tag{2.53}$$

with

$$\chi_{\pm} = \frac{1}{\sqrt{\left(\hbar\Omega - \Delta \pm \hbar\omega_R\right)^2 + \left(eF\right)^2}}. \tag{2.54}$$

Here we get two results that call our attention. The first one is that the Floquet Hamiltonian has a quasienergy gap

$$\Delta_F = |\epsilon_+ - \epsilon_-|, \tag{2.55}$$

called Floquet gap, that is equal to ω_R instead of the original energy gap of the unperturbed system, Δ. The other interesting thing is that when $\Delta = \hbar\Omega$, the Floquet modes are equally weighted superpositions of $|\sigma\rangle$, and vice versa.

From Eq. (2.2) and using the evolution of the Floquet modes on Eq. (2.12), we obtain the Floquet states for this problem

$$|\psi_{\pm}(t)\rangle = e^{-i(\pm\omega_R - \Omega)t/2}\langle -1|u_{\pm}\rangle\,|-1\rangle + e^{-i(\pm\omega_R + \Omega)t/2}\langle +1|u_{\pm}\rangle\,|+1\rangle \tag{2.56}$$

and observe that the amplitudes of the Floquet states rotate with Ω.

Substituting the respective factors in Eq. (2.20), the evolution of the system is given by

$$\overrightarrow{\mathbf{\Psi}}(t) = \begin{bmatrix} e^{i\Omega t} & 0 \\ 0 & 1 \end{bmatrix} \cdot \mathbf{U}_F \cdot \begin{bmatrix} e^{-i\epsilon_- t/\hbar} & 0 \\ 0 & e^{-i\epsilon_+ t/\hbar} \end{bmatrix} \cdot \mathbf{U}_F^{\dagger} \cdot \overrightarrow{\mathbf{\Psi}}(0) \tag{2.57}$$

or rewriting the product of the first three matrices,

$$\overrightarrow{\mathbf{\Psi}}(t) = \begin{bmatrix} e^{i\Omega t/2} & 0 \\ 0 & e^{-i\Omega t/2} \end{bmatrix} \cdot \mathbf{U}_F \cdot \begin{bmatrix} e^{i\omega_R t/2} & 0 \\ 0 & e^{-i\omega_R t/2} \end{bmatrix} \cdot \mathbf{U}_F^{\dagger} \cdot \overrightarrow{\mathbf{a}}(0) \tag{2.58}$$

with $[\mathbf{U}_F]_{\sigma n} = \langle\sigma|u_n\rangle$ which in this case is equal to

$$\mathbf{U}_F = \begin{bmatrix} \frac{\hbar\Omega - \Delta + \hbar\omega_R}{\sqrt{(\hbar\Omega - \Delta + \hbar\omega_R)^2 + (eF)^2}} & \frac{\hbar\Omega - \Delta - \hbar\omega_R}{\sqrt{(\hbar\Omega - \Delta - \hbar\omega_R)^2 + (eF)^2}} \\ \frac{eF}{\sqrt{(\hbar\Omega - \Delta - \hbar\omega_R)^2 + (eF)^2}} & \frac{eF}{\sqrt{(\hbar\Omega - \Delta - \hbar\omega_R)^2 + (eF)^2}} \end{bmatrix}. \tag{2.59}$$

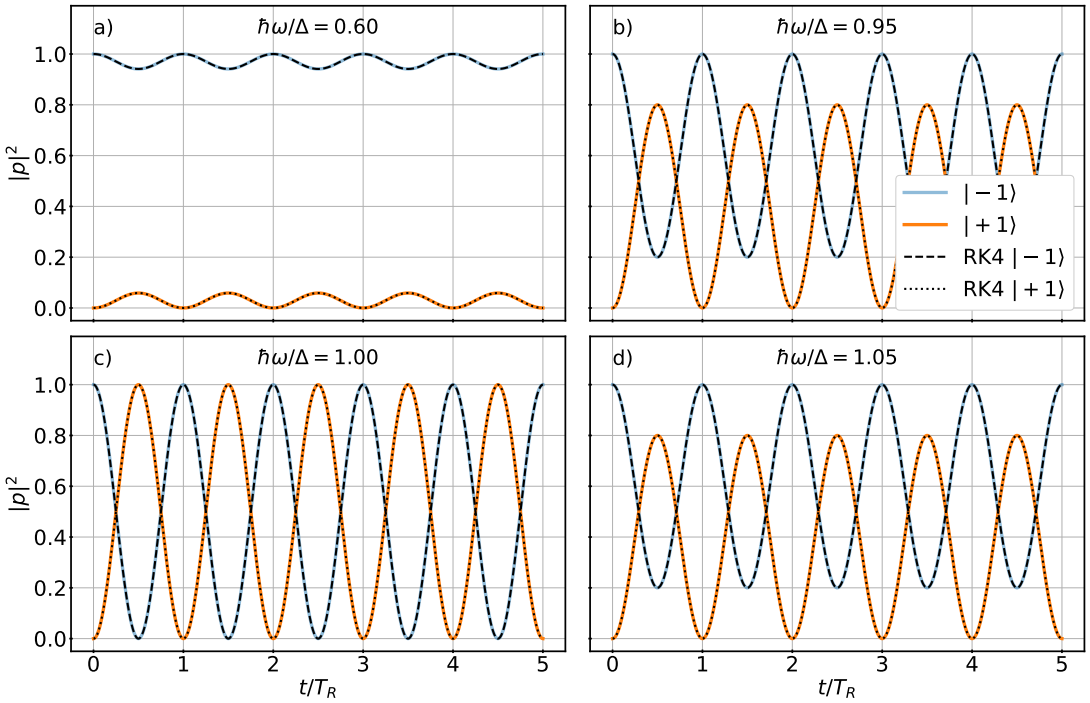

Figure 2.1.: Representation of the time evolution with Floquet formalism (solid lines) of the levels' populations, $|p|^2$, of the two-level system pumped with a circularly polarized field with $eF/\Delta = 0.1$, and $|\psi(0)\rangle = |-1\rangle$, compared with RK4 (black dashed lines).

To illustrate these results, we set a system with field strength $eF/\Delta = 0.1$ and calculate the time evolution of the system from the initial state $|\psi(0)\rangle = |-1\rangle$ for four fields with different frequencies, $\hbar\Omega/\Delta = \{0.7, 0.95, 1, 1.05\}$. The time evolution of the probability of the system being in one of the states $|\sigma\rangle$, mentioned below as the levels' populations of the system, is represented in Fig. 2.1, for both states $|+1\rangle$ and $|-1\rangle$. The evolution was computed using the Floquet formalism and also using a numerical method to solve ordinary differential equations, the fourth-order Runge-Kutta [14], that solve directly the equation

$$\frac{\partial}{\partial t}|\psi(t)\rangle = -\frac{i}{\hbar}\hat{H}(t)\,|\psi(t)\rangle\,. \tag{2.60}$$

As we see in the figure, the results are in perfect agreement, which validates the Floquet formalism.

In the graphs of Fig. 2.1, we represent the time evolution of the populations as function of t/T_R, with $T_R = 2\pi/\omega_R$ the period associated to the Rabi frequency. So, we verify that the level's populations oscillate with Rabi frequency, ω_R. It is interesting to note that despite the Floquet states rotate with external frequency Ω the level's populations oscillate with the Floquet energy gap, so the quantities with non-diagonal elements, such as the $x-$component of the spin $\hat{\sigma}^x$ will oscillate with both Floquet gap and the driven frequency. This is a result that follows from the fact that the operator $\hat{P}(t)$ is diagonal in $|\sigma\rangle$ basis.

As aforementioned, when $\hbar\Omega = \Delta$ the states $|\sigma\rangle$ are equally weighted superposition of the Floquet states and because of the phase $\exp(-i\omega_R t)$, the populations vary between 1 and 0 at Rabi frequency (Fig. 2.1 c)). In the scenario where $\hbar\Omega \ll \Delta$, the states $|\sigma\rangle$ are superpositions of the Floquet states with one principal amplitude, and the result is that the populations oscillate around the initial configuration (Fig. 2.1 a)).

2.3.2. Two-level system pumped with a linearly polarized field

The following example is similar to the previous one, but there is no obvious choice for the auxiliary operator $\hat{P}(t)$. So, we will compute the results in the extended space. The case considered is a two-level system driven by a linear polarized field. The nonperturbed system has a gap Δ and the field has an intensity F and frequency Ω:

$$\hat{H} = \frac{\Delta}{2}\hat{\sigma}^z + eF\hat{\sigma}^x \cos(\Omega t), \tag{2.61}$$

All numerical results were obtained using natural units ($e = \hbar = 1$) and Δ as energy unit.

We first compute the EFH. Substituting the Hamiltonian of the problem in Eq. (2.32), we get

$$\hat{\mathcal{H}}_{\sigma m;\sigma' p} = \frac{1}{T}\int_0^T dt\, \langle\sigma|\, \frac{\Delta}{2}\hat{\sigma}^z + eF\hat{\sigma}^x \cos(\Omega t)\, |\sigma'\rangle\, e^{-i(m-p)\Omega t}, \tag{2.62}$$

and rewriting $\cos(\Omega t)$ using the complex exponentials, the only non-zero matrix elements are

$$\hat{\mathcal{H}}_{m;m} = \frac{\Delta}{2}\hat{\sigma}^z, \tag{2.63}$$

$$\hat{\mathcal{H}}_{m;m+1} = \frac{eF}{2}\hat{\sigma}^x, \tag{2.64}$$

$$\hat{\mathcal{H}}_{m;m-1} = \frac{eF}{2}\hat{\sigma}^x. \tag{2.65}$$

The EFH is a sparse matrix with the principal and the secondary diagonals filled with 2×2 blocks. Then the eigenvalue equation, Eq. (2.31), becomes

$$\left(\frac{\Delta}{2}\sigma^z + \hbar p\Omega\hat{\mathbb{1}}\right) \cdot \overrightarrow{\mathbf{a}}_m^{(n)} + \frac{eF}{2}\sigma^x \cdot \left(\overrightarrow{\mathbf{a}}_{m+1}^{(n)} + \overrightarrow{\mathbf{a}}_{m-1}^{(n)}\right) = \epsilon_n \overrightarrow{\mathbf{a}}_m^{(n)}. \tag{2.66}$$

We need to diagonalise this matrix to compute the system's time evolution. The EFH gives the exact solution of the time evolution equation in the limit of infinitely extended Hilbert space. Computationally, we need to truncate the dimension of the space to perform the calculations. For this system, we truncate the indices in Fourier expansion, Eq. (2.29), between $-M$ and M with $M = 12$. The time evolution is then given by

$$|\psi(t)\rangle = \frac{1}{T}\sum_{p=-M}^{M}\sum_{q=-M}^{M}\sum_{n,\alpha,\beta} |\varphi_\alpha\rangle\, a_{\alpha p}^{(n)} e^{ip\Omega t} e^{-i\epsilon_n t/\hbar} a_{\beta q}^{(n)}\, \langle\varphi_\beta|\psi(0)\rangle\,, \quad M = 12, \tag{2.67}$$

where the coefficients $a_{\alpha p}^{(n)}$ are the coefficients of the selected eigenvectors of Hamiltonian from Eq. (2.62). As mentioned before, to solve the time evolution problem, it is only necessary to select d eigenvectors with energies in different sets of the form $\{\epsilon_n + m\hbar\Omega, \quad m \in \mathbb{Z}\}$, since the eigenvectors with eigenvectors from the same set of quasi-energies are redundant. For this system with only two levels, the dimension of the original Hilbert space, we only need to choose two eigenvectors.

The consequence of truncating the Hamiltonian is that the obtained result is an approximation to the exact result. In Fig. 2.2, we represent the absolute value of the entries indexing by (j, i) of the matrix which each column is an eigenvector of the EFH, i.e. the absolute value of the coefficients of the eigenvectors of Eq. (2.62), $a_{\alpha m}^{(n)}$. As we can see, the matrix is sparse, i.e., most of the coefficients of the eigenvectors are zero, and the nonzero coefficients are together. This means we can choose a truncation that preserves the nonzero indices of at least two eigenvectors and does not introduce significant errors.

We can see from Fig. 2.2 a) that not all eigenvectors are good choices. The eigenvectors with finite elements close to where truncation takes place will introduce more approximation errors. This effect is reflected in the value of the Floquet quasi-energies. In Fig. 2.2 b), we represent the value of the Floquet energies mapped into the first Brillouin zone in time, $-\hbar\Omega/2 \leq \epsilon_n < \hbar\Omega/2$. Related to the observation done before, the quasi-energies that correspond to the edge vectors ($m = -12$ e $m = 12$) are far from the correct value. The dark blue dot should correspond to a negative Floquet energy, and the red dot should be positive.

To see the effect of the truncation in the system's time evolution, we compare the time evolution of the system when choosing the vectors with less influence of the truncation (most central eigenvectors) against those with more influence (closer to the truncation), in Fig. 2.3 a). The plot has the level occupation of the system for both cases. To have a reference for the correct evolution, we computed the evolution using the RK4. As we can see, the evolution using the central vectors matches the RK4 very well, while the evolution using the edge vectors is entirely incorrect.

To select the adequate vectors numerically, we think of a way to look for the two vectors with the non-zero coefficients located far away from the limits of the matrix. We opt to calculate the average of the square value of the index, $-M \leq m \leq M$, weighted by the absolute value of the coefficients of the eigenvectors and choose the two vectors whose average is closest to 0. The only care we have to take is that the corresponding eigenvalues cannot be part of the same set of energies $\{\epsilon_n + m\Omega, m \in \mathbb{Z}\}$.

In Fig. 2.4 from a) to d), we plot the evolution of the levels' populations for a system with field intensity $eF/\Delta = 0.1$ and four different frequencies, $\hbar\Omega/\Delta = \{0.7, 0.95, 1, 1.05\}$. The system is perturbed from its initial state $|-1\rangle$. From the results, we see some similarities with the previous example. When $\hbar\Omega \ll \Delta$ the populations oscillate around the initial state. In other words, the probability of the system being in the state $|-1\rangle$ oscillates close to 1 and the opposite probability oscillates close to 0 (Fig. 2.4 a)). With the increasing frequency of the field, the amplitude of the main oscillation also increases until $\hbar\Omega = \Delta$, when the populations oscillate between 0 and 1 (Fig. 2.4 c)).

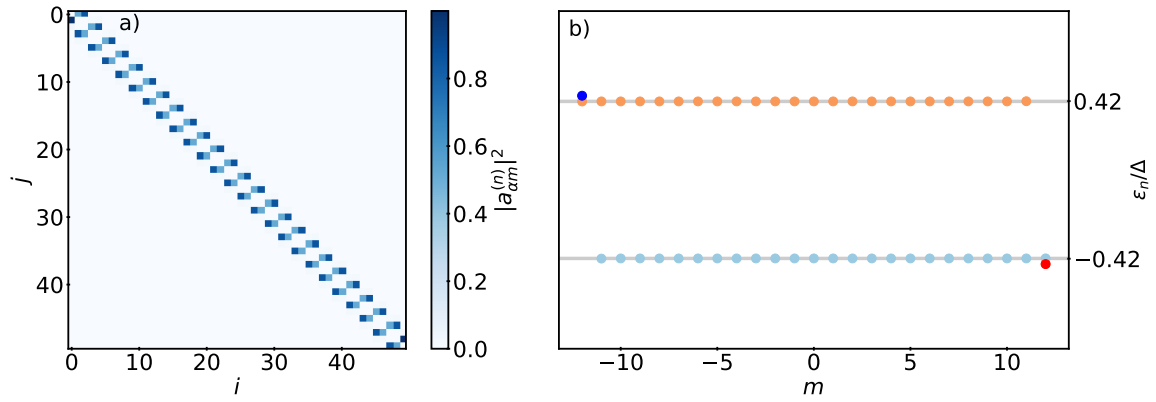

Figure 2.2.: Representation of a) the absolute value of the entries indexing by (j, i) of the matrix which each column is an eigenvector of the EFH and b) the respective eigenvalues mapped into the first Brillouin zone in time, $-\hbar\Omega/2 \leq \epsilon_n < \hbar\Omega/2$. The x-axis of the plot b) is the index of each pair of energies between $-M$ and M inclusive.

Regarding to the response for $\hbar\Omega = \Delta$, we can notice that the system pumped with a circularly polarized field approximates the one pumped with a linearly polarized field. The linear polarized field can be written as a sum of two counter-rotating fields:

$$\begin{aligned}\overrightarrow{\mathbf{E}} = \cos(\Omega t)\,\overrightarrow{\mathbf{e}}_x = &\frac{1}{2}\left(\cos(\Omega t)\,\overrightarrow{\mathbf{e}}_x + \sin(\Omega t)\,\overrightarrow{\mathbf{e}}_y\right) \\ &+ \frac{1}{2}\left(\cos(-\Omega t)\,\overrightarrow{\mathbf{e}}_x + \sin(-\Omega t)\,\overrightarrow{\mathbf{e}}_y\right).\end{aligned} \tag{2.68}$$

In the rotating frame used in the previous example, the perturbation that rotates in the same direction becomes stationary, and the other rotates with twice the frequency Ω. In resonance, the intensity of the response at frequency Ω is strong, and we can neglect the 2Ω component, such that the evolution is approximately the evolution of the system pumped with a circularly polarized field. This is called the Rotating Wave Approximation. In Fig. 2.4 f), we see that the lower frequency of the linear solution corresponds to the frequency of the response of the system pumped with a circularly polarized field, in contrast to in Fig. 2.4 e).

To analyse the frequencies present in the time evolution of the occupation of level $|-1\rangle$, we compute the Fourier transform and represent in Fig. 2.5 and explicitly point out the

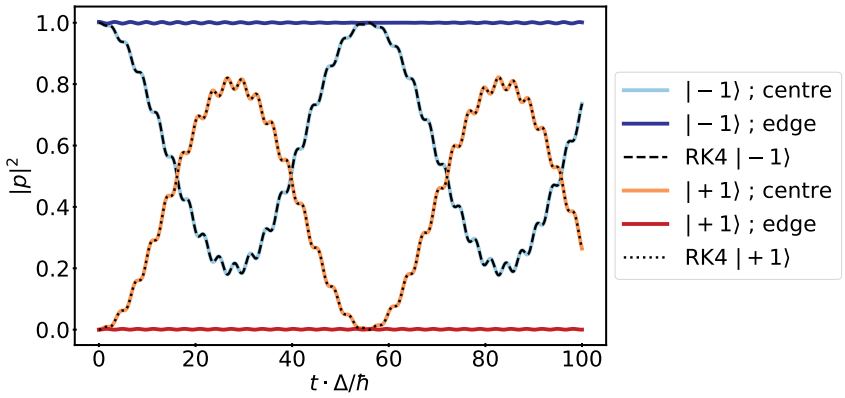

Figure 2.3.: Illustration of the truncation effect on the edge eigenvectors of the EFH through the time evolution of the level's population of the two-level system pumped with a linearly polarized field, with $eF/\Delta = 0.1$, $\hbar\Omega/\Delta = 0.95$, and $|\psi(0)\rangle = |-1\rangle$, comparing the result with Floquet formalism (coloured solid lines) with RK4 (black dashed lines).

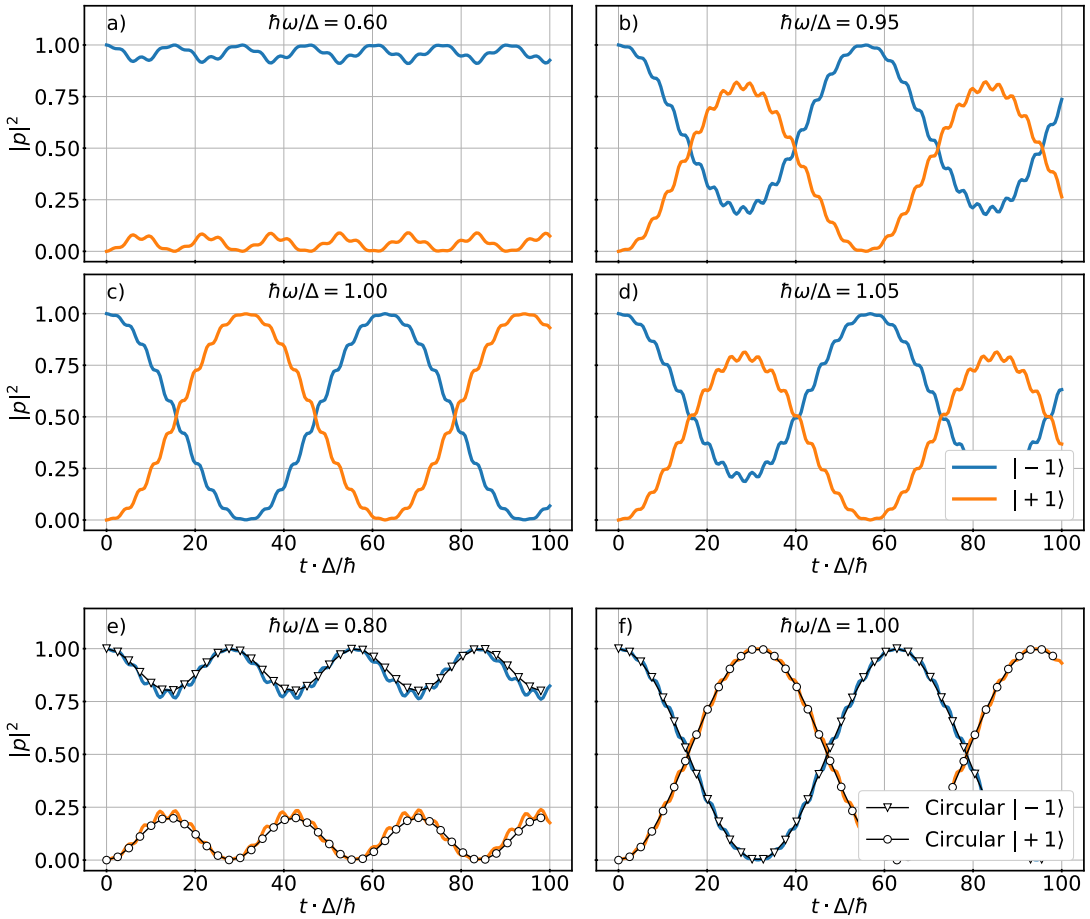

Figure 2.4.: Representation of the time evolution with Extended Floquet Hamiltonian formalism ($M = 12$) of the levels' populations, $|p|^2$, of the two-level system with Hamiltonian from Eq.(2.45), with $eF/\Delta = 0.1$, and $|\psi(0)\rangle = |-1\rangle$(from a) to d)). The calculation was performed with Extended Floquet Hamiltonian formalism with truncation $M = 12$. Comparison of the time evolution of the levels' populations, $|p|^2$, of the two-level system pumped with a circularly polarized field and the system pumped with a linearly polarized field (plots e) and f)).

frequencies related to the Floquet gap Δ_F, defined similarly to the previous example as the difference between the two Floquet quasienergies. From this analysis, we can see that only appear frequencies that are $\pm\Delta_F/\hbar$ modulo Ω and multiples of the external frequency Ω. This agrees with the result of Eqs. (2.40) and (2.41) that show that the components of the system's state are linear combinations of complex exponentials with frequency $(\epsilon_n - \epsilon_m)/\hbar - (p-s)\,\Omega$:

$$|\langle -1|\psi(t)\rangle|^2 = \frac{1}{T^2}\sum_{\substack{n,m\\p,q\\r,s}}\sum_{\sigma,\sigma'}\langle\psi(0)|\sigma'\rangle\, a^{(m)}_{\sigma' r}\, a^{(m)*}_{-1s}\, a^{(n)}_{-1p}\, a^{(n)*}_{\sigma q}\,\langle\sigma|\psi(0)\rangle\, e^{-i[(\epsilon_n-\epsilon_m)/\hbar-(p-s)\Omega]t}. \quad (2.69)$$

When $n = m$ the frequency that appears is a multiple of the external frequency, but when $m \neq n$ the frequency is $\pm\Delta_F/\hbar$ modulo Ω.

These two examples were useful for gaining intuition on applying the Floquet formalism in calculating the optical response of the 1D two-band semiconductor that we will do in Chapters 3 and 4. As explained before, the main problem can be described in velocity gauge, and using the Bloch vectors basis, the operators are diagonal in k by blocks. These blocks are two dimensional from the two-band of the semiconductor. This means that for each vector k, the problem is the evolution of a two-level system pumped with a time periodic electromagnetic field. The solution will be addressed in the same way we did for this second example, and we expect that the optical response will have frequencies related to the Floquet gap and the integer multiples of the frequency of the field. An important aspect of applying the Floquet formalism is the need to choose an initial time, Eqs. (2.18) and (2.40). By doing this, we are fixing the system to that state regardless of the history of the system, as we did in these two examples, fixing the systems at $|-1\rangle$ at $t = 0$. This is equivalent to switching the perturbation suddenly.

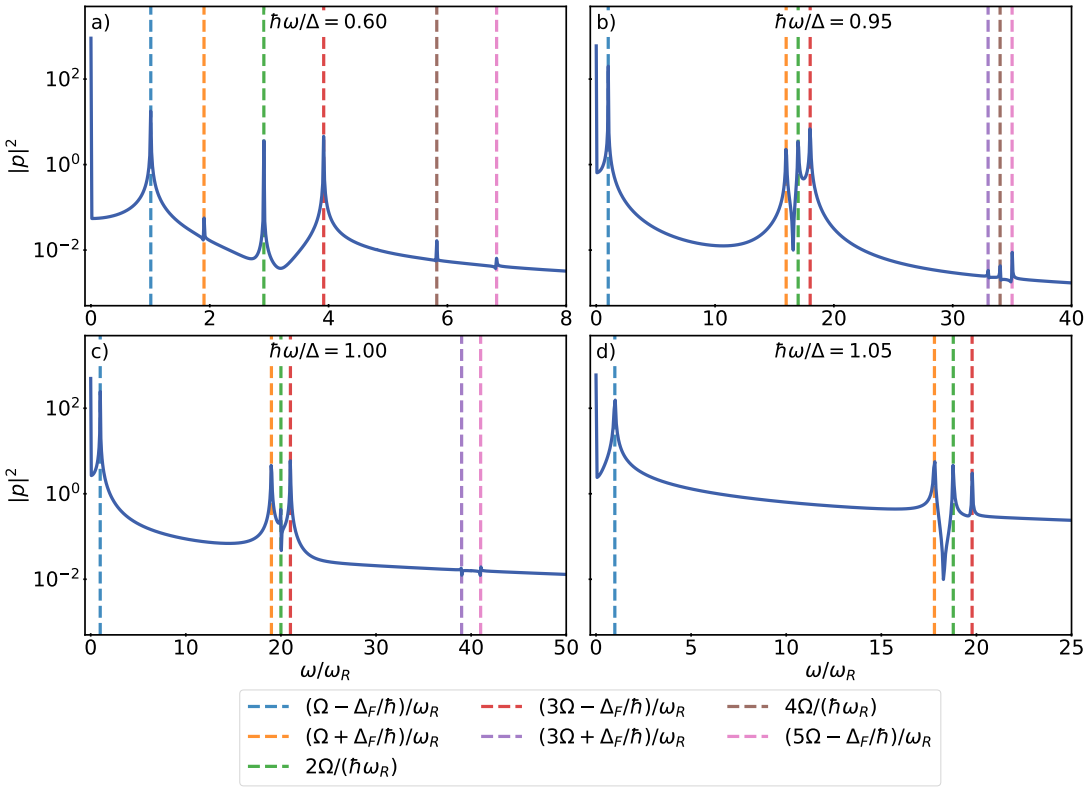

Figure 2.5.: Discrete Fourier transform of initial state's occupation of the two-level system pumped with a linearly polarized field, $|\langle -1|\psi(t)\rangle|^2$, represented as a function of the ratio between the response frequency and the Rabi frequency.

3. Optical response of a 1D two-band semiconductor

This work aims to study the utility of the Floquet Formalism to compute the nonlinear optical response of a crystal system under a periodic electromagnetic perturbation beyond the range of validity of perturbation theory. In this chapter, we begin to study the optical response of the 1D two-band semiconductor at zero temperature under a periodic electromagnetic perturbation. First, in Section 3.1, we introduce the model and the time evolution equations. Then, in Section 3.2, we compute the first order current in perturbation theory, closely following the notes [34]. In the end, we construct the EFH for this problem following the reasoning of the Chapter 2 to perform the time evolution of the system using the Floquet formalism and to obtain the response of the system to the perturbation by computing the current in time and frequency space, Section 3.3.

3.1. Introduction to the model

In this work, we consider a 1D lattice structure with periodic boundary conditions where each unit cell contains two different orbitals, in other words, a linear chain of alternating A and B orbitals, with respective on-site energies $\Delta/2$ and $-\Delta/2$, within each unit cell, Fig. 3.1.

We consider the crystal to be described by the tight binding model, i.e. the electrons are tightly bound to the respective orbital. In this model, only transitions between the nearest neighbour orbitals are allowed, with the intercell and the intracell hopping having the same real value. Therefore, the tight binding Hamiltonian that describes the system in equilibrium is given by:

$$\begin{aligned}\hat{H}_0 = &\sum_n \frac{\Delta}{2}\Big(|n,A\rangle\langle n,A| - |n,B\rangle\langle n,B|\Big) \\ &- t_h \sum_n \Big(|n,B\rangle\langle n,A| + |n-1,B\rangle\langle n,A| + h.c.\Big).\end{aligned} \tag{3.1}$$

Here $|n,A\rangle$ is the single particle state in the position basis for the A orbital in the n-th unit cell, while $|n,B\rangle$ is the corresponding states for the B orbital. The parameter Δ represents the energy gap between the two orbitals and t_h denotes the hopping amplitude between the two orbitals so that t_h^2 is the transition probability. The numerical results that follow will be shown in natural units ($e = \hbar = 1$) and with t_h as energy and a as length units.

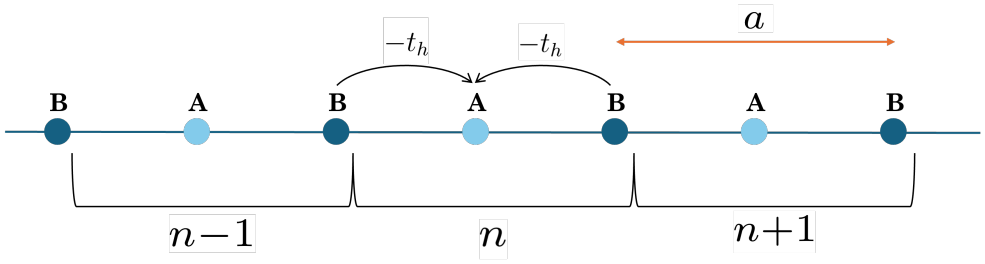

Figure 3.1.: Scheme of a 1D lattice with two orbitals A and B. The index n is the numbering of the unit cells, t_h is the hopping between nearest orbitals and a is the lattice parameter.

Since we aim to study the application of Floquet's formalism to calculating the optical response of a material, in this case, a crystal, we have to respect certain requirements of the formalism. The most important is that the problem must be periodic in time. This means that the field with which we perturb the system has to be periodic along the time interval in which we calculate the evolution of the system; in other words, it cannot be switched adiabatically, nor can it have damping. The other requirement we find in Chapter 2 is that we have to choose an initial state to calculate the time evolution, which is equivalent to imposing that the field is suddenly switched on at that moment.

So, as proof of concept, we chose to study the optical response of the AB chain under the perturbation of a monochromatic and uniform electromagnetic field suddenly switched on at the initial time $t = 0$. The assumption is that the system is at 0 temperature before applying the field, i.e. the system evolves from a full valence band.

As discussed in Chapter 1, when the problem is described in the velocity gauge, the Hamiltonian, the DM and other operators are block-diagonal in the Bloch basis. This simplifies the solution of the time evolution once the time evolution equations for the DM are independent for each k. For this specific problem, those equations are two dimensional (2D) due to the two orbitals in each unit cell. For these reasons, we studied the nonlinear optical response introducing the electromagnetic field using a vector potential (velocity gauge) defined by

$$A(t) = A_0 \sin(\Omega t)\,. \tag{3.2}$$

We introduce the perturbation in the system via the Peierls substitution, which consists of adding a phase to the bond between orbitals in the lattice as

$$t_{ij} \to t_{ij} e^{-i(e/\hbar)\int_{\vec{\mathbf{R}}_j}^{\vec{\mathbf{R}}_i} d\vec{\mathbf{r}}\cdot\vec{\mathbf{A}}(\vec{\mathbf{r}},t)}$$

where t_{ij} is the hopping between positions $\vec{\mathbf{R}}_j$ and $\vec{\mathbf{R}}_i$. This integral is calculated with the minimum path between $\vec{\mathbf{R}}_j$ and $\vec{\mathbf{R}}_i$, and in this problem since we only work in one dimension and uniform electric field

$$\vec{\mathbf{R}}_i \to x_i, \tag{3.3}$$

$$\vec{\mathbf{A}}(\vec{\mathbf{r}},t) \to A(t), \tag{3.4}$$

the new hopping takes the form

$$t_{ij}e^{-i(e/\hbar)\Delta x\, A(t)}, \qquad \Delta x A(t) = \int_{x_j}^{x_i} dx A(t). \tag{3.5}$$

So, to apply the electromagnetic field in the 1D semiconductor, we have to define the positions of the orbitals in the unit cell.

3.1.1. Two descriptions of the 1D two-band chain

There are two possibilities to define the positions x_i, represented in Fig. 3.2. The first one, Fig. 3.2a, where the two orbitals take two different positions in the unit cell, and other case, Fig. 3.2b, where the two orbitals are in the same positions in each unit cell.

In the first possibility, the position operator is defined as

$$\hat{r}^{(I)} = \sum_n \Big((na + r_A) \left|n, A\right\rangle \left\langle n, A\right| + (na + r_B) \left|n, B\right\rangle \left\langle n, B\right| \Big) \tag{3.6}$$

where a is the lattice parameter, and r_A and r_B are the positions of each orbital in the unit cell. To simplify the calculation, we defined $r_A = 0$ and $r_B = a/2$. With this definition, the perturbed Hamiltonian is

$$\begin{aligned} \hat{H}^{(I)}(t) = &\sum_n \frac{\Delta}{2} \Big(\left|n, A\right\rangle \left\langle n, A\right| - \left|n, B\right\rangle \left\langle n, B\right| \Big) \\ &- t_h \sum_n \Big(e^{-i\delta(t)} \left|n, B\right\rangle \left\langle n, A\right| + e^{i\delta(t)} \left|n-1, B\right\rangle \left\langle n, A\right| + h.c. \Big) \end{aligned} \tag{3.7}$$

where

$$\delta(t) = \frac{e}{\hbar}\frac{a}{2} A(t), \tag{3.8}$$

is the Peierls phase, and the DM evolves as

$$i\hbar \frac{\partial \hat{\rho}^{(I)}(t)}{\partial t} = \left[\hat{H}^{(I)}(t), \hat{\rho}^{(I)}(t) \right]. \tag{3.9}$$

The other choice corresponds to the following position operator

$$\hat{r}^{(II)} = \sum_n \Big(na \left|n, A\right\rangle \left\langle n, A\right| + na \left|n, B\right\rangle \left\langle n, B\right| \Big), \tag{3.10}$$

which leads to the following Hamiltonian

$$\begin{aligned} \hat{H}^{(II)}(t) = &\sum_n \frac{\Delta}{2} \Big(\left|n, A\right\rangle \left\langle n, A\right| - \left|n, B\right\rangle \left\langle n, B\right| \Big) \\ &- t_h \sum_n \Big(\left|n, B\right\rangle \left\langle n, A\right| + e^{i2\delta(t)} \left|n-1, B\right\rangle \left\langle n, A\right| + h.c. \Big) \end{aligned} \tag{3.11}$$

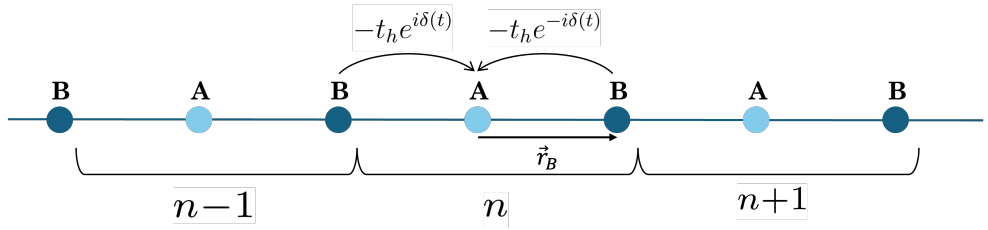

(a) Scheme of the AB chain where the two orbitals are in two different and equidistant positions in the same unit cell: the orbital A is in the centre of the unit cell, $r_A = 0$, and the orbital B is on the right edge, $r_B = a/2$.

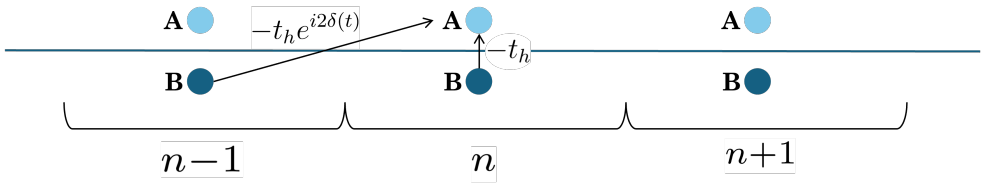

(b) Scheme of the AB chain where the two orbitals are in the same position in each unit cell.

Figure 3.2.: Scheme of the chain of the two orbitals A and B with two different descriptions for the position of each orbital in a unit cell. The index n is the numbering of the unit cells, t_h is the hopping of the unperturbed system and $\delta(t)$ is the Peierls phase.

and the evolution of the DM is

$$i\hbar\frac{\partial\hat{\rho}^{(II)}(t)}{\partial t} = \left[\hat{H}^{(II)}(t), \hat{\rho}^{(II)}(t)\right]. \tag{3.12}$$

There is a unitary transformation that transforms $\hat{H}^{(a)}(t)$ into $\hat{H}^{(b)}(t)$ that is written as:

$$\hat{H}^{(II)}(t) = \hat{U}(t)\hat{H}^{(II)}(t)\hat{U}^{\dagger}(t)\,, \qquad \hat{U}(t) = \sum_n \left(|n,A\rangle\langle n,A| + e^{i\delta(t)}|n,B\rangle\langle n,B|\right). \tag{3.13}$$

As the transformation is time-dependent, the evolution of the two systems is not equivalent to that described in Eqs. (3.9) and (3.12). If we start from the time evolution equation of the system (I), Eq. (3.9), and write the transformed equation, we will see that the time evolution of the transformed DM:

$$\hat{\tilde{\rho}}(t) = \hat{U}(t)\hat{\rho}^{(I)}(t)\hat{U}^{\dagger}(t), \tag{3.14}$$

is not the same as the evolution of $\hat{\rho}^{(II)}(t)$. Inverting unitary transformation and rewriting the DM operator $\hat{\rho}^{(I)}(t)$ in terms of $\hat{\tilde{\rho}}(t)$, the evolution equation (3.9) takes the form:

$$i\hbar\frac{\partial\left(\hat{U}(t)\hat{\tilde{\rho}}(t)\hat{U}^{\dagger}(t)\right)}{\partial t} = \left[\hat{H}^{(I)}(t), \hat{U}(t)\hat{\tilde{\rho}}(t)\hat{U}^{\dagger}(t)\right]. \tag{3.15}$$

Expanding the derivative of the product and multiplying with $\hat{U}^{\dagger}(t)$ on the left and $\hat{U}(t)$ on the right, the evolution equation can be written as:

$$i\hbar\left(\hat{U}^{\dagger}(t)\frac{\partial\hat{U}(t)}{\partial t}\hat{\tilde{\rho}}(t) + \frac{\partial\hat{\tilde{\rho}}(t)}{\partial t} + \hat{\tilde{\rho}}(t)\frac{\partial\hat{U}^{\dagger}(t)}{\partial t}\hat{U}(t)\right) = \left[\hat{H}^{(II)}(t), \hat{\tilde{\rho}}(t)\right]. \tag{3.16}$$

If, at this point, we use the following equality

$$\hat{U}^\dagger(t)\partial_t\hat{U}(t) = -\left(\partial_t\hat{U}^\dagger(t)\right)\hat{U}(t), \tag{3.17}$$

consequence of the unitarity of the transformation, $\hat{U}^\dagger(t)\hat{U}(t) = \hat{\mathbb{1}}$, the evolution equation becomes

$$i\hbar\frac{\partial\hat{\tilde{\rho}}(t)}{\partial t} = \left[\hat{H}^{(II)}(t) - \hat{U}^\dagger(t)\frac{\partial\hat{U}(t)}{\partial t}, \hat{\tilde{\rho}}(t)\right]. \tag{3.18}$$

With this equation, the DM $\hat{\tilde{\rho}}(t)$ describes a systems equivalent to $\hat{\rho}^{(I)}$. This means that for the two systems to be equivalent, we needed to do the correction

$$-\hat{U}^\dagger(t)\frac{\partial\hat{U}(t)}{\partial t} \tag{3.19}$$

in the Hamiltonian $\hat{H}^{(II)}(t)$.

Beyond the differences in dynamics, there is an important contrast between the two descriptions. The first one, Fig. 3.2a, has inversion symmetry, while the second description, Fig. 3.2b, does not.

Regarding the description (I), if we apply the inversion transformation $\hat{P}$ (see Appendix A for explicit calculation), the Hamiltonian of the system becomes:

$$\begin{aligned}\hat{P}\hat{H}^{(I)}(t)\hat{P}^\dagger = &\sum_n \frac{\Delta}{2}\Big(|n,A\rangle\langle n,A| - |n,B\rangle\langle n,B|\Big)\\ &- t_h\sum_n\Big(e^{-i\delta(t)}|n-1,B\rangle\langle n,A| + e^{i\delta(t)}|n,B\rangle\langle n,A| + h.c.\Big)\end{aligned} \tag{3.20}$$

The scheme of the transformed system is represented in Fig. 3.3 where it is possible to see that by changing the direction of the field in the Hamiltonian, i.e. changing the direction of the purple and green arrows, the system remains unchanged. This means that (Appendix A):

$$\hat{P}\hat{H}^{(I)}(A)\hat{P}^\dagger = \hat{H}^{(I)}(-A) \tag{3.21}$$

and we can conclude that the system described by (I) has inversion symmetry.

For description (II), this is not the case. Applying the inversion transformation $\hat{P}$ (see Appendix A for explicit calculation), the system is described as

$$\begin{aligned}\hat{P}\hat{H}^{(II)}(t)\hat{P}^\dagger = &\sum_n \frac{\Delta}{2}\Big(|n,A\rangle\langle n,A| - |n,B\rangle\langle n,B|\Big)\\ &- t_h\sum_n\Big(|n,B\rangle\langle n,A| + e^{i2\delta(t)}|n+1,B\rangle\langle n,A| + h.c.\Big)\end{aligned} \tag{3.22}$$

It is clear from the representation of the transformation in Fig. 3.4 that if we change the direction of vector potential, i.e. changing the direction of the purple arrows, the system is not the same:

$$\hat{P}\hat{H}^{(II)}(A)\hat{P}^\dagger \neq \hat{H}^{(II)}(-A) \tag{3.23}$$

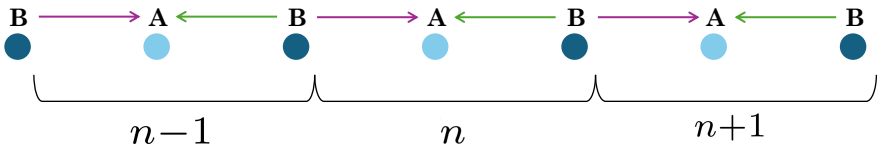

(a) 1D two-band chain with the orbitals A and B in different positions in the unit cell without the inversion transformation.

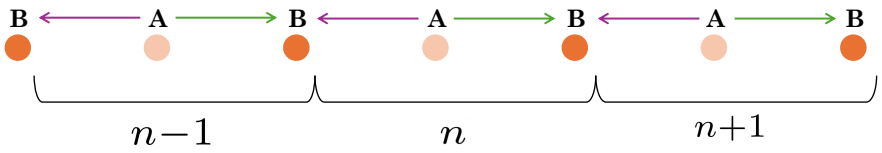

(b) 1D two-band chain with the orbitals A and B in different positions in the unit cell after the application inversion transformation around the centre of n-th cell.

Figure 3.3.: Scheme of the application of the inversion transformation in the 1D two-band chain with the orbitals A and B in different positions. The green arrows represent the hopping between two orbitals in the same unit cell, and the purple arrows represent the hopping between two orbitals in different unit cells. The hopping in the scheme corresponds to the transitions from orbitals B to A.

The original lattice has a hopping between the less energetic orbital and the more energetic orbital inside the unit cell and between the cells n and $n+1$. As a result of the transformation, the same hopping is observed between two orbitals in the same unit cell and between the cells n and $n-1$. This shows that the system described in this way does not have inversion symmetry, which means we expect that the optical response of the system (II) has even order harmonic generation (Appendix A), in contrast to the system (I).

3.1.2. Bloch's basis and current operator

As mentioned before, the Hamiltonian written in velocity gauge is block-diagonal in k-basis; Considering that the system has periodic boundary conditions we use the Bloch's theorem

$$|n, A\rangle = \frac{1}{\sqrt{N}} \sum_k e^{-ikna} |k, A\rangle \,, \tag{3.24}$$

$$|n, B\rangle = \frac{1}{\sqrt{N}} \sum_k e^{-ikna} |k, B\rangle \,, \tag{3.25}$$

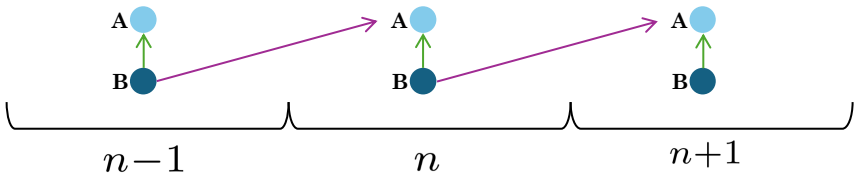

(a) Two 2D bands chain with the orbitals A and B in the same position in the unit cell without the inversion transformation.

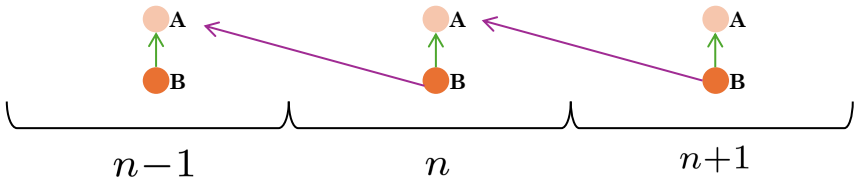

(b) Two 1D bands chain with the orbitals A and B in the same position in the unit cell after the application inversion transformation around the centre of n-th cell.

Figure 3.4.: Scheme of the application of the inversion transformation in the two 1D bands chain with the orbitals A and B in the same position in the unit cell. The green arrows represent the hopping between two orbitals in the same unit cell, and the purple arrows represent the hopping between two orbitals in different unit cells. The hopping in the scheme corresponds to the transitions from orbitals B to A.

where $k = 2\pi/(Na)\, k_{int}$, with Na the length of the system and $k_{int} \in \mathbb{Z}$, and substituting this in the previous Hamiltonians (Eqs. (3.7) and (3.11)), we obtain

$$\begin{aligned}\hat{\mathcal{H}}^{(I)}(t) = &\sum_k \left\{ \frac{\Delta}{2}\Big(|k,A\rangle \langle k,A| - |k,B\rangle \langle k,B| \Big) \right. \\ &\left. - t_h \left[\Big(e^{-i\delta(t)} + e^{i(ka+\delta(t))} \Big) |k,B\rangle \langle k,A| + h.c \right] \right\},\end{aligned} \tag{3.26}$$

and

$$\begin{aligned}\hat{\mathcal{H}}^{(II)}(t) = &\sum_k \left\{ \frac{\Delta}{2}\Big(|k,A\rangle \langle k,A| - |k,B\rangle \langle k,B| \Big) \right. \\ &\left. - t_h \left[\Big(1 + e^{i(ka+2\delta(t))} \Big) |k,B\rangle \langle k,A| + h.c \right] \right\}.\end{aligned} \tag{3.27}$$

As expected, the Hamiltonians are block-diagonal in k, i.e. the terms of the sum in k are independent from each other. We will focus on each term independently, $\hat{\mathcal{H}}^{(I)}(k,t)$ and $\hat{\mathcal{H}}^{(II)}(k,t)$. Factoring out the complex exponentials $\exp(ika/2)$ and $\exp(ika/2 + i\delta(t))$ in the previous equations, respectively, we obtain

$$\begin{aligned}\hat{\mathcal{H}}^{(I)}(k,t) = &\frac{\Delta}{2}\Big(|k,A\rangle \langle k,A| - |k,B\rangle \langle k,B| \Big) \\ &- 2t_h \cos\left(\frac{k(t)a}{2} \right) \left[e^{ika/2} |k,B\rangle \langle k,A| + h.c \right],\end{aligned} \tag{3.28}$$

and

$$\hat{\mathcal{H}}^{(II)}(k,t) = \frac{\Delta}{2}\Big(|k,A\rangle\langle k,A| - |k,B\rangle\langle k,B|\Big) - 2t_h\cos\left(\frac{k(t)a}{2}\right)\left[e^{ik(t)a/2}|k,B\rangle\langle k,A| + h.c\right], \tag{3.29}$$

with $k(t) = k + 2\delta(t)/a$.

These two operators can be represented by matrix notation

$$\hat{\mathcal{H}}^{(1)}(k,t) = \frac{\Delta}{2}\hat{\sigma}^z - 2t_h\cos\left(\frac{k(t)a}{2}\right)\hat{\sigma}^1\left(\frac{ka}{2}\right), \tag{3.30}$$

$$\hat{\mathcal{H}}^{(2)}(k,t) = \frac{\Delta}{2}\hat{\sigma}^z - 2t_h\cos\left(\frac{k(t)a}{2}\right)\hat{\sigma}^1\left(\frac{k(t)a}{2}\right), \tag{3.31}$$

where

$$\hat{\sigma}^1(k) = \cos(k)\,\hat{\sigma}^x + \sin(k)\,\hat{\sigma}^y, \tag{3.32}$$

and σ_x and σ_y are the usual Pauli matrices [39].

Without perturbation, $A_0 = 0$, both Hamiltonian are equal and the energy bands are represented in Fig. 3.5. As can be seen, this model exhibits a gap of value Δ.

Recalling to the Chapter 1, in velocity gauge, the current operator is given by

$$\hat{\mathcal{J}}(t) = -\frac{1}{L}\frac{\partial\hat{\mathcal{H}}(t)}{\partial A(t)}, \qquad L = Na. \tag{3.33}$$

For the present problem, we have

$$\hat{\mathcal{J}}^{(I)}(t) = -\frac{et_h}{\hbar N}\sum_k \sin\left(\frac{k(t)a}{2}\right)\sigma^1\left(\frac{ka}{2}\right), \tag{3.34}$$

and

$$\hat{\mathcal{J}}^{(II)}(t) = -\frac{et_h}{\hbar N}\sum_k\left[\sin\left(\frac{k(t)a}{2}\right)\sigma^1\left(\frac{k(t)a}{2}\right) - \cos\left(\frac{k(t)a}{2}\right)\sigma^2\left(\frac{k(t)a}{2}\right)\right], \tag{3.35}$$

where

$$\hat{\sigma}^2(k) = \frac{\partial\sigma^1(k)}{\partial k} = -\sin(k)\,\hat{\sigma}^x + \cos(k)\,\hat{\sigma}^y. \tag{3.36}$$

Note that the second current can also be written as

$$\hat{\mathcal{J}}^{(II)}(t) = -\frac{1}{L}\frac{e}{\hbar}\frac{\partial\hat{\mathcal{H}}^{(II)}(t)}{\partial k}. \tag{3.37}$$

In the following section, we will compute the first order current of the semiconductor described by (II) under the monochromatic electromagnetic field. We choose the second description because of the lack of inversion symmetry, which will allows to see second order effects.

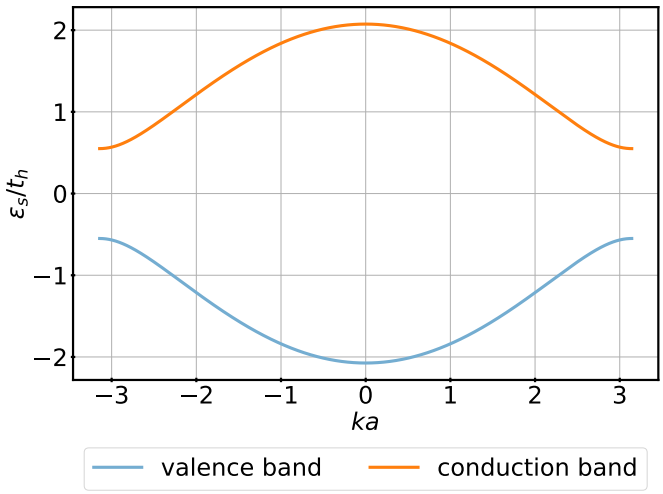

Figure 3.5.: Illustration of the energy bands of the unperturbed 1D lattice with two orbitals in each unit cell setting the parameters as $\Delta/t_h = 1.1$.

3.2. Solution in first order in perturbation theory

The calculations done in this section are based on reference [40]. To simplify the calculations, we will use the fact that all operators are block-diagonal in k and write them as a sum over k of auxiliary operators, as we did for the Hamiltonian in the previous section. The current operator[1] is

$$\hat{\mathcal{J}}(t) = \frac{1}{N}\sum_k \hat{j}(k,t), \tag{3.38}$$

where

$$\begin{aligned}\hat{j}(k,t) = -\frac{et_h}{\hbar}\Bigg[&\sin\left(\frac{k(t)a}{2}\right)\sigma^1\left(\frac{k(t)a}{2}\right)\\ &-\cos\left(\frac{k(t)a}{2}\right)\sigma^2\left(\frac{k(t)a}{2}\right)\Bigg].\end{aligned} \tag{3.39}$$

The same thinking is applied to the DM

$$\hat{\rho}(t) = \sum_k \hat{\rho}(k,t), \tag{3.40}$$

where the operator $\hat{\rho}(k,t)$ obeys

$$\mathrm{i}\hbar\partial_t\hat{\rho}(k,t) = \left[\hat{\mathcal{H}}(k,t), \hat{\rho}(k,t)\right], \tag{3.41}$$

in which $\hat{\mathcal{H}}(k,t)$ is given by Eq. (3.31). Note that these auxiliary operators are 2D, resulting from the system's number of bands (internal degrees of freedom).

[1] In what follows, we will refer the quantities relative to the system (II) without the superior index, for example $\hat{\mathcal{O}}^{(II)} \equiv \hat{\mathcal{O}}$.

As seen in Chapter 1, the current of any system can be defined as a function of the velocity operator

$$\hat{\mathcal{J}}(t) = e\hat{v}(t), \tag{3.42}$$

and the velocity operator can also be written as

$$\hat{v}(t) = \sum_k \hat{v}(k,t), \tag{3.43}$$

with

$$\begin{aligned}\hat{v}(k,t) = -\frac{t_h}{\hbar}\Bigg[&\sin\left(\frac{k(t)a}{2}\right)\sigma^1\left(\frac{k(t)a}{2}\right)\\ &-\cos\left(\frac{k(t)a}{2}\right)\sigma^2\left(\frac{k(t)a}{2}\right)\Bigg].\end{aligned} \tag{3.44}$$

With this in mind, the average value of the current is given by

$$\left\langle\hat{\mathcal{J}}(t)\right\rangle = \frac{1}{N}\sum_k\left\langle\hat{j}(k,t)\right\rangle, \tag{3.45}$$

$$= \frac{e}{N}\sum_k \mathrm{Tr}\left[\hat{v}(k,t)\hat{\rho}(k,t)\right]. \tag{3.46}$$

To find the linear order response in $A(t)$ we expand the velocity in the first order

$$\begin{aligned}\hat{v}(k,t) &= \hat{v}(k,t)\Big|_{A_0=0} + \frac{\delta\hat{v}}{\delta A(t)}\Big|_{A_0=0}A(t) + \mathcal{O}\left(A^2(t)\right)\\ &= \hat{v}(k) + \frac{e}{\hbar}\frac{\partial\hat{v}(k)}{\partial k}A(t) + \mathcal{O}\left(A^2(t)\right),\end{aligned} \tag{3.47}$$

as well as the density matrix

$$\hat{\rho}(k,t) = \hat{\rho}^{(0)}(k) + \hat{\rho}^{(1)}(k,t) + \mathcal{O}\left(A^2(t)\right). \tag{3.48}$$

We fixed the initial conditions ($t_0 = 0$) as

$$\rho_{ss'}(k,0) = \rho^{(0)}_{ss'}(k) = \delta_{ss'}f_{ks} \tag{3.49}$$

written in the unperturbed Hamiltonian eigenbasis

$$\hat{\mathcal{H}}_0(k) = \sum_{s,s'}\delta_{ss'}\epsilon_s(k)\left|k,s\right\rangle\left\langle k,s'\right|, \tag{3.50}$$

where $s, s' = \{c, v\}$ are the conduction and valence bands, respectively, and where f_{ks} is the Fermi-Dirac distribution:

$$f_{ks} = \frac{1}{e^{(\epsilon_s(k)-\mu)/k_BT}+1}, \tag{3.51}$$

with μ the chemical potential, k_B the Boltzmann constant and T the temperature.

So, we get the following expression for the expected value of the operator $\hat{j}(k,t)$

$$\begin{aligned}\left\langle \hat{j}(k,t) \right\rangle = &- e\mathrm{Tr}\left[\hat{v}(k)\hat{\rho}^{(0)}(k)\right] - \frac{e^2}{\hbar}\mathrm{Tr}\left[\frac{\partial \hat{v}(k)}{\partial k}\hat{\rho}^{(0)}(k)\right] A(t) \\ &- e\mathrm{Tr}\left[\hat{v}(k)\hat{\rho}^{(1)}(k,t)\right],\end{aligned} \tag{3.52}$$

where the first term is the zero order, the second term is the diamagnetic term, $\hat{j}_d(k,t)$, and the last term is the paramagnetic term, $\hat{j}_p(k,t)$. The first two terms are equal to the semiclassical approximation (Appendix (B)), so they are related to the intraband dynamics. At the same time the paramagnetic component is the response resulting from the interband virtual transitions, as we will show in the following calculations.

To compute the current, we first start by computing the first order of the density matrix, $\hat{\rho}^{(1)}(k,t)$. We expand the Hamiltonian

$$\begin{aligned}\hat{\mathcal{H}}(k,t) &= \hat{\mathcal{H}}_0(k) + \left.\frac{\partial \hat{\mathcal{H}}}{\partial A(t)}\right|_{A=0} A(t) + \mathcal{O}\left(A^2(t)\right) \\ &= \hat{\mathcal{H}}_0(k) + e\hat{v}(k)A(t) + \mathcal{O}\left(A^2(t)\right).\end{aligned} \tag{3.53}$$

Retaining the first order terms in the Liouville equation, we get

$$i\hbar\partial_t \hat{\rho}^{(1)}(k,t) = \left[\hat{\mathcal{H}}_0(k,t), \hat{\rho}^{(1)}(k,t)\right] + e\left[\hat{v}(k), \hat{\rho}^{(0)}(k)\right] A(t). \tag{3.54}$$

Because $\hat{\mathcal{H}}_0(k,t)$ and $\hat{\rho}^{(0)}(k)$ are diagonal, the commutators in the Eq. (3.54) are given by

$$\left[\hat{\mathcal{H}}_0(k,t), \hat{\rho}^{(1)}(k,t)\right] = \Delta_{ss'}(k)\rho^{(1)}_{ss'}(k,t), \tag{3.55}$$

where

$$\Delta_{ss'}(k) = \epsilon_s(k) - \epsilon_{s'}(k) \tag{3.56}$$

is the difference between the valence and conduction bands at each point k and

$$\left[\hat{v}(k), \hat{\rho}^{(0)}(k)\right] = \left(f_{ks} - f_{ks'}\right) v_{ss'}(k), \tag{3.57}$$

which results in

$$\left[i\hbar\partial_t - \Delta_{ss'}(k)\right] \rho^{(1)}_{ss'}(k,t) = e v_{ss'}(k)\left(f_{ks} - f_{ks'}\right) A(t). \tag{3.58}$$

Defining a new operator $\tilde{\hat{\rho}}(k,t)$ as

$$\rho^{(1)}_{ss'}(k,t) = e^{-\mathrm{i}\Delta_{ss'}t/\hbar}\tilde{\rho}_{ss'}(k,t), \tag{3.59}$$

the Eq. (3.58) takes the form

$$[i\hbar\partial_t - \Delta_{ss'}(k)]\, e^{-\mathrm{i}\Delta_{ss'}t/\hbar}\tilde{\rho}_{ss'}(k,t) = ev_{ss'}(k)\,(f_{ks} - f_{ks'})\,A(t). \tag{3.60}$$

By expanding the temporal derivative and simplifying the equation, the terms with $\tilde{\rho}_{ss'}(k,t)$ cancel, and it reduces to an equation whose solution is

$$\tilde{\rho}(k,t) = -i\frac{e}{\hbar}v_{ss'}(k)\,(f_{ks} - f_{ks'})\int_0^t dt' e^{\mathrm{i}\Delta_{ss'}t'/\hbar}A(t'). \tag{3.61}$$

The solution to the first order contribution to the DM is, therefore

$$\rho^{(1)}_{ss'}(k,t) = -\mathrm{i}\frac{e}{\hbar}v_{ss'}(k)\,(f_{ks} - f_{ks'})\int_0^t dt' e^{-\mathrm{i}\Delta_{ss'}(t-t')/\hbar}A(t'). \tag{3.62}$$

In this problem, the field that perturbs the semiconductor is a monochromatic field described by $A(t) = A_0 \sin(\Omega t)$. If we look closer at the integral

$$G(\Delta_{ss'},t) = i\int_0^t dt' e^{-\mathrm{i}\Delta_{ss'}(t-t')/\hbar}\sin(\Omega t'), \tag{3.63}$$

we can expand the $\sin(\Omega t')$ with complex exponentials and solve the integral, obtaining the solution

$$G(\Delta_{ss'},t) = \frac{1}{2i}\left(\frac{e^{\mathrm{i}\Omega t}}{\Delta_{ss'}/\hbar + \Omega} - \frac{e^{-\mathrm{i}\Omega t}}{\Delta_{ss'}/\hbar - \Omega} + \frac{2\Omega e^{-\mathrm{i}\Delta_{ss'}t/\hbar}}{(\Delta_{ss'}/\hbar)^2 - \Omega^2}\right). \tag{3.64}$$

We can write the paramagnetic term as

$$-e\mathrm{Tr}\left[\hat{v}(k)\hat{\rho}^{(1)}(k,t)\right] = -e\sum_{s,s'} v_{ss'}(k)\rho^{(1)}_{s's}(k,t) \tag{3.65}$$

$$= \frac{e^2}{\hbar}A_0\sum_{s,s'} v_{ss'}(k)v_{s's}(k)\,(f_{ks'} - f_{ks})\,G(\Delta_{ss'},t). \tag{3.66}$$

The terms in the sum with $s = s'$ are null as the paramagnetic term only has contributions interband interactions, and because of that the sum can be rewritten as follows

$$-e\mathrm{Tr}\left[\hat{v}(k)\hat{\rho}^{(1)}(k,t)\right] = \frac{e^2}{\hbar}A_0 v_{vc}(k)v_{cv}(k)\,(f_{kc} - f_{kv})\,(G(\Delta_{cv},t) - G(\Delta_{vc},t)) \tag{3.67}$$

Now, simplifying the difference of the integrals using the relations between complex exponentials and trigonometric functions, we obtain

$$G(\Delta_{cv},t) - G(\Delta_{vc},t) = 2\frac{(\Delta_{cv}/\hbar\sin(\Omega t) - \Omega\sin(\Delta_{cv}t/\hbar))}{(\Delta_{cv}/\hbar)^2 - \Omega^2}, \tag{3.68}$$

and the paramagnetic component is written as

$$\begin{aligned}-e\mathrm{Tr}\left[\hat{v}(k)\hat{\rho}^{(1)}(k,t)\right] =& 2\frac{e^2}{\hbar}A_0 v_{vc}(k)v_{cv}(k)\left(f_{kc}-f_{kv}\right)\\ &\cdot\frac{\left(\Delta_{cv}/\hbar\sin\left(\Omega t\right)-\Omega\sin\left(\Delta_{cv}t/\hbar\right)\right)}{\left(\Delta_{cv}/\hbar\right)^2-\Omega^2}.\end{aligned} \tag{3.69}$$

The next step is to sum over the first Brillouin zone (FBZ) to obtain the total current. Observing the average value of the velocity operator, Fig. (3.6), with $A_0 = 0$ we see that it is periodic in k, so the sum over the FBZ of the zero order term is null.

So, the total current to first order in the electric field is written as

$$\begin{aligned}J(t) =& \frac{1}{N}\sum_k\left(-\frac{e^2}{\hbar}\mathrm{Tr}\left[\frac{\partial\hat{v}(k)}{\partial k}\hat{\rho}^{(0)}(k)\right]A(t)\right.\\ &\left.+2\frac{e^2}{\hbar}A_0 v_{vc}(k)v_{cv}(k)\left(f_{kc}-f_{kv}\right)\cdot\frac{\left(\Delta_{cv}/\hbar\sin\left(\Omega t\right)-\Omega\sin\left(\Delta_{cv}t/\hbar\right)\right)}{\left(\Delta_{cv}/\hbar\right)^2-\Omega^2}\right).\end{aligned} \tag{3.70}$$

In the limit of an infinite system ($L\to+\infty$), this sum turns into an integral. In the first two terms, the time dependency is only a $\sin(\Omega t)$ function:

$$\begin{aligned}J_\Omega(t) =& -A_0\frac{e^2}{\hbar}\frac{a}{2\pi}\int_{-\pi/a}^{\pi/a}dk\left(\mathrm{Tr}\left[\frac{\partial\hat{v}(k)}{\partial k}\hat{\rho}^{(0)}(k)\right]\right.\\ &\left.-2v_{vc}(k)v_{cv}(k)\left(f_{kc}-f_{kv}\right)\frac{\Delta_{cv}(k)/\hbar}{\left(\Delta_{cv}(k)/\hbar\right)^2-\Omega^2}\right)\cdot\sin\left(\Omega t\right)\end{aligned} \tag{3.71}$$

while the last term is a little more curious since it depends on the gap energy between the conductance and valence band at each point k of the FBZ.

$$\begin{aligned}J_\Delta(t) =& -A_0\frac{e^2}{\hbar}\frac{a}{2\pi}\int_{-\pi/a}^{\pi/a}dk\left(2\Omega v_{vc}(k)v_{cv}(k)\left(f_{kc}-f_{kv}\right)\right.\\ &\left.\cdot\frac{\Delta_{cv}(k)/\hbar}{\left(\Delta_{cv}(k)/\hbar\right)^2-\Omega^2}\sin\left(\Delta_{cv}(k)t/\hbar\right)\right).\end{aligned} \tag{3.72}$$

It depends on the gap energy between the conductance and valence band in each k. This integral can be estimated within the long time limit using the Stationary Phase Method. We can write this term as

$$J_\Delta(t) = A_0\frac{e^2}{\hbar}\frac{a}{2\pi}\Im\int_{-\pi/a}^{\pi/a}dk\, f(k)e^{i\Delta_{cv}(k)t/\hbar} \tag{3.73}$$

at long times after turning on the perturbation ($t\gg\hbar/\Delta_{cv}$), where $f(k)$ is

$$f(k) = 2\Omega v_{vc}(k)v_{cv}(k)\left(f_{kc}-f_{kv}\right)\frac{\Delta_{cv}(k)/\hbar}{\left(\Delta_{cv}(k)/\hbar\right)^2-\Omega^2}. \tag{3.74}$$

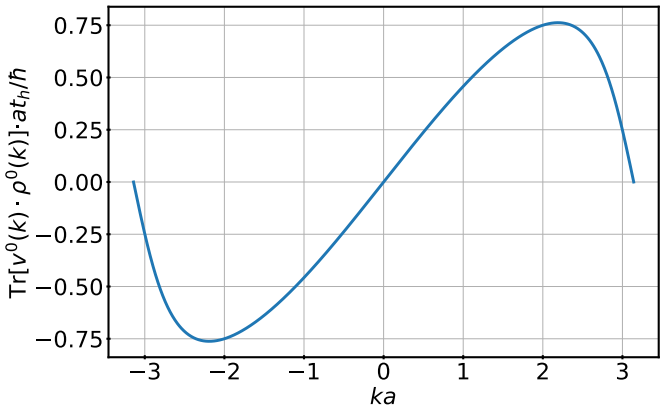

Figure 3.6.: Representation of the average value of the unperturbed velocity operator of the AB chain in equilibrium state, $\mathrm{Tr}\left[\hat{v}(k)\hat{\rho}^{(0)}(k)\right]$, setting $\Delta/t_h = 1.1$.

Since we are in the perturbative regime, meaning small perturbations and small responses, we only consider field frequencies below the gap $(\Delta_{cv}(k)/\hbar)^2 - \Omega^2 > 0$ and the current contribution from Eq. (3.72) does not diverge, such that the function $f(k)$ is a real function of the Bloch vector k and takes finite values.

In long time limit, there is a strong oscillation of the integrand, coming from the exponential, so we can use the Stationary Phase Method to solve this integral. This means that the value of the integral is dominated by the vicinity of the extrema of $\Delta_{cv}(k)$, because at these points the phase is stationary up to quadratic corrections

$$\Delta_{cv}(k) = \Delta_{cv}(k_0) + \frac{1}{2}\Delta''_{cv}(k_0)k^2 + \mathcal{O}\left(k^3\right), \tag{3.75}$$

with k_0 the extrema of the function $\Delta_{cv}(k)$ and $\Delta''_{cv}(k)$ the second derivative in order of k. Since $\Delta_{cv}(k)$ is the energy difference between the valence and the conduction bands, it will have a minimum at $ka = \pm\pi$ and a maximum at $k = 0$ (see Fig. 3.5). So if we rewrite the integral as

$$J_\Delta(t) \;=\; A_0\frac{e^2}{\hbar}\frac{a}{2\pi}\Im\int_{-\pi/(2a)}^{\pi/(2a)} dk\; f(k)e^{i\Delta_{cv}(k)t/\hbar} + \Im\int_{\pi/(2a)}^{3\pi/(2a)} dk\; f(k)e^{i\Delta_{cv}(k)t/\hbar}, \tag{3.76}$$

it is possible to approximate its value to

$$\begin{aligned} J_\Delta(t) \approx & A_0\frac{e^2}{\hbar}\frac{a}{2\pi}\left[\Im f(0)e^{i\Delta_{cv}(0)t/\hbar}\int_{-\infty}^{+\infty} dk\; e^{i\Delta''_{cv}(0)k^2t/\hbar}\right. \\ & \left. + \Im f\left(\frac{\pi}{a}\right)e^{i\Delta_{cv}(\pi/a)t/\hbar}\int_{-\infty}^{+\infty} dk\; e^{i\Delta''_{cv}(\pi/a)k^2t/\hbar}\right]. \end{aligned} \tag{3.77}$$

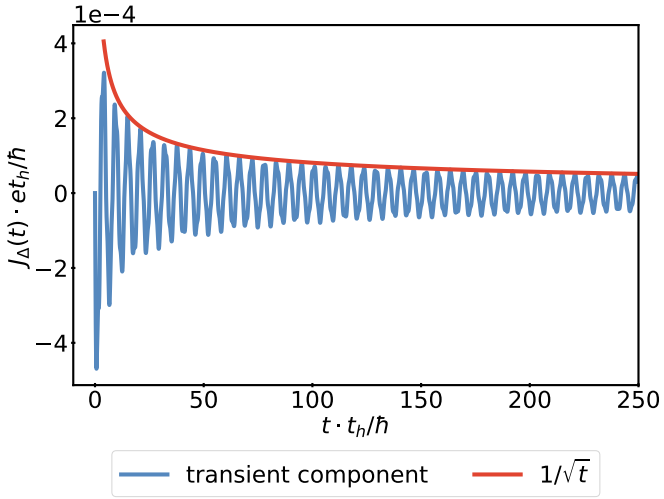

Figure 3.7.: Representation of the term $J_\Delta(t)$ with $\Delta/t_h = 1.1$ under a monochromatic electromagnetic field with frequency $\hbar\Omega/t_h = 0.2$ and the amplitude of vector potential equal to $e/\hbar \cdot aA_0 = 0.01$.

Now the problem is reduced to the calculation of the complex gaussian integral:

$$\begin{aligned} J_\Delta(t) =& A_0 \frac{e^2}{\hbar}\frac{a}{2\pi}\left[f(0)\sqrt{\frac{2\pi\hbar}{|\Delta''_{cv}(0)|\,t}}\sin\left(\frac{\Delta_{cv}(0)t}{\hbar}+\frac{\pi}{4}\right)+\right. \\ &\left. + f\left(\frac{\pi}{a}\right)\sqrt{\frac{2\pi\hbar}{|\Delta''_{cv}(\pi/a)|\,t}}\sin\left(\frac{\Delta_{cv}(\pi/a)t}{\hbar}-\frac{\pi}{4}\right)\right]. \end{aligned} \tag{3.78}$$

This part of the linear response decays very slowly at a rate of $t^{-1/2}$, as shown in the left panel of Fig. 3.7.

The final current is the sum of the terms $J_\Omega(t)$ and $J_\Delta(t)$. This is written as a sum of three sine functions with frequencies Ω, $\Delta_{cv}(0)/\hbar$ and $\Delta_{cv}(\pi/a)/\hbar$:

$$\begin{aligned} \hat{J}(t) =& -A_0\frac{e^2}{\hbar}\frac{a}{2\pi}\left[\int_{-\pi}^{\pi} dk \left(\mathrm{Tr}\left[\frac{\partial\hat{v}(k)}{\partial k}\hat{\rho}^{(0)}(k)\right]\right.\right. \\ &\left. -2v_{vc}(k)v_{cv}(k)\left(f_{kc}-f_{kv}\right)\frac{\Delta_{cv}(k)/\hbar}{\left(\Delta_{cv}(k)/\hbar\right)^2-\Omega^2}\right)\cdot\sin\left(\Omega t\right) \\ &+ f(0)\sqrt{\frac{2\pi\hbar}{|\Delta''_{cv}(0)|\,t}}\sin\left(\frac{\Delta_{cv}(0)t}{\hbar}+\frac{\pi}{4}\right) \\ &\left. +f\left(\frac{\pi}{a}\right)\sqrt{\frac{2\pi\hbar}{|\Delta''_{cv}(\pi/a)|\,t}}\sin\left(\frac{\Delta_{cv}(\pi/a)t}{\hbar}-\frac{\pi}{4}\right)\right], \end{aligned} \tag{3.79}$$

which is represented in Fig. 3.8.

In the left panel, we see the transient expressed by the current component with time dependent amplitude. This is a consequence of the sudden switching of the field. As

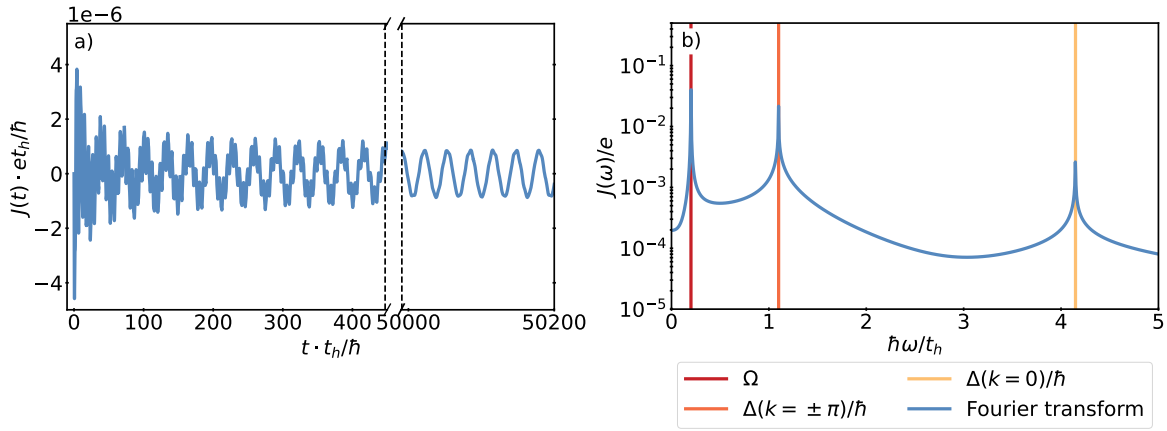

Figure 3.8.: Representation of the first order current of the system with $\Delta/t_h = 1.1$ under a monochromatic electromagnetic field with frequency $\hbar\Omega/t_h = 0.2$ and the amplitude of vector potential $e/\hbar \cdot aA_0 = 0.01$. The plot a) illustrates the time response for initial times until $t \cdot t_h/\hbar = 450$ and the response in a time interval for long times. The plot b) shows the Fourier transform of the current with the three frequencies: the field frequency Ω and the frequencies corresponding to extremes of the gap between the energy bands $\Delta(k = \pm\pi)/\hbar$ and $\Delta(0)/\hbar$.

the amplitude of this component decays with $1/\sqrt{T}$, the effect of suddenly switch the field almost disappeared. In the right panel are represented the three frequencies that we expect from Eq. (3.79): the field frequency, Ω, and the frequencies corresponding to extremes of the gap between the energy bands, Fig. 3.5, $\Delta(k = \pm\pi)/\hbar$ and $\Delta(0)/\hbar$. Note that the peaks corresponding to the extremes of the gap also appear in the right panel in Fig. 3.7.

In this section, we arrive at an expression of the first order current in perturbation theory, Eq. (3.79). In the following section, we will compute the current using Floquet formalism in time and frequency space. Further in the work, Chapter 4, we will compute these two results numerically and compare them.

3.3. Solution in Floquet formalism

Similar to what we have done in Section 2.3.2, to apply the Floquet formalism to the nonlinear optical problem, we start by constructing the EFH. At this point, it is useful to recall its form

$$\hat{H}^{Ext} = \sum_{\alpha,\beta} \sum_{m,p\in\mathbb{Z}} |\varphi_{\alpha m}\rangle \left(\mathcal{H}_{\alpha m;\beta p} + \hbar p\Omega\delta_{m,p}\delta_{\alpha,\beta}\right) \langle\varphi_{\beta p}|, \tag{3.80}$$

where

$$\mathcal{H}_{\alpha m;\beta p} = \frac{1}{T}\int_0^T dt\, \langle\phi_\alpha|\, \hat{H}\, |\phi_\beta\rangle\, e^{-i(m-p)\Omega t} \tag{3.81}$$

with $T = 2\pi/\Omega$.

As discussed before, the Hamiltonian of this problem is diagonal in k-basis by blocks, and we can write the evolution equation for each k independently. We will use this fact to compute the evolution of the equations of each k individually, which are 2D problems, and then get the full evolution summing over the FBZ. Choosing the $|\phi_\alpha\rangle = |\pm 1\rangle$ as the eigenbasis of the Pauli matrix $\hat{\sigma}^z$, the EFH for each k is given by

$$\begin{aligned}\hat{H}^{\text{Ext}} = &\sum_{\alpha,\beta}\sum_{m,p\in\mathbb{Z}} |\varphi_{\alpha m}\rangle \left\{ \left(\frac{\Delta}{2}\sigma^z_{\alpha\beta} + m\Omega\delta_{\alpha\beta}\right)\delta_{pm} \right. \\ &\left. -2t_h\frac{1}{T}\int_0^T dt \cos\left(\frac{ka}{2}+\delta(t)\right)\sigma^1_{\alpha\beta}\left(\frac{ka}{2}+\delta(t)\right)e^{-i(p-m)\Omega t}\right\}\langle\varphi_{\beta p}| \end{aligned} \tag{3.82}$$

We can use trigonometric identities to isolate the time dependent factors in the integral and write the Hamiltonian in an easier way to compute it

$$H^{\text{Ext}}_{\alpha p,\beta m} = \left(\frac{\Delta}{2}\sigma^z_{\alpha\beta} + m\Omega\delta_{\alpha\beta}\right)\delta_{pm} - 2t_h\frac{1}{T}\int_0^T dt\frac{1}{2}\sigma^x_{\alpha\beta}e^{-i(p-m)\Omega t} + \tag{3.83}$$

$$+\frac{1}{T}\int_0^T dt\left(\cos\left(2\delta(t)\right)\sigma^1_{\alpha\beta}\left(ka\right) + \sin\left(2\delta(t)\right)\sigma^2_{\alpha\beta}\left(ka\right)\right)e^{-i(p-m)\Omega t}, \tag{3.84}$$

where $\hat{\sigma}^1(k)$ and $\hat{\sigma}^2(k)$ are given by Eqs. (3.32) and (3.36).

In this way, to compute the Hamiltonian, we need to calculate the three integrals above. The first one has a trivial result

$$\frac{1}{T}\int_0^T dt e^{-i(p-m)\Omega t} = \delta_{p,m}. \tag{3.85}$$

In the other two, we start by doing a change of variable $t \to t' = \Omega t$ and then we expand the complex exponential in real and imaginary parts. The integral with the cosine simplifies as

$$\begin{aligned}\frac{1}{T}\int_0^T dt\cos\left(q_A a\sin\left(\Omega t\right)\right)e^{-i(p-m)\Omega t} &= \frac{1}{2\pi}\int_0^{2\pi} dt'\cos\left(q_A a\sin\left(t'\right)\right)\cos\left((p-m)t'\right) \\ &\equiv c(p-m, q_A a),\end{aligned} \tag{3.86}$$

where only the real part remains, because the imaginary part is the integral of an odd function. Conversely, for the sine integral, we get:

$$\begin{aligned}\frac{1}{T}\int_0^T dt\sin\left(q_A a\sin\left(\Omega t\right)\right)e^{-i(p-m)\Omega t} &= -i\frac{1}{2\pi}\int_0^{2\pi} dt'\sin\left(q_A a\sin\left(t'\right)\right)\sin\left((p-m)t'\right) \\ &\equiv -i\ s(p-m, q_A a).\end{aligned} \tag{3.87}$$

In the last two equations, we defined $q_A = e/\hbar A_0$ and the two functions $c\,(p-m, q_A a)$ and $s\,(p-m, q_A a)$ that can be identified as the Bessel function of the first kind (Appendix C) such that

$$c(p-m, q_A a) = \begin{cases} J_{p-m}(q_A a) & ,\ p-m \text{ even} \\ 0 & ,\ p-m \text{ odd} \end{cases}, \tag{3.88}$$

and

$$s(p-m, q_A a) = \begin{cases} 0 & ,\ p-m \text{ even} \\ J_{p-m}(q_A a) & ,\ p-m \text{ odd} \end{cases}, \tag{3.89}$$

where $J_{p-m}(q_A a)$ are the Bessel functions of the first kind.

Then we arrive at

$$\begin{aligned} H^{\text{Ext}}_{\alpha p,\beta m} = &\left(\frac{\Delta}{2}\sigma^z_{\alpha\beta} + m\Omega\delta_{\alpha\beta} - t_h\sigma^x_{\alpha\beta}\right)\delta_{pm} - \\ &- t_h\left(c\,(p-m, q_A a)\,\sigma^1_{\alpha\beta}\,(ka) - i\,s\,(p-m, q_A a)\,\sigma^2_{\alpha\beta}\,(ka)\right). \end{aligned} \tag{3.90}$$

To obtain the time evolution of the system for each k we follow the same procedure used to compute the time evolution of a two level system pumped with a periodic linearly polarized field in Section 2.3.2. After calculating the EFH for this problem, we diagonalize it. Since we are in the extended space, we choose two of the eigenvectors of the matrix with coefficients described by Eq. (3.90) with eigenvalues of different sets of the form $\{\epsilon_n + m\Omega, m \in \mathbb{Z}\}$. In the numerical results presented in Chapter 4, we truncate the matrix such that the indices p and m are limited between $-M$ and M. To choose the eigenvectors, we use the same criteria discussed in Section 2.3.2 that choose the two vectors whose coefficients have less influence of the truncation.

From the two chosen eigenvectors of EFH, a general state of the system is, recalling to Eqs. (2.40) and (2.41), written as:

$$|\psi(k,t)\rangle = \frac{1}{T}\sum_{n=1}^{2}\sum_{p\in\mathbb{Z}}\sum_{\alpha,\beta}|\phi_\alpha\rangle\, a^{(n)}_{\alpha p}\,\langle u_n|\psi(0)\rangle\, e^{-i(\epsilon_n/\hbar - p\Omega)t}, \tag{3.91}$$

where $a^{(n)}_{\alpha p}$ are the coefficients of the chosen eigenvectors of the EFH, $|u_n\rangle$ and ϵ_n the respective Floquet mode at $t=0$ and the eigenvalue. As the EFH is different for each k, the coefficients $a^{(n)}_{\alpha p}$ and the quasienergy ϵ_n are functions of k, as well as the Floquet gap defined as the difference between the quasienergies ϵ_n will be dependent of k, $\Delta_F(k)$.

For the following calculations we use the result that we have just obtained for the system's time evolution, (3.91), and compute the total current in time and frequency space.

3.3.1. Frequency analysis

A good characteristic of the Floquet formalism is that the frequencies of the response are explicit in the expression of the evolution of the system's state. If it is possible to write the current operator as a linear combination of complex exponentials we can extract the frequencies present in the optical response directly from the current computed with Floquet formalism and the amplitude of each component.

In this problem, we can do that. We rewrite the current operator of Eq. (3.35) as

$$\hat{j}(k,t) = -\frac{e}{\hbar}t_h \left[\sin(ka)\begin{pmatrix} 0 & e^{-i2\delta(t)} \\ e^{i2\delta(t)} & 0 \end{pmatrix} + \cos(ka)\begin{pmatrix} 0 & ie^{-i2\delta(t)} \\ -ie^{i2\delta(t)} & 0 \end{pmatrix}\right], \tag{3.92}$$

where the time dependency is exclusively in $\exp[\pm i2\delta(t)]$, with $\delta(t) = (a/2)(e/\hbar)A_0\sin(\Omega t)$. This function can be expanded in complex exponentials using the Jacobi-Anger expansion [41]:

$$e^{ix\sin(\pm\Omega t)} = \sum_{n=-\infty}^{+\infty} J_n(x)e^{\pm in\Omega t}, \tag{3.93}$$

where $x = a(e/\hbar)A_0$ and $J_n(z)$ are the Bessel functions of the first kind with the property $J_{-n}(x) = (-1)^n J_n(x)$. Then, the current operator can be written as

$$\hat{j}(k,t) = -\frac{e}{\hbar}t_h \sum_{n=-\infty}^{+\infty} J_n(x)\begin{pmatrix} 0 & (-1)^n(\sin(ka)+i\cos(ka)) \\ (\sin(ka)-i\cos(ka)) & 0 \end{pmatrix} e^{in\Omega t}. \tag{3.94}$$

Using the states of the system written as Eq. (3.91), the average value of the current is

$$\begin{aligned} \left\langle \hat{j}(k,t)\right\rangle &= \langle\psi(t)|\,\hat{j}(k,t)\,|\psi(t)\rangle \\ &= -\frac{e}{\hbar}t_h \sum_{m,n}\sum_{p,q,l\in\mathbb{Z}}\sum_{\alpha,\beta}\Big\{\langle\psi(0)|u_m\rangle\, a_{\beta q}^{*(m)}\,\langle\phi_\beta|\,\hat{\mathcal{O}}_l\,|\phi_\alpha\rangle\, a_{\alpha p}^{(n)}\,\langle u_n|\psi_0\rangle \\ &\quad \cdot\exp\left[i\left(\left(\epsilon_m-\epsilon_n\right)/\hbar-(q-l-p)\,\Omega\right)t\right]\Big\}, \end{aligned} \tag{3.95}$$

where

$$\hat{\mathcal{O}}_l = J_l(z)\begin{pmatrix} 0 & (-1)^l(\sin(ka)+i\cos(ka)) \\ (\sin(ka)-i\cos(ka)) & 0 \end{pmatrix}. \tag{3.96}$$

This extensive definition can be resumed to

$$\left\langle \hat{j}(k,t)\right\rangle = -\frac{e}{\hbar}\sum_{\{m_i;p_j;l\}} f_{\{m_i;p_j;l\}}(k)\cdot\exp\left[i\left(\left(\epsilon_m-\epsilon_n\right)/\hbar-(q-l-p)\,\Omega\right)t\right], \tag{3.97}$$

where the function $f_{\{m_i;p_i\}}(k)$ is the amplitude of the frequency mode of the time response defined as

$$f_{\{m_i;p_i;l\}}(k) = \sum_{\alpha,\beta}\langle\psi(0)|u_m\rangle\, a_{\beta q}^{*(m)}\,\langle\phi_\beta|\,\hat{\mathcal{O}}_l\,|\phi_\alpha\rangle\, a_{\alpha p}^{(n)}\,\langle u_n|\psi_0\rangle. \tag{3.98}$$

The notation $\{m_i\,;p_j;l\}$ represents all the indices of the sum, where m_i condenses the indices of the Floquet states, $\{m,n\}$, and the p_j condenses the indices $\{p,q\}$, that run over $\mathbb{Z}$.

If we rearrange the indices in Eqs. (3.97) and (3.98), we can isolate the terms that contribute to the response with the same frequency:

$$\left\langle \hat{j}(k,t) \right\rangle = -\frac{e}{\hbar} \sum_{r} \sum_{\{m_i\,;p_j\}} f_{\{m_i\,;p_j\}}(k) \cdot \exp\left[i\left(\left(\epsilon_m - \epsilon_n\right)/\hbar + r\Omega\right)t\right] \tag{3.99}$$

with

$$f_{\{m_i\,;p_i\}}(k) = \sum_{\alpha,\beta} \langle\psi(0)|u_m\rangle\, a^{*(m)}_{\beta q}\, \langle\phi_\beta|\, \hat{\mathcal{O}}_{r+q-p}\, |\phi_\alpha\rangle\, a^{(n)}_{\alpha p}\, \langle u_n|\psi_0\rangle \tag{3.100}$$

controlling only the indices of the Extended Floquet space, p and q, and the integer that multiply the external frequency, r. However, with the aim of obtaining a function of the current that we can plot for a range of frequencies, we did the Laplace transform:

$$\mathcal{J}(\omega) = -\frac{1}{N}\frac{e}{\hbar} \sum_{k\in fbz} \sum_{r} \sum_{\{m_i\,;p_j\}} f_{\{m_i\,;p_j\}}(k) \int_{-\infty}^{+\infty} dt\Theta(t) e^{i\bar{\omega}t} e^{-i(\omega - i\eta)t}. \tag{3.101}$$

where $\bar{\omega} = \left(\epsilon_m - \epsilon_n\right)/\hbar + r\Omega$. The presence of the Heaviside function is because of the need to fix the initial state of the system with the Floquet calculation, which means the field is suddenly switched in $t = 0$ and there has been no response before. Solving the time integral, we obtain:

$$\mathcal{J}(\omega) = \frac{1}{N} \sum_{k\in fbz} j(\omega, k). \tag{3.102}$$

where

$$j(\omega,k) = -\frac{e}{\hbar} \sum_{r} \sum_{\{m_i\,;p_j\}} \frac{f_{\{m_i\,;p_j\}}(k)}{\eta - i(\bar{\omega} - \omega)} \tag{3.103}$$

In the limit $\eta \to 0^+$, according to Sokhotski–Plemelj theorem, the result of this calculation is

$$\lim_{\eta\to 0^+} j(\omega,k) = -\frac{e}{\hbar} \sum_{r} \sum_{\{m_i\,;p_j\}} f_{\{m_i\,;p_j\}}(k) \left(\pi\delta(\bar{\omega} - \omega) + i\mathcal{P}\left(\frac{1}{\bar{\omega} - \omega}\right)\right), \tag{3.104}$$

where $\delta\left(\bar{\omega} - \omega\right)$ is the Dirac delta function and $\mathcal{P}\left(1/(\bar{\omega} - \omega)\right)$ denotes the Cauchy principal value, which is the Fourier transform of the current. So, if η is small enough we can compute the value of the amplitude of the frequency mode exactly.

At this point, we have an expression of the current of the system that includes all the frequencies that appear in the response without any restriction on the field intensity or the frequency. In the next section, we compare this expression to n-th order of the current expanded in powers of the vector potential amplitude for the condition of adiabatic and sudden switching.

3.3.2. Adiabatic vs sudden switching

As we can see from previous discussions, the Floquet formalism is limited to periodic problems and fixes an initial state, so the formalism solves problems where the time dependence is suddenly switched in the initial time. One of our interests is to relate the response obtained by Floquet formalism to the solution of time dependent perturbation theory with adiabatic switching of the perturbation, i.e. the perturbation is switched slowly at $t \to -\infty$.

As we see in Section 1.2, the n-th order of perturbation theory can be given by

$$J^{(n)}(k,t) = \int_{-\infty}^{t} dt_1 \cdots \int_{-\infty}^{t} dt_n \chi^{(n)}\left(k, t-t_1, \ldots, t-t_n\right) A\left(t_1\right) \ldots A\left(t_n\right), \tag{3.105}$$

where $\chi^{(n)}$ is the response function.

For adiabatic switching, the vector potential takes de form

$$A_{\mathrm{abd}}(t) = A_\Omega e^{-i(\Omega+i\eta)t} + A_\Omega^* e^{i(\Omega-i\eta)t}, \tag{3.106}$$

where $A_\Omega = iA_0$ and for sudden switching

$$A_{\mathrm{sdn}}(t) = \left(A_\Omega e^{-i\Omega t} + A_\Omega^* e^{i\Omega t}\right)\Theta(t). \tag{3.107}$$

The response function does not depend on vector potential, so supposing that the response is discrete in frequencies, we can expand it in Fourier series for each time argument such that

$$\chi^{(n)}\left(k, t-t_1, \ldots, t-t_n\right) = \sum_{\{m\}} \tilde{\chi}^{(n)}_{\{m\}}(k) e^{-i\omega_{m_1}(t-t_1)} \ldots e^{-i\omega_{m_n}(t-t_n)}. \tag{3.108}$$

Introducing this in the expression of the current, for adiabatic switching, we have

$$\begin{aligned} J^{(n)}_{\mathrm{adb}}(k,t) = &\sum_{\{m\}} \tilde{\chi}^{(n)}_{\{m\}}(k) e^{-i\left(\omega_{m_1}+\ldots+\omega_{m_n}\right)t} \\ &\cdot \int_{-\infty}^{t} dt_1 \cdots \int_{-\infty}^{t} dt_n \sum_{\{\sigma\}} A_{\sigma_1\Omega} e^{-i(\sigma_1\Omega-\omega_{m_1}+i\eta)t_1} \ldots A_{\sigma_n\Omega} e^{-i(\sigma_n\Omega-\omega_{m_n}+i\eta)t_n}, \end{aligned} \tag{3.109}$$

where we define a variable $\sigma_i = \pm 1$ such that we can write $A^*_{\pm\Omega} = A_{\mp\Omega}$. Solving the time integral of the form

$$\mathcal{I} = \int_{-\infty}^{t} dt_1 e^{-i(\sigma_1\Omega-\omega_{m_1}+i\eta)t_1} = i\frac{e^{-i(\sigma_1\Omega-\omega_{m_1}+i\eta)t}}{(\sigma_1\Omega-\omega_{m_1}+i\eta)}, \tag{3.110}$$

the current takes the form

$$\begin{aligned} J^{(n)}_{\mathrm{adb}}(k,t) = &\sum_{\{m\}} \tilde{\chi}^{(n)}_{\{m\}}(k) e^{-i\left(\omega_{m_1}+\ldots+\omega_{m_n}\right)t} \\ &\cdot \sum_{\{\sigma\}} iA_{\sigma_1\Omega} \frac{e^{-i(\sigma_1\Omega-\omega_{m_1}+i\eta)t}}{(\sigma_1\Omega-\omega_{m_1}+i\eta)} \cdot \ldots \cdot iA_{\sigma_n\Omega} \frac{e^{-i(\sigma_n\Omega-\omega_{m_n}+i\eta)t}}{(\sigma_n\Omega-\omega_{m_n}+i\eta)} \end{aligned} \tag{3.111}$$

and by computing the multiplication and simplifying the expression, we arrive at an expression for the time response for a perturbation with adiabatic switching of the form

$$J^{(n)}_{\text{adb}}(k,t) = \sum_{\{m,\sigma\}} \frac{i^n \tilde{\chi}^{(n)}_{\{m\}}(k) A_{\sigma_1\Omega} \cdot \ldots \cdot A_{\sigma_n\Omega}}{(\sigma_1\Omega - \omega_{m_1} + i\eta)\ldots(\sigma_n\Omega - \omega_{m_n} + i\eta)} \cdot \exp\left(-i\left(\left(\sigma_1 + \ldots + \sigma_n\right)\Omega + in\eta\right)t\right) . \tag{3.112}$$

For the sudden switching case, the current is

$$J^{(n)}_{\text{sdn}}(k,t) = \sum_{\{m\}} \tilde{\chi}^{(n)}_{\{m\}}(k) e^{-i\left(\omega_{m_1}+\ldots+\omega_{m_n}\right)t} \cdot \int_0^t dt_1 \cdots \int_0^t dt_n \sum_{\{\sigma\}} A_{\sigma_1\Omega} e^{-i(\sigma_1\Omega-\omega_{m_1})t_1} \ldots A_{\sigma_n\Omega} e^{-i(\sigma_n\Omega-\omega_{m_n})t_n}. \tag{3.113}$$

By performing the integrals of the form

$$\mathcal{I} = \int_0^t dt_1 e^{-i(\sigma_1\Omega-\omega_{m_1})t_1} = i\frac{e^{-i(\sigma_1\Omega-\omega_{m_1})t} - 1}{(\sigma_1\Omega - \omega_{m_1})} \tag{3.114}$$

the current takes the form

$$J^{(n)}_{\text{sdn}}(k,t) = \sum_{\{m\}} \tilde{\chi}^{(n)}_{\{m\}}(k) e^{-i\left(\omega_{m_1}+\ldots+\omega_{m_n}\right)t} \cdot \sum_{\{\sigma\}} iA_{\sigma_1\Omega}\frac{e^{-i(\sigma_1\Omega-\omega_{m_1})t} - 1}{(\sigma_1\Omega - \omega_{m_1})} \cdot \ldots \cdot iA_{\sigma_n\Omega}\frac{e^{-i(\sigma_n\Omega-\omega_{m_n})t} - 1}{(\sigma_n\Omega - \omega_{m_n})} \tag{3.115}$$

and after simplifications, the final expression is

$$J^{(n)}_{\text{sdn}}(k,t) = \sum_{\{m,\sigma\}} \frac{i^n \tilde{\chi}^{(n)}_{\{m\}}(k) A_{\sigma_1\Omega} \cdot \ldots \cdot A_{\sigma_n\Omega}}{(\sigma_1\Omega - \omega_{m_1})\ldots(\sigma_n\Omega - \omega_{m_n})} \cdot \left[\left(e^{-i(\sigma_1\Omega)t} - e^{-i\omega_{m_1}t}\right) \cdot \ldots \cdot \left(e^{-i(\sigma_n\Omega)t} - e^{-i\omega_{m_n}t}\right)\right] \tag{3.116}$$

Comparing Eqs. (3.112) and (3.116), we can see that the terms that correspond to a response with multiples of the frequency of the electromagnetic field proportional to $\exp\left(-i\left(\left(\sigma_1 + \ldots + \sigma_n\right)\Omega\right)t\right)$:

$$J_{\Omega}(k,t) = \sum_{\{m,\sigma\}} \frac{i^n \tilde{\chi}^{(n)}_{\{m\}}(k) A_{\sigma_1\Omega} \cdot \ldots \cdot A_{\sigma_n\Omega}}{(\sigma_1\Omega - \omega_{m_1})\ldots(\sigma_n\Omega - \omega_{m_n})} \exp\left(-i\left(\left(\sigma_1 + \ldots + \sigma_n\right)\Omega\right)t\right). \tag{3.117}$$

are identical in both currents, apart from the $i\eta$ terms. Note that the response from a field suddenly switched contains the information of the system's response with adiabatic switching. The terms that are left in Eq. (3.116) are related to the transient in the current.

Now, comparing these expressions with the current obtained with Floquet formalism, Eq. (3.97), we can identify the terms with frequency multiple of the field frequency Ω, when $\epsilon_m = \epsilon_n$, and the other frequencies present in the response. Regarding the terms in multiples of Ω we can write an expression for the response function

$$\tilde{\chi}^{(n)}_{\{m\}}(k) = \sum_{r,q} \frac{f_{\{m_i;p\}}(k)(\sigma_1\Omega - \omega_{m_1})\dots(\sigma_n\Omega - \omega_{m_n})}{i^n A_{\sigma_1\Omega}\cdot\ldots\cdot A_{\sigma_n\Omega}} \tag{3.118}$$

that is valid only for the set of indices $\{\sigma\}$ and $\{p_j\}$ such that

$$\sigma_1 + \ldots + \sigma_n = s - l - p. \tag{3.119}$$

Note that, as these terms, Eq. (3.117), are common in adiabatic and sudden switching responses, the adiabatic response can be extracted from the Floquet formalism, despite the restriction of the Floquet formalism must be applied to a system suddenly perturbed.

Comparing Eqs. (3.116) and (3.97) reveal that the remaining frequencies ω_{m_i} are related to the Floquet gap, Δ_F, so we can relate the transient to the Floquet spectrum.

Note that in Eq. (3.116) seems to have resonance when $\sigma_i\Omega - \omega_{m_i} = 0$. As shown above, the frequency ω_{m_i} are related to the Floquet gap, which depends on the external frequency, Ω, so if we change the frequency to match the Floquet gap, the system will have a new Floquet gap, and there will not be resonance.

4. Results

In this chapter, we discuss the results derived from the analysis done in Chapter 3. We start by analysing the evolution of the average value of the current and DM auxiliary operators. Then, summing over the FBZ, we study the response of the 1D two-band semiconductor at zero temperature perturbed by a periodic electromagnetic field, focusing on the variation of the intensity of the field in perturbative and nonperturbative regimes.

4.1. Partial current for each quasi-momentum k

The final goal is to compute the response of the AB chain at zero temperature to a periodic electromagnetic field. As we saw in Chapter 3, the problem is diagonal by blocks in k-basis in velocity gauge so we can solve the time evolution of the system with Floquet formalism for each vector k reducing the problem to a 2D problem. This is equivalent to solving a problem of one particle in the two-level system perturbed with an electromagnetic field.

To understand which values of field intensity correspond to small perturbations, we can start by thinking of the effect of the field in the quasi-momentum k. For this system, we conclude, Eq. (3.31), that the perturbed Hamiltonian is equal to the original Hamiltonian with the transformation $k \to k + 2\delta(t)/a$:

$$\hat{\mathcal{H}}(k,t) = \hat{\mathcal{H}}_0\left(k + \frac{2}{a}\delta(t)\right). \tag{4.1}$$

Remembering that

$$\delta(t) = \frac{e}{\hbar}\frac{a}{2}A_0 \sin(\Omega t), \tag{4.2}$$

the translation in k is periodic with a maximum deviation equal to $e/\hbar \cdot A_0$. So, we consider that a small perturbation means that the amplitude of the translation of k is much smaller than the width of the FBZ:

$$2\frac{e}{\hbar}A_0 \ll \frac{2\pi}{a}. \tag{4.3}$$

To compare the resulting current from Floquet formalism, Eq. (2.40), and the first order response in perturbation theory calculated in Section 3.2, we compute the current for different quasi-momentum k for a system with a gap $\Delta/t_h = 1$ and an electromagnetic field with intensity $e/\hbar \cdot aA_0 = 0.01$ and frequency $\hbar\Omega/t_h = 0.2$. In Fig. 4.1 from a) to

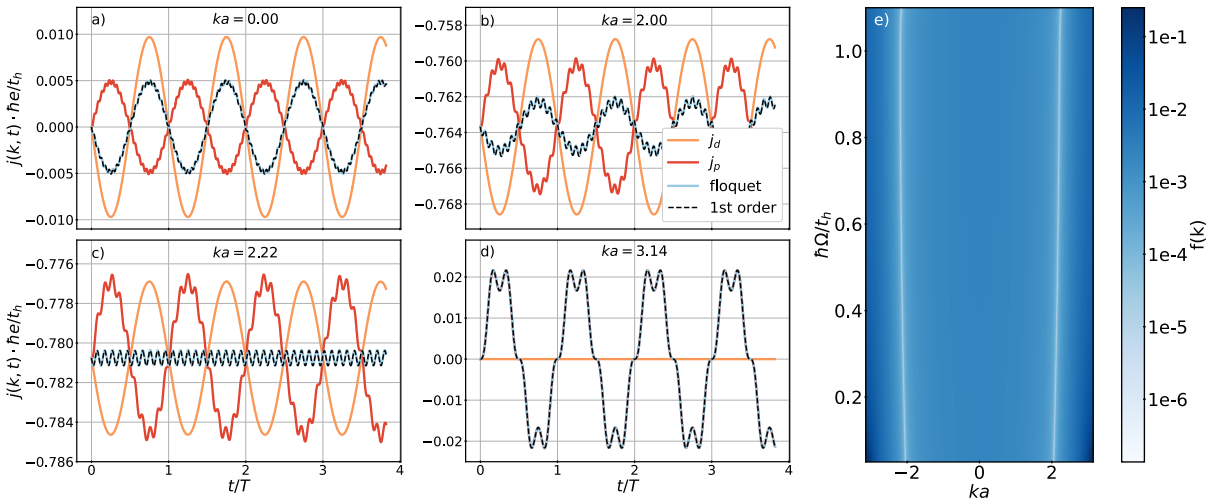

Figure 4.1.: Time evolution of the system with $\Delta/t_h = 1$, $e/\hbar \cdot aA_0 = 0.01$ and $\hbar\Omega/t_h = 0.2$, (plots from a) to d)) computed with Floquet formalism (blue lines) of the partial current for a Bloch vector with quasi-momentum k as a function of the ratio between the time instant t and the period of the field $T = 2\pi/\Omega$, compared with first order response (black dashed line). Representation of the diamagnetic (red line) and paramagnetic (orange line) components of the first order current. In plot e) is represented the amplitude of the oscillation of the current in the field frequency, the first harmonic, for all points of the FBZ for a range of fields frequencies.

d), we represent the current for the points of the FBZ $ka = \{0, \pi/4, 2.22, \pi\}$. We see that the results from Floquet formalism and perturbation theory overlap, which gives us two pieces of informations:

- A field with intensity $e/\hbar \cdot aA_0 = 0.01$ is considered within the perturbative regime;
- With the Floquet formalism, we can obtain the correct current of the perturbed system.

In Fig. 4.1, we also represent the diamagnetic component

$$j_d(k,t) = -\frac{e^2}{\hbar}\mathrm{Tr}\left[\frac{\partial \hat{v}(k)}{\partial k}\hat{\rho}^{(0)}(k)\right]A(t) \tag{4.4}$$

and paramagnetic component

$$j_p(k,t) = 2\frac{e^2}{\hbar}A_0 v_{vc}(k)v_{cv}(k)\left(f_{kc} - f_{kv}\right)\cdot\frac{\left(\Delta_{cv}/\hbar\sin\left(\Omega t\right) - \Omega\sin\left(\Delta_{cv}t/\hbar\right)\right)}{\left(\Delta_{cv}/\hbar\right)^2 - \Omega^2} \tag{4.5}$$

of the first order current $j(k,t) = j_0(k) + j_d(k,t) + j_p(k,t)$, with $j_0(k)$ the zero order of the current. As mentioned in Section 3.2, the diamagnetic component represented by the orange curve is related to the intraband effects and the paramagnetic component represented by the red curve corresponds to the interband interactions. In the centre of the FBZ, $k = 0$, the intraband effects are more important resulting in a stronger component.

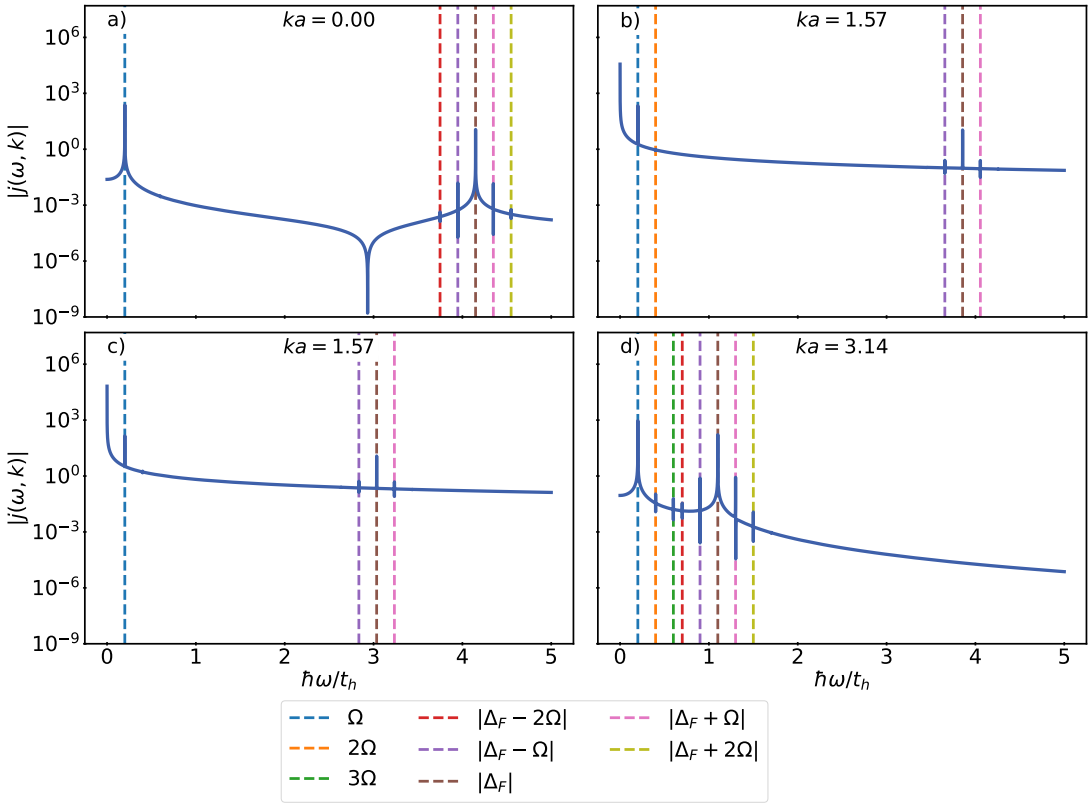

Figure 4.2.: Representation of the current response in frequency space for four different points of the FBZ, in perturbative regime; The results were obtained with Floquet formalism computed from Eq. (3.103) with $\eta = 1 \times 10^{-5}$.

As we move to the edge of the FBZ, the interband interactions become stronger. On the edge of the FBZ, $k = \pi$, the diamagnetic current is zero, and the current is only due to interband effects. This is a consequence of a decrease in the energy gap as we go from the centre to the edges of FBZ.

As we saw in Section 3.2, the diamagnetic current has the same frequency as the field, Eq. (3.52). The diamagnetic current and the component of the paramagnetic current with the field frequency have opposite signs and interfere destructively. For example, for $\hbar\Omega/t_h = 0.2$ and $k = 2.22$, they have the same amplitude and cancel out. The value of the k where this is observed is solution of the equation

$$\mathrm{Tr}\left[\frac{\partial \hat{v}(k)}{\partial k}\hat{\rho}^{(0)}(k)\right] - 2v_{vc}(k)v_{cv}(k)\left(f_{kc} - f_{kv}\right)\frac{\Delta_{cv}(k)/\hbar}{\left(\Delta_{cv}(k)/\hbar\right)^2 - \Omega^2} = 0 \tag{4.6}$$

resulting from the amplitude of the Ω oscillation of the current, Eq. (3.71), to be null, so it depends on the field frequency. In Fig. 4.1 c), we see that the partial current $j(k,t)$ does not oscillate with frequency Ω. In Fig. 4.1 e) are represented the amplitude of the oscillation of the current in the field frequency, the first harmonic, for all points of the FBZ for fields frequencies from $\hbar\Omega/t_h = 0.05$ to $\hbar\Omega/t_h = 1.1$. The two symmetric lines correspond to the values of $\pm k$ in the FBZ, where the amplitude of the first harmonic is

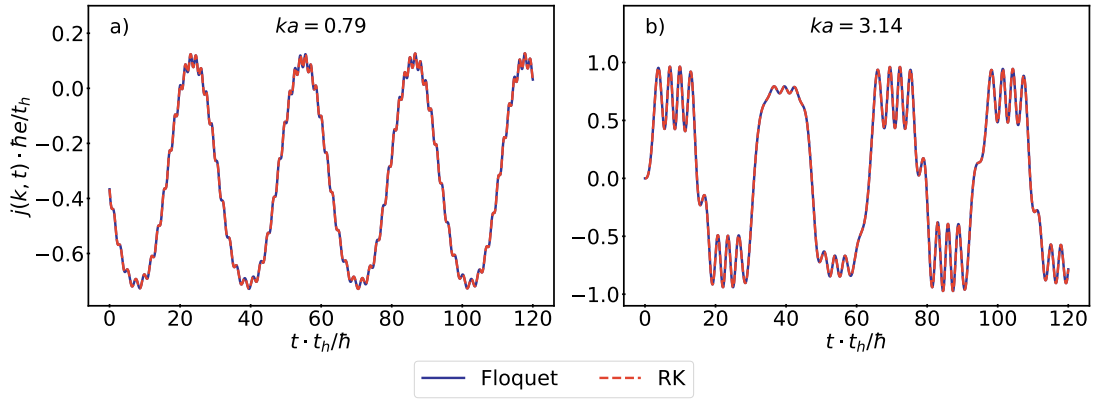

Figure 4.3.: Evolution of the expected value of the current operator for ka: (1) $\pi/4$, (2) π. The results were obtained with Floquet formalism and RK4 for a system with gap $\Delta/t_h = 1.1$ perturbed with a field with intensity $e/\hbar \cdot aA_0 = 1$ and frequency $\hbar\Omega/t_h = 0.2$.

null for each field frequency. With this, we observe that the effect of the second band is not negligible even if there are no real band transitions, i.e. if the external frequency is smaller than the gap, $\hbar\Omega < \Delta$.

To analyse the frequencies that appear in the response for each k, we compute the current response in frequency space for different quasi-momentum k with Floquet formalism, Eq. (3.103), represented in Fig. 4.2. As expected from the Floquet formalism, the system response with discrete frequencies:

- multiples of the external frequency, $r\Omega$, $r \in \mathbb{Z}$;
- Floquet gap plus multiples of field frequency, $\Delta_F(k)/\hbar + r\Omega$, $r \in \mathbb{Z}$.

Note that despite not being visible in the plots of the time response observed in Fig. 4.1, response in multiples of external frequency appears in the Fourier spectrum with much lower intensity.

Looking at frequency plots (Fig. 4.2), we see that they have in common the peaks at $m\Omega$, however, the peaks at Floquet gap plus multiples of field frequency depend on k. These peaks are within a region between the maximum and the minimum of $\Delta_F(k)$ that are $\Delta_F(\pi)$ and $\Delta_F(0)$ respectively.

After observing the response at perturbative regime, we increase the value of the field intensity, $e/\hbar \cdot aA_0 = 1$, for two points of FBZ $ka = \{\pi/4, \pi\}$, and computed the time response via the Floquet Formalism, Eq. (2.40), and RK4. Remember that $\Delta k = e/\hbar \cdot A(t)$, so that this field intensity corresponds to a maximum translation is about 1/3 of the FBZ. Fig. 4.3 shows both results and we can see that they overlap. The choice of the field intensity was not very large, so more frequencies are observed at the edge of the FBZ ($k = \pi$) where the energy gap ($\Delta(k)$) is smaller.

Until here, we analyse the current associated with each Bloch vector with quasi-momentum k, computing the response for low and higher field intensity and comparing the result obtained with Floquet formalism with the first order current and the solution obtained with

RK4. In the following section, we will sum over the FBZ to obtain the total current of the system.

4.2. Total current

To obtain the total nonlinear optical response from the response of each quasi-momentum k we sum over the FBZ. To simulate an infinite system, we take the limit used in Section 3.2 and transform the sum into an integral. We use the Simpson integration method to do it numerically. There are some aspects to consider when we compute the sum. As we seen in the previous section in Fig. 4.2, there are peaks in the response $j(\omega$,k) related to the Floquet gap $\Delta_F(k)$ that depend on the quasi-momentum k, so that they are dislocated from each other. As we said before, the current function in frequency space in the limit of $\eta \to 0^+$ is equal to the exact Fourier transform, which is a Dirac delta function plus a Cauchy principal value. So, the width of the peak is in the order of η. Considering two consecutive points k_a and k_b, the partial current for each k will have peaks centred at $\omega_a = \Delta_F(k_a) + r\Omega$ and $\omega_b = \Delta_F(k_b) + r\Omega$, respectively. If we want to obtain a continuum function in frequency, instead of separated peaks, the separation between ω_a and ω_b must be smaller than η, so that

$$\omega_a - \omega_b < \eta \Leftrightarrow \Delta_F(k_a) - \Delta_F(k_b) \ll \eta. \tag{4.7}$$

Note that we can write $k_b = k_a + \Delta k$ and if $\Delta k \ll 1$ we have

$$\Delta_F(k_b) = \Delta_F(k_a) + \left.\frac{d\Delta_F(k)}{dk}\right|_{k_a} (k_b - k_a) + \mathcal{O}(k^2) \tag{4.8}$$

and we find a relation between Δk and the parameter η

$$\Delta k \ll \eta \left(\frac{d\Delta_F(k)}{dk}\right)^{-1}. \tag{4.9}$$

To compute the integration in the FBZ, we choose a number of points N that determines $\Delta k = 2\pi/N$, which means that the number of points used to compute the integral must be larger than $N_{\min}$ given by

$$N_{\min} = \frac{2\pi}{\eta} \left(\frac{d\Delta_F(k)}{dk}\right)_{\max}. \tag{4.10}$$

To observe the effect of the number of points on the integral in FBZ, we compute the total current for $\eta = 0.1$ for several numbers of points. The results are shown in Fig. 4.4.

As expected, the region where it takes more points to converge is between $\Delta(\pi)$ and $\Delta(0)$. In this case, we obtain a smooth curve for $N = 256$, and computing the current for different values of η we find smooth curves for $N \sim 2/\eta$ as expected.

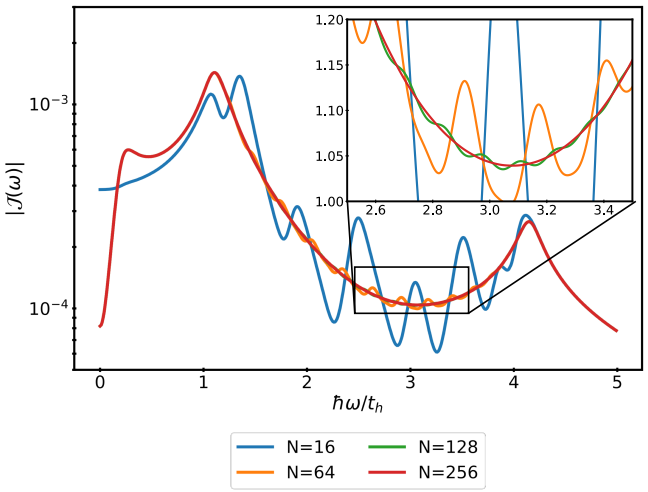

Figure 4.4.: Representation of the dependency on the total current response with the number of points used to compute the integral over the FBZ for a system with $\Delta/t_h = 1$, $e/\hbar \cdot aA_0 = 0.01$ and $\hbar\Omega/t_h = 0.2$, computed with $\eta = 1 \times 10^{-1}$.

Focusing on the choice of the parameter η, we can use it as a measurement of resolution. In Fig. 4.5, we see that as we increase the parameter η the curve becomes less defined in some regions, and some details disappear. Otherwise, when we decrease the value of the parameter η we see more details of the function. Observe that in the two curves computed with $\eta = \{1 \times 10^{-2}, 1 \times 10^{-3}\}$ we cannot see the peak in $\omega = 0.4$ correspondent to the second harmonic.

As we saw before, the number of the points needed to compute the integral in k depend on the parameter η in a way that if we want more resolution, we will need to compute the integral using more points. However, we can compute the curve using for different regions of frequency different values of η. With that in mind, we obtain the plot in Fig. 4.6, which represents the total current in frequency space for the interval $\hbar\omega/t_h \in [0, 5]$.

As we saw in Fig. 3.8, the Fourier transform of the first order current analysed in Section 3.2 also the first harmonic and in the site of the Floquet gap peaks are the unperturbed energy gap ones. Because the field intensity is low the floquet gap and the unperturbed gap are very close and the peaks coincide. With Floquet formalism, we can also observe the presence of the second harmonic with much lower intensity.

From the Section 4.1, we see that the response for each k has discrete frequencies at $r\Omega$ and $\Delta_F + r\Omega$ as expected from the Eq. (3.95). After the sum over the FBZ, the majority of the peaks in frequency space disappear. To understand this effect, we will discuss in the following calculations the result of the integral over the FBZ around the peaks that appear for each k.

First, we can rewrite the total current in frequency space, Eqs. (3.102) and (3.103), as

$$\mathcal{J}(\omega) = -\frac{e}{\hbar}\frac{a}{2\pi}\sum_{r,\sigma}\int_{-\pi/a}^{\pi/a} dk\, \frac{F_{r,\sigma}(k)}{\eta - i\left(g_\sigma(k) + r\Omega - \omega\right)}, \tag{4.11}$$

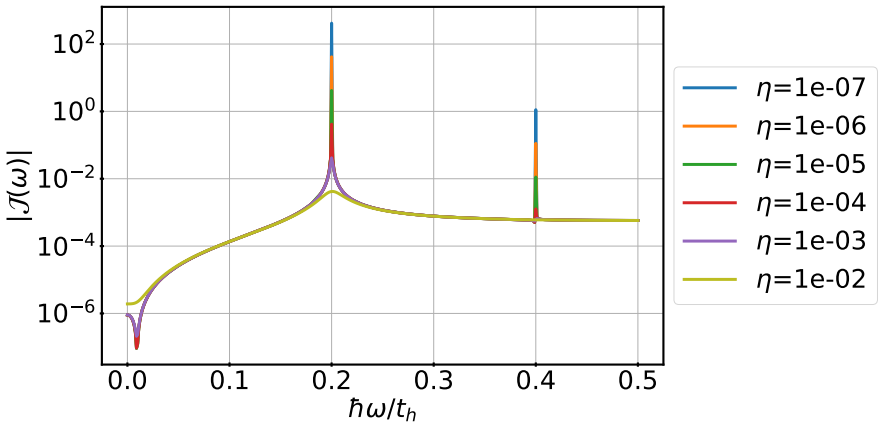

Figure 4.5.: Representation of the dependency of the total current response with the parameter η for a system with $\Delta/t_h = 1$, $e/\hbar \cdot aA_0 = 0.01$ and $\hbar\Omega/t_h = 0.2$, computed with $N = 256$.

where $F_{r,\sigma}(k)$ is the amplitude of the frequency $g_\sigma(k) + r\Omega$ and $g_\sigma(k)$ as a function that takes the value of the Floquet gap or is null. When we evaluate the integrand function at $\tilde{\Delta}_F(k) + r\Omega = \omega$, the function diverges with $1/\eta$ and in the limit $\eta \to 0^+$ it is equal to a Dirac delta function plus a Cauchy principal value. We can discuss the value of the total current around these points dividing the calculation in three cases.

First case: Focusing in the terms of the integral where $g_\sigma(k) = 0$, the only part of the integrand that depends on k is the amplitude function $F_{r,\sigma}(k)$, so

$$\mathcal{J}(r\Omega) = -\frac{e}{\hbar}\frac{a}{2\pi}\frac{1}{\eta}\int_{-\pi/a}^{\pi/a} dk\, F_{r,\sigma}(k). \tag{4.12}$$

In the same way that the integrand function in Eq. (4.11) diverges, the current $\mathcal{J}(\omega)$ for $\omega = r\Omega$ also diverges with $1/\eta$. For a finite η, we can obtain the value of the amplitude of the current component with this frequency, by multiplying the computed current in frequency space by the parameter η:

$$\mathcal{A}(r\Omega) \equiv -\frac{e}{\hbar}\frac{a}{2\pi}\int_{-\pi/a}^{\pi/a} dk\, F_{r,\sigma}(k) = \lim_{\eta\to o^+} \eta\mathcal{J}(r\Omega). \tag{4.13}$$

In Fig. 4.7 a), we compute the amplitude $\mathcal{A}(\omega)$ for different values of η and we see that for peaks $\omega = \Omega$ and $\omega = 2\Omega$, the value of the amplitude is independent of η.

Second case: Regarding the current at $\omega = \Delta_F(k) + r\Omega$, the integrand function diverges at the point k^* where $\Delta_F(k^*) = \omega - r\Omega$, in the limit of $\eta \to 0^+$. In a small region around k^*, we can make the following approximation:

$$\Delta_F(k) + r\Omega - \omega \approx a\,(k - k^*)\,, \qquad k^* - C \leq k \leq k^* + C, \tag{4.14}$$

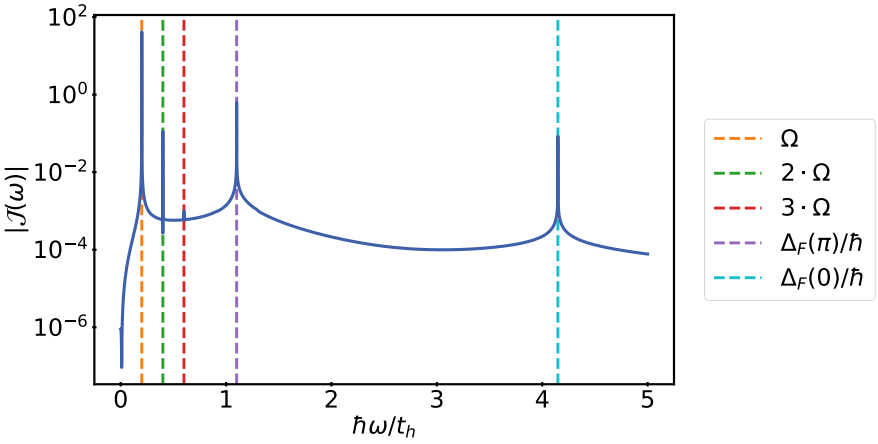

Figure 4.6.: Representation of the current response in frequency space of the 1D two-band semiconductor model at zero temperature with energy gap $\Delta/t_h = 1$ suddenly perturbed by a monochromatic electromagnetic field with intensity $e/\hbar \cdot aA_0 = 0.01$ and frequency $\hbar\Omega/t_h = 0.2$.

where a is the first derivative of the Floquet gap evaluated in k^* and $C \ll 1$ delimits the interval where this approximation is valid, considering $C \gg \eta$. Now, we can compute the integral using this approximation in this region (Appendix D) and obtain an expression in powers of η:

$$\int_{k^*-C}^{k^*+C} dk \, \frac{F_{r,\sigma}(k)}{\eta - i\left(\Delta_F(k) + r\Omega - \omega\right)} = \frac{9\pi F_{r,\sigma}(k^*) + i18C\, F'_{r,\sigma}(k^*) + iC^3\, F^{(3)}_{r,\sigma}(k^*)}{9a} + \mathcal{O}(\eta), \tag{4.15}$$

where $F'_{r,\sigma}(k)$ is the first derivative of the amplitude function and $F^{(n)}_{r,\sigma}(k)$ is the n-th order derivative. Note that the result is written as a series in C, such that these corrections can be neglected in the limit where $C \ll 1$. Given that $\eta \ll C$, we can take the limit $\eta \to 0^+$ and we see that the result of the integral is finite. Since the parts of the integral outside of the interval $k^* - C \leq k \leq k^* + C$ are independent of η, we can conclude that the singularity in the integrand does not generate any singularity in the current $\mathcal{J}(\omega)$.

Third case: Following on from the previous case, we may ask about the points k^* where $\Delta_F(k^*) = \omega - r\Omega$ and the first derivative of the Floquet gap is null. In those cases, we must use the approximation:

$$\Delta_F(k) + r\Omega - \omega \approx \frac{b}{2}\left(k - k^*\right)^2, \qquad k^* - C \leq k \leq k^* + C, \tag{4.16}$$

where b in the second derivative of the Floquet gap at k^*, and C delimits the interval where this approximation is valid, with $c \gg \eta$.

Using a similar process we use in previous case to compute the integral in k around the

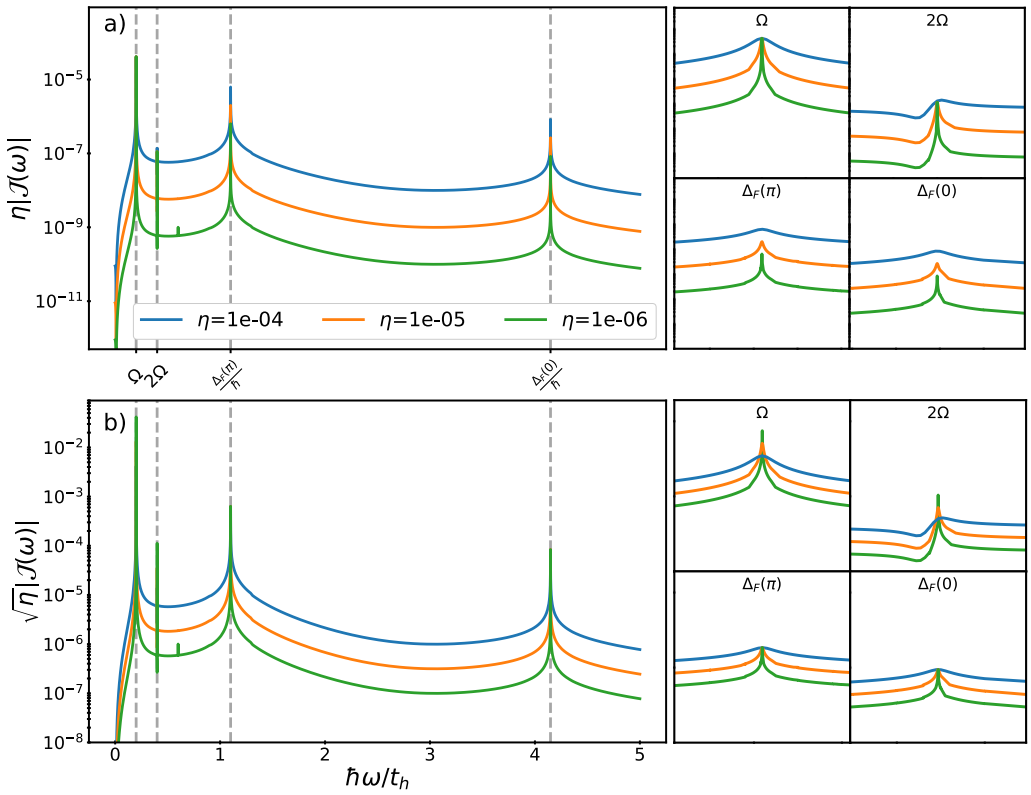

Figure 4.7.: Representation of the collapse of a) the maximum of the peak $\mathcal{J}(r\Omega)$ with $1/\eta$ and b) the maximum of the peaks $\mathcal{J}\left(\Delta_F(\pi)\right)$ and $\mathcal{J}\left(\Delta_F(0)\right)$ with $1/\sqrt{\eta}$. The plots in the right panels are the zoom in around the frequencies marked with the vertical dashed lines.

point k^* (Appendix D) we get

$$\int_{k^*-C}^{k^*+C} dk\, \frac{F_{r,\sigma}(k)}{\eta - i\left(\Delta_F(k) + r\Omega - \omega\right)} = \frac{1}{\sqrt{\eta}} \frac{(1+i)\pi F_{r,\sigma}(k^*)}{\sqrt{|b|}} + \mathcal{O}\left(\eta^0\right). \tag{4.17}$$

This time the integral diverges with $1/\sqrt{\eta}$. In Fig. 4.7 b), we represent the current $\mathcal{J}(\omega)$ multiplied by $\sqrt{\eta}$ and we see that the curves coincide for $\hbar\omega = \Delta_F(\pi)$ and $\Delta_F(0)$, where we can see that the amplitude $\sqrt{\eta}\mathcal{J}(\omega)$ for the frequencies in the Floquet gap coincide.

We can conclude that after we sum over the FBZ the only peaks that does not disappear are the multiples of the field frequency, $r\Omega$, and the peaks associated with the extremes of the Floquet gap, as we saw in Fig. 4.6.

To analyse the appearance of the non-perturbative regime, we compute the amplitude for the current response in frequency space for the first three harmonics as a function of the field intensity, from $e/\hbar \cdot aA_0 = 0.01$ to $e/\hbar \cdot aA_0 = 1$. When we start to increase the value of A_0 we need a larger truncation to compute the EFH. As we saw in Section 2.3.2, to obtain the correct solution of the system evolution, there must be at least two orthogonal eigenvectors of the EFH unaffected by the truncation. To analyse the behaviour of the

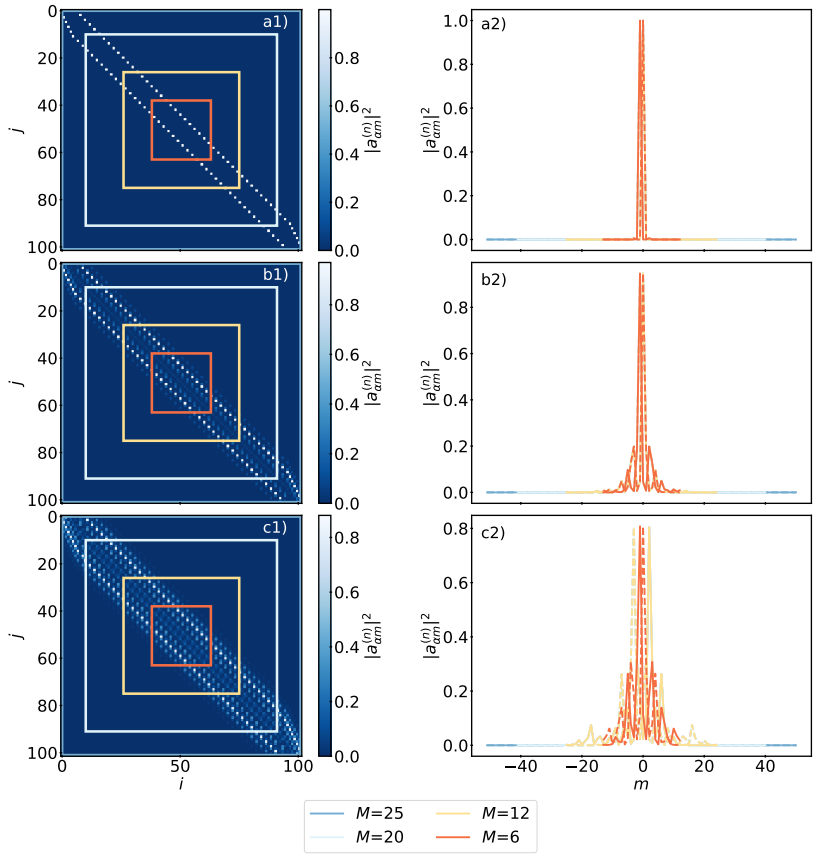

Figure 4.8.: Schematic representation of the convergence of the eigenvectors of the EFH with the increase of the truncation M and the dependency on the field intensity. The results correspond to the eigenvectors of the EFH for the system with $\hbar\Omega/t_h = 0.2$ and (a) $e/\hbar \cdot aA_0 = 0.01$; (b) $e/\hbar \cdot aA_0 = 0.5$; (c) $e/\hbar \cdot aA_0 = 1$. Panels (1) representation of the absolute value of the entries indexing by (j, i) of the matrix which each column is an eigenvector of the EFH with $M = 25$ and size of the matrices with different truncation. Panels (2), representation of the pairs (with dashed and solid lines) chosen for each truncation.

coefficients of the eigenvectors of the EFH with the increase of the field intensity, we compute and diagonalize the EFH for different field intensity values. In Fig. 4.8, we see the representation of the coefficients of eigenvectors of the EFH with the increase of the truncation M and with the field intensity A_0. In panels (1), we represent the matrix whose columns are the eigenvectors of the EFH with truncation $M = 25$. The coloured squares delimit the places where the different truncations, $M = \{6, 12, 20, 25\}$, take place. From panels (1) to panels (2), we chose the two orthogonal eigenvectors with the most minor influence on the truncation for each value of M.

Similarly to what we saw for the two levels system pumped with a linearly polarized electromagnetic field, for a sufficiently large truncation, the matrix of the eigenvectors of the EFH in columns is sparse (panels (1) Fig. 4.8). Note that with the increase of the field

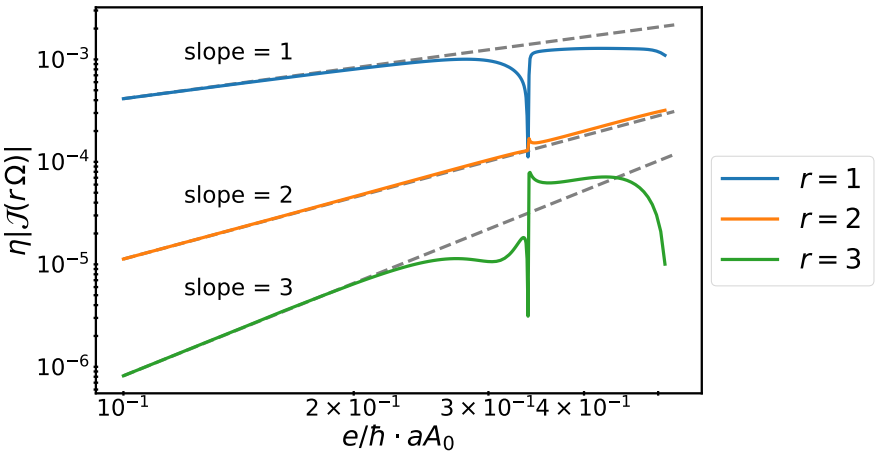

Figure 4.9.: Representation of the dependency of the amplitude of current response for the first three harmonics, $\omega = r\Omega$, $r = \{1, 2, 3\}$, with the field intensity. The result corresponds to the system with energy gap $\Delta/t_h = 1$ perturbed by an electromagnetic field with frequency $\hbar\Omega/t_h = 0.2$.

intensity from (a) to (c), the number of nonzero coefficients on the eigenvector increases. We can use a smaller truncation for low field intensities and obtain the correct evolution. For $e/\hbar \cdot aA_0 = 0.01$, the lines plotted in the panel (a2) in the Fig. 4.8 overlap, which means that the coefficients of the eigenvectors of the EFH are the same for all truncations. Besides that, the amplitudes of the edge coefficients are equal to zero, even for $M = 6$. However, when we look at $e/\hbar \cdot aA_0 = 2$, panel (c2) in Fig. 4.8, the eigenvectors of the EFH truncated at $M = 6$ and $M = 12$ depend highly on the edges, and the coefficients do not match the results obtained for $M = 20$ and $M = 25$ (the lines do not overlap).

To decide which truncation value we were going to use to calculate the current amplitudes for the first three harmonics (Fig. 4.9), we calculated the Floquet modes for a field intensity $e/\hbar \cdot aA_0 = 1$ and checked from which value of M the modes were normalized. We find that a suitable truncation was $M = 17$. Then, using the results from the EFH with $M = 17$, we compute the current amplitudes for $\omega = \{\Omega, 2\Omega, 3\Omega\}$ using the function of the current in the frequency space, Eq. (3.102), and multiply by η to obtain the coefficients that multiply the complex exponentials in time response. In Fig. 4.9, we see that for low fields, until $e/\hbar \cdot aA_0 = 0.2$, the optical response is perturbative as the amplitude depends with the expected power law on the field intensity

$$\mathcal{J}(r\Omega) \propto A_0^r, \tag{4.18}$$

with $r = \{1, 2, 3\}$. Recalling the result of 3.3.2, where we showed the equivalence between the response of a system perturbed by a field with adiabatic switching and the components of the response resulting from a suddenly switched field with multiples of the field frequency in perturbative regime, the amplitudes of current for weak fields presented in Fig. 4.9 computed for sudden switching are also valid for adiabatic switching. As we increase the field intensity, nonperturbative behaviour starts to appear, i.e., the dependency of the amplitudes on the field intensity changes drastically, expressing the perturbative

behaviour breakdown. The study of the behaviour seen in Fig. 4.9 for larger $e/\hbar \cdot aA_0$ shall be material for future work.

5. Conclusion and Outlook

In this thesis we used the Floquet formalism to obtain the optical response of a 1D two band semiconductor at zero temperature perturbed by a periodic electromagnetic field in velocity gauge. We compute the system's time evolution for each quasi-momentum k and sum over the FBZ within perturbative and nonpertubative regime.

Regarding the system's time evolution for each k we compared the result for low field intensities to first order perturbation theory and the result for high field intensities with RK4. In the regime of low field intensity and frequency $\hbar\Omega \ll \Delta$, where there are no real interband transitions, we found a limitation of the semiclassical dynamics. The virtual interband transitions have a large effect on the amplitude of the first harmonic, contributing to its significant decrease.

In what concerns the total current, we compute the current in frequency space for low field intensity for $\hbar\omega/t_h = [0, 5]$ and observe that the only frequencies that survive after summing over the FBZ are the multiples of the field frequency and the frequencies associated to the extremes of the Floquet gap. We studied the behaviour of the current around these frequencies and observed that the limit towards the exact Fourier transform of the current follows different laws for each one. We also observed how the amplitude of the first three harmonics depend on the field intensity, observing nonperturbative responses. Analysing the perturbation theory with adiabatic and sudden switching, we conclude that the Floquet formalism can respond to both cases. Despite the formalism's limitations, which require the system's perturbation to be periodic so that the perturbation must be switched suddenly, we saw that the components of multiples of the perturbation frequency are common for both adiabatic and sudden switches, i.e. the results obtained for the first three harmonics for weak fields are valid not only for the system perturbed with sudden switching as we formulated the problem but also for a system perturbed with a field switch adiabatically.

To perform the numerical calculations, we numerically implemented the EFH for this system and wrote a code to compute the time evolution with the Floquet formalism for two-level systems, as well as the implementation of the density current for this problem with Floquet formalism in frequency space. Concerning the way we opted to calculate the current in the frequency space, we found some numerical issues. In order to be able to calculate very small perturbations and high harmonics, it is necessary to consider the response with high resolution, i.e. with low values of the parameter η. This, as we saw in Chapter 4, requires the use of a larger number of points to calculate the integral in k. Another problem we found was the need to increase the truncation of the EFH as we increase the field intensity. These two parameters of the calculation, the number of

points to calculate the integral, N, and the truncation, M, are crucial to obtain the exact response.

The results presented in this thesis are only preliminary, as there was no time to explore the method further. We have a lot of open space for future work. As we saw in the calculation of the optical response for high field intensities, the coefficients of the EFH eigenvectors depend on the field intensity, and the truncation must be adapted to this and any other parameters of the problem. Understanding the correct measure of convergence of the Floquet states is essential to create a general way of implementing this formalism in calculating optical responses that adapts the truncation of the EFH.

Specifically for this system, it would be interesting to analyse how the amplitude of the harmonics of the response depends on other system parameters, such as the gap of the unperturbed system or the external frequency. Another interesting analysis for future work is how the frequency and amplitude of the transient, that appear after summing over the FBZ, depend on the intensity and frequency of the field and the parameters of the unperturbed system. Besides the analysis of the optical response of this system, we also can using this method to compute the optical response of other materials such as 2D materials or materials with more bands. An example is the other possible description of this chain mentioned at the beginning of the 3, which, from the outset, differed from the one explored in terms of inversion symmetry.

A. Inversion symmetry

The idea is that a system has inversion symmetry if the system remains invariant under the transformation of $\overrightarrow{\mathbf{r}} \to -\overrightarrow{\mathbf{r}}$. In the problem of a system with an electromagnetic perturbation, inverting the direction of the position implies the inversion of the direction of vector potential, $\overrightarrow{\mathbf{A}}$. This means that if we characterise the inversion by the transformation operator $\hat{P}$, the system has inversion symmetry if the transformation of the Hamiltonian of the system was

$$\hat{P}\hat{H}(\overrightarrow{\mathbf{A}})\hat{P}^{\dagger} = \hat{H}(-\overrightarrow{\mathbf{A}}) \tag{A.1}$$

and the transformation of the current operator was

$$\hat{P}\hat{\overrightarrow{\mathbf{J}}}(\overrightarrow{\mathbf{A}})\hat{P}^{\dagger} = -\hat{\overrightarrow{\mathbf{J}}}(\overrightarrow{\mathbf{A}}) \tag{A.2}$$

such that the transform current operator is odd in the vector potential:

$$\hat{\overrightarrow{\mathbf{J}}}(-\overrightarrow{\mathbf{A}}) = -\hat{\overrightarrow{\mathbf{J}}}(\overrightarrow{\mathbf{A}}). \tag{A.3}$$

Consequently the terms in perturbation theory that depend on even powers of the field doesn't exist.

Considering the problem of a chain with two orbital explored in Chapter 3 we start by defining the actuation of the parity operator, $\hat{P}^{(I)}$, in the basis of position for the description of the two band in different positions in the same unit cell:

$$|n, A\rangle \to \hat{P}^{(I)} |n, A\rangle = |-n, A\rangle , \tag{A.4}$$

$$|n, B\rangle \to \hat{P}^{(I)} |n, B\rangle = |-n-1, B\rangle . \tag{A.5}$$

So the transformation of the system Hamiltonian is computed by

$$\begin{aligned}
\hat{P}^{(I)}\hat{H}^{(I)}\hat{P}^{(I)\dagger} =& \sum_n \frac{\Delta}{2}\Big(|-n, A\rangle\langle -n, A| - |-n-1, B\rangle\langle -n-1, B|\Big) \\
& - t_h \sum_n \Big(e^{-i\delta(t)} |-n-1, B\rangle\langle -n, A| + e^{i\delta(t)} |-n, B\rangle\langle -n, A| + h.c.\Big), \\
\underset{n\to -n}{=}& \sum_n \frac{\Delta}{2}\Big(|n, A\rangle\langle n, A| - |n, B\rangle\langle n, B|\Big) \\
& - t_h \sum_n \Big(e^{-i\delta(t)} |n-1, B\rangle\langle n, A| + e^{i\delta(t)} |n, B\rangle\langle n, A| + h.c.\Big).
\end{aligned} \tag{A.6}$$

If we invert the direction of the vector potential in the original Hamiltonian, i.e. $\delta(t) \to -\delta(t)$:

$$\begin{aligned}\hat{H}^{(I)}\left(-\delta(t)\right) =& \sum_n \frac{\Delta}{2}\Big(|n,A\rangle\langle n,A| - |n,B\rangle\langle n,B|\Big) \\ & - t_h \sum_n \Big(e^{i(-\delta(t))}|n-1,B\rangle\langle n,A| + e^{-i(-\delta(t))}|n,B\rangle\langle n,A| + h.c.\Big),\end{aligned}$$

the equality is observed:

$$\hat{P}^{(I)}\hat{H}^{(I)}(A)\hat{P}^{(I)\dagger} = \hat{H}^{(I)}(-A). \tag{A.7}$$

For the second description, the actuation of the parity operator, $\hat{P}^{(II)}$, is given by

$$|n,\alpha\rangle \underset{n\to -n}{\to} \hat{P}\,|n,\alpha\rangle = |-n,\alpha\rangle\,, \tag{A.8}$$

and the transformed Hamiltonian is computed by

$$\begin{aligned}\hat{P}\hat{H}^{(II)}(t)\hat{P}^{\dagger} =& \sum_n \frac{\Delta}{2}\Big(|-n,A\rangle\langle -n,A| - |-n,B\rangle\langle -n,B|\Big) \\ & - t_h \sum_n \Big(|-n,B\rangle\langle -n,A| + e^{i2\delta(t)}|-n+1,B\rangle\langle -n,A| + h.c.\Big), \\ \underset{n\to -n}{=}& \sum_n \frac{\Delta}{2}\Big(|n,A\rangle\langle n,A| - |n,B\rangle\langle n,B|\Big) \\ & - t_h \sum_n \Big(|n,B\rangle\langle n,A| + e^{i2\delta(t)}|n+1,B\rangle\langle n,A| + h.c.\Big).\end{aligned} \tag{A.9}$$

In this case, if we change the direction of the field of the original Hamiltonian the symmetry does not appear:

$$\begin{aligned}\hat{H}^{(II)}\left(-\delta(t)\right) =& \sum_n \frac{\Delta}{2}\Big(|n,A\rangle\langle n,A| - |n,B\rangle\langle n,B|\Big) \\ & - t_h \sum_n \Big(|n,B\rangle\langle n,A| + e^{-i2(-\delta(t))}|n-1,B\rangle\langle n,A| + h.c.\Big)\end{aligned}$$

such that

$$\hat{P}\hat{H}^{(II)}(t)\hat{P}^{\dagger} \neq \hat{H}(-A). \tag{A.10}$$

B. Semiclassical approximation

In a single band system, the electronic response to an applied electric field is given by [42]:

$$k(t) = k(0) - \frac{e}{\hbar}\int_0^t dt' E(t') = k(0) + \frac{e}{\hbar}\left(A(t) - A(0)\right), \tag{B.1}$$

which coincides with the second semiclassical equation. The current of the system can be written as

$$j(t,k) = ev\left(k(t)\right), \tag{B.2}$$

and by expanding in first order in vector potential $A(t)$ we get

$$j(k,t) = ev\left(k(0)\right) + \frac{e^2}{\hbar}\frac{\partial v\left(k(0)\right)}{\partial k}A(t). \tag{B.3}$$

For a two bands system, we can take this approximation by considering that the interband interactions are negligible. Suppose that the electron is in the band with lower energy, the valence band, such that

$$\begin{aligned} j(t,k) &= e\mathrm{Tr}\left[\hat{v}\left(k(t)\right)\hat{\rho}\right], \\ &= ev_{vv}\left(k(t)\right). \end{aligned}$$

The current in first order for that system in semiclassical approximation is then

$$j(k,t) = ev_{vv}\left(k(0)\right) + \frac{e^2}{\hbar}\frac{\partial v_{vv}\left(k(0)\right)}{\partial k}A(t). \tag{B.4}$$

C. Bessel function of the first kind

A definition of the Bessel function of the first kind is [43]

$$J_n(x) = \frac{1}{\pi}\int_0^{\pi} \cos\left(n\tau - x\sin\tau\right) d\tau. \tag{C.1}$$

Using trigonometric equalities we can rewrite it as

$$\begin{aligned} J_n(x) &= \frac{1}{\pi}\int_0^{\pi} \left(\cos\left(n\tau\right)\cos\left(x\sin\tau\right) + \sin\left(n\tau\right)\cos\left(x\sin\tau\right)\right) d\tau, \\ &= \frac{1}{2\pi}\int_{-\pi}^{\pi} \left(\cos\left(n\tau\right)\cos\left(x\sin\tau\right) + \sin\left(n\tau\right)\cos\left(x\sin\tau\right)\right) d\tau, \end{aligned}$$

where from the first line to the second line we use the fact that both terms of the integrand are even functions. Note that the functions are invariant under the translation

$$\tau \to \tau' = \tau + 2\pi \tag{C.2}$$

so the Bessel function can be finally written as

$$J_n(x) = \frac{1}{2\pi}\int_0^{2\pi} \left(\cos\left(n\tau\right)\cos\left(x\sin\tau\right) + \sin\left(n\tau\right)\cos\left(x\sin\tau\right)\right) d\tau. \tag{C.3}$$

Looking closely to the first term

$$\begin{aligned} &\frac{1}{2\pi}\int_0^{2\pi} \cos\left(n\tau\right)\cos\left(x\sin\tau\right) d\tau \\ =&\frac{1}{2\pi}\left(\int_0^{\pi} \cos\left(n\tau\right)\cos\left(x\sin\tau\right) d\tau + \int_{\pi}^{2\pi} \cos\left(n\tau\right)\cos\left(x\sin\tau\right) d\tau\right) \\ =&\frac{1}{2\pi}\left(\int_0^{\pi} \cos\left(n\tau\right)\cos\left(x\sin\tau\right) d\tau + \int_0^{\pi} \cos\left(n(\tau-\pi)\right)\cos\left(x\sin\left(\tau-\pi\right)\right) d\tau\right) \\ =&\frac{1}{2\pi}\left(\int_0^{\pi} \cos\left(n\tau\right)\cos\left(x\sin\tau\right) d\tau + \int_0^{\pi} (-1)^n\cos\left(n\tau\right)\cos\left(x\sin\left(\tau\right)\right) d\tau\right) \end{aligned}$$

if n is odd the integral is null.

For the other term

$$\begin{aligned} &\frac{1}{2\pi}\int_0^{2\pi} \sin\left(n\tau\right)\sin\left(x\sin\tau\right) d\tau \\ =&\frac{1}{2\pi}\left(\int_0^{\pi} \sin\left(n\tau\right)\sin\left(x\sin\tau\right) d\tau + \int_{\pi}^{2\pi} \sin\left(n\tau\right)\sin\left(x\sin\tau\right) d\tau\right) \\ =&\frac{1}{2\pi}\left(\int_0^{\pi} \sin\left(n\tau\right)\sin\left(x\sin\tau\right) d\tau + \int_0^{\pi} \sin\left(n(\tau-\pi)\right)\sin\left(x\sin\left(\tau-\pi\right)\right) d\tau\right) \\ =&\frac{1}{2\pi}\left(\int_0^{\pi} \sin\left(n\tau\right)\sin\left(x\sin\tau\right) d\tau - \int_0^{\pi} (-1)^n\sin\left(n\tau\right)\sin\left(x\sin\left(\tau\right)\right) d\tau\right) \end{aligned}$$

the integral is null when n is even.

So the Bessel function reduces to

$$J_n(x) = \begin{cases} \frac{1}{2\pi} \int_0^{2\pi} \cos(n\tau) \cos(x \sin \tau)\, d\tau & n \text{ is even} \\ \frac{1}{2\pi} \int_0^{2\pi} \sin(n\tau) \cos(x \sin \tau)\, d\tau & n \text{ is odd} \end{cases} \tag{C.4}$$

D. Integral of the partial current in k around the singularities

In Chapter 4, we discuss the result of the total current in frequency space around the frequencies where the partial current, $j(\omega, k)$, has singularities. In this appendix, we compute explicitly the integral around the point k^* where $\Delta_F(k^*) = \omega - r\Omega$, i.e. we compute the integral of $j(\omega, k)$ between $k^* - C$ and $k^* + C$ for the case $\Delta'_F(k^*) \neq 0$ and the case $\Delta'_F(k^*) = 0$.

$\Delta'_F(k^*) \neq 0$

In the region around k^* we can use the following approximation:

$$\Delta_F(k) + r\Omega - \omega \approx \Delta'_F(k - k^*), \qquad -C \leq k \leq C \tag{D.1}$$

with $C \ll 1$ and $C \gg \eta$. The integral take the form, redefining $\Delta'_F(k^*) \equiv a$:

$$\int_{k^*-C}^{k^*+C} dk \, \frac{F_{r,\sigma}(k)}{\eta - i\left(\Delta_F(k) + r\Omega - \omega\right)} = \int_{k^*-C}^{k^*+C} dk \, \frac{F_{r,\sigma}(k)}{\eta - i\Delta'_F(k - k^*)}$$

Redefining $\Delta'_F(k^*) \equiv a$ and making the change of variable

$$\begin{cases} \delta = \frac{|a|}{\eta}(k - k^*)/\eta \\ \frac{\eta}{|a|} d\delta = dk \end{cases} \tag{D.2}$$

we obtain

$$\int_{k^*-C}^{k^*+C} dk \, \frac{F_{r,\sigma}(k)}{\eta - i\left(\Delta_F(k) + r\Omega - \omega\right)} = \frac{\eta}{|a|} \int_{-C|a|/\eta}^{C|a|/\eta} dk \, \frac{F_{r,\sigma}\left(k^* + \frac{\eta}{|a|}\delta\right)}{\eta - i\eta\delta \, \mathrm{sign}(a)} \tag{D.3}$$

$$= \frac{1}{|a|} \int_{-C|a|/\eta}^{C|a|/\eta} dk \, \frac{F_{r,\sigma}\left(k^* + \frac{\eta}{|a|}\delta\right)}{1 - i\delta \, \mathrm{sign}(a)}. \tag{D.4}$$

To compute the integral, we expand the amplitude function $F_r\left(k^* + \frac{\eta}{|a|}\delta\right)$ in powers of δ:

$$\begin{aligned} \frac{1}{|a|} \frac{F_{r,\sigma}\left(k^* + \frac{\eta}{|a|}\delta\right)}{1 - i\delta \, \mathrm{sign}(a)} =& \frac{F_{r,\sigma}(k^*)}{|a|(1 - i\delta)} + \frac{\delta F'_{r,\sigma}(k^*)}{|a|^2(1 - i\delta)}\eta \\ &+ \frac{\delta^2 F''_{r,\sigma}(k^*)}{2|a|^3(1 - i\delta)}\eta^2 + \frac{\delta^3 F^{(3)}_{r,\sigma}(k^*)}{6|a|^4(1 - i\delta)}\eta^3 + \mathcal{O}\left(\eta^3\right) \end{aligned} \tag{D.5}$$

and we get

$$\begin{aligned}\int_{k^*-C}^{k^*+C} dk\, \frac{F_{r,\sigma}(k)}{\eta - i\left(\Delta_F(k) + r\Omega - \omega\right)} \\ =&\frac{9\pi F_{r,\sigma}\left(k^*\right) + \text{sign}(a)18iCF'_{r,\sigma}\left(k^*\right) + \text{sign}(a)iC^3F^{(3)}_{r,\sigma}\left(k^*\right)}{9|a|} \\ &+ \frac{-2F_{r,\sigma}\left(k^*\right) + C\left(-\text{sign}(a)i\pi F'_{r,\sigma}\left(k^*\right) + CF''_{r,\sigma}\left(k^*\right)\right)}{|a|^2C}\eta \\ &+ \frac{12\text{sign}(a)iF'_{r,\sigma}\left(k^*\right) - 3\pi CF''_{r,\sigma}\left(k^*\right) - 2\text{sign}(a)ic^2F^{(3)}_{r,\sigma}\left(k^*\right)}{6|a|^3C}\eta^2 + \mathcal{O}\left(\eta^3\right)\end{aligned} \tag{D.6}$$

$\Delta'_F\left(k^*\right) = 0$

Following the same procedure used in section above, this time with the approximation:

$$\Delta_F(k) + r\Omega - \omega \approx \frac{\Delta''_F}{2}\left(k - k^*\right)^2, \qquad -C \le k \le C \tag{D.7}$$

The integral take the form:

$$\int_{k^*-C}^{k^*+C} dk\, \frac{F_{r,\sigma}(k)}{\eta - i\left(\Delta_F(k) + r\Omega - \omega\right)} = \int_{k^*-C}^{k^*+C} dk\, \frac{F_{r,\sigma}(k)}{\eta - i\frac{\Delta''_F}{2}\left(k - k^*\right)^2}$$

Now we can make the following change of variable

$$\begin{cases}\delta = \sqrt{\frac{|b|}{2\eta}}\left(k - k^*\right) \\ \sqrt{\frac{2\eta}{|b|}}\, d\delta = dk\end{cases} \tag{D.8}$$

where we define $b = \Delta''_F\left(k^*\right)$ and the integral become

$$\int_{k^*-C}^{k^*+C} dk\, \frac{F_{r,\sigma}(k)}{\eta - i\left(\Delta_F(k) + r\Omega - \omega\right)} = \sqrt{\frac{2\eta}{|b|}}\int_{-C\sqrt{|a|/2\eta}}^{C\sqrt{|a|/2\eta}} dk\, \frac{F_{r,\sigma}\left(k^* + \sqrt{\frac{2\eta}{|b|}}\delta\right)}{\eta - i\eta\delta^2\,\text{sign}(b)} \tag{D.9}$$

$$= \sqrt{\frac{1}{2|b|\eta}}\int_{-C|a|/\eta}^{C|a|/\eta} dk\, \frac{F_{r,\sigma}\left(k^* + \sqrt{\frac{2\eta}{|b|}}\delta\right)}{1 - i\delta^2\,\text{sign}(b)}. \tag{D.10}$$

Now we expand the integrand function in powers of δ:

$$\sqrt{\frac{1}{2|b|\eta}}\frac{F_{r,\sigma}\left(k^* + \sqrt{\frac{2\eta}{|a|}}\delta\right)}{1 - i\delta^2\,\text{sign}(b)} = \sqrt{\frac{2}{|b|}}\frac{iF_{r,\sigma}\left(k^*\right)}{i + \delta^2}\frac{1}{\sqrt{\eta}} + \frac{2i\delta F'_{r,\sigma}\left(k^*\right)}{|b|\left(i + \delta^2\right)} \tag{D.11}$$

$$+ \frac{i\sqrt{2}\delta^2F''_{r,\sigma}\left(k^*\right)}{|b|^{3/2}\left(i + \delta^2\right)}\sqrt{\eta} + \frac{2i\delta^3F^{(3)}_{r,\sigma}\left(k^*\right)}{3|b|^2\left(i + \delta^2\right)}\eta + \mathcal{O}\left(\eta^{3/2}\right) \tag{D.12}$$

and the result of the integral is given by

$$\begin{aligned}
&\int_{k^*-C}^{k^*+C} dk\, \frac{F_{r,\sigma}(k)}{\eta - i\left(\Delta_F(k) + r\Omega - \omega\right)} \\
&\quad = \frac{(1+\mathrm{sign}(b)i)\,\pi F_{r,\sigma}(k^*)}{\sqrt{|b|}} \frac{1}{\sqrt{\eta}} \\
&\qquad + \frac{1}{|b|^2 C}\Big[392\,\mathrm{sign}(b)i\left(-3600 F_{r,\sigma}(k^*) + 1800\, C^2 F''_{r,\sigma}(k^*)\right. \\
&\qquad \left. + 50\, C^4 F^{(4)}_{r,\sigma}(k^*) + C^6 F^{(6)}_{r,\sigma}(k^*)\right) + 5\mathrm{sign}(b)i C^8 F^{(8)}_{r,\sigma}(k^*)\Big]\eta \\
&\qquad + \frac{(1-\mathrm{sign}(b)i)\pi F''_{r,\sigma}(k^*)}{|b|^{3/2}}\sqrt{\eta} + \mathcal{O}\left(\eta^3\right)
\end{aligned} \tag{D.13}$$

Bibliography

[1] John Kerr. Xl. A new relation between electricity and light: Dielectrified media birefringent. *The London, Edinburgh, and Dublin Philosophical Magazine and Journal of Science*, 50(332):337–348, November 1875. doi:10.1080/14786447508641302. [Cited on page 1.]

[2] F. Pockels. *Ueber den Einfluss des elektrostatischen Feldes auf das optische Verhalten piëzoelektrischer Krystalle*, volume 39. Dieterichsche Verlags-Buchhandlung, 1894. ISBN 978-3836440820. [Cited on page 1.]

[3] P.A. Franken, A.E. Hill, C.W. Peters, and G. Weinreich. Generation of Optical Harmonics. *Phys. Rev. Lett*, 7(4):118–119, August 1961. doi:10.1103/PhysRevLett.7.118. [Cited on pages 1 and 2.]

[4] Robert W. Boyd, Alexander L. Gaeta, and Enno Giese. Nonlinear optics. In *Springer Handbook of Atomic, Molecular, and Optical Physics*, pages 1097–1110. Springer, 2008. ISBN 978-3-030-73892-1. [Cited on page 1.]

[5] Y R Shen. *The Principles of Nonlinear Optics*. Wiley-Interscience, New York, NY, USA, 1984. ISBN 978-0471430803. [Cited on page 1.]

[6] J. E. Sipe and Ed Ghahramani. Nonlinear optical response of semiconductors in the independent-particle approximation. *Phys. Rev. B*, 48:11705–11722, October 1993. doi:10.1103/PhysRevB.48.11705. [Cited on page 1.]

[7] Claudio Aversa, J. E. Sipe, M. Sheik-Bahae, and E. W. Van Stryland. Third-order optical nonlinearities in semiconductors: The two-band model. *Phys. Rev. B*, 50:18073–18082, December 1994. doi:10.1103/PhysRevB.50.18073. [Cited on page 1.]

[8] J. E. Sipe and A. I. Shkrebtii. Second-order optical response in semiconductors. *Phys. Rev. B*, 61:5337–5352, Feb 2000. doi:10.1103/PhysRevB.61.5337. [Cited on page 1.]

[9] Geoffrey New. *Introduction to Nonlinear Optics*. Cambridge University Press, 2011. ISBN 978-0521877015. [Cited on page 1.]

[10] D Ter Haar. Theory and applications of the density matrix. *Reports on Progress in Physics*, 24(1):304, January 1961. doi:10.1088/0034-4885/24/1/307. [Cited on page 1.]

[11] Ole Keller. *Density Matrix Formalism: Hamilton and Current Density Operators – Gauge Invariance*, pages 187–215. Springer Berlin Heidelberg, Berlin, Heidelberg, 2011. ISBN 978-3-642-17410-0. [Cited on page 1.]

[12] Ryogo Kubo. Statistical-mechanical theory of irreversible processes. i. general theory and simple applications to magnetic and conduction problems. *Journal of the Physical Society of Japan*, 12(6):570–586, March 1957. doi:10.1143/JPSJ.12.570. [Cited on page 1.]

[13] D J Passos, G B Ventura, J M B Lopes dos Santos, and J M Viana Parente Lopes. Nonlinear optical conductivity of a two-band crystal I. *Journal of Physics: Condensed Matter*, 33(46):465701, August 2021. doi:10.1088/1361-648X/ac1c2d. [Cited on pages 1 and 7.]

[14] Mark Newman. *Computational Physics*. University of Michigan, 2013. ISBN 978-148014551-1. [Cited on pages 2 and 17.]

[15] Julian Schwinger. On nonadiabatic processes in inhomogeneous fields. *Phys. Rev.*, 51(8):648–651, April 1937. doi:10.1103/PhysRev.51.648. [Cited on page 2.]

[16] F. Bloch and A. Siegert. Magnetic resonance for nonrotating fields. *Phys. Rev.*, 57(6):522–527, March 1940. doi:10.1103/PhysRev.57.522. [Cited on page 2.]

[17] I. I. Rabi, N. F. Ramsey, and J. Schwinger. Use of rotating coordinates in magnetic resonance problems. *Reviews of Modern Physics*, 26(2):167–171, April 1954. doi:10.1103/revmodphys.26.167. [Cited on page 2.]

[18] Jon H. Shirley. Solution of the Schrodinger Equation with a Hamiltonian Periodic in Time. *Physical Review*, 138(4B):979–987, May 1965. doi:10.1103/physrev.138.b979. [Cited on pages 2 and 14.]

[19] G. Floquet. Sur les équations différentielles linéaires à coefficients périodiques. *Annales scientifiques de l'École Normale Supérieure*, 12(2):47–88, 1883. doi:10.24033/asens.220. [Cited on page 2.]

[20] Takuya Kitagawa, Erez Berg, Mark Rudner, and Eugene Demler. Topological characterization of periodically-driven quantum systems. *Physical Review B*, 82(23):235114, December 2010. doi:10.1103/PhysRevB.82.235114. [Cited on page 2.]

[21] Takahiro Morimoto, Shudan Zhong, Joseph Orenstein, and Joel E. Moore. Semiclassical theory of nonlinear magneto-optical responses with applications to topological Dirac/Weyl semimetals. *Physical Review B*, 94(24):245121, December 2016. doi:10.1103/PhysRevB.94.245121. [Cited on page 2.]

[22] Marco Merboldt, Michael Schüler, David Schmitt, Jan Philipp Bange, Wiebke Bennecke, Karun Gadge, Klaus Pierz, Hans Werner Schumacher, Davood Momeni, Daniel Steil, Salvatore R. Manmana, Michael A. Sentef, Marcel Reutzel, and Stefan Mathias. Observation of Floquet states in graphene. Preprint, April 2024. arXiv:2404.12791v1 [cond-mat.mes-hall]. [Cited on page 2.]

[23] Netanel H. Lindner, Gil Refael, and Victor Galitski. Floquet Topological Insulator in Semiconductor Quantum Wells. *Nature Physics*, 7(6):490–495, June 2011. doi:10.1038/nphys1926. [Cited on page 2.]

[24] Mikael C. Rechtsman, Julia M. Zeuner, Yonatan Plotnik, Yaakov Lumer, Daniel Podolsky, Felix Dreisow, Stefan Nolte, Mordechai Segev, and Alexander Szameit. Photonic Floquet topological insulators. *Nature*, 496(7444):196–200, April 2013. doi:10.1038/nature12066. [Cited on page 2.]

[25] S. Sajad Dabiri, Hosein Cheraghchi, and Ali Sadeghi. Floquet states and optical conductivity of an irradiated two dimensional topological insulator. *Physical Review B*, 106(16):165423, October 2022. doi:10.1103/PhysRevB.106.165423. [Cited on page 2.]

[26] Y. Zhou and M. W. Wu. Optical response of graphene under intense terahertz fields. *Physical Review B*, 83(24):245436, June 2011. doi:10.1103/PhysRevB.83.245436. [Cited on page 2.]

[27] Hossein Dehghani and Aditi Mitra. Optical Hall conductivity of a Floquet Topological Insulator. *Physical Review B*, 92(16):165111, October 2015. doi:10.1103/PhysRevB.92.165111. [Cited on page 2.]

[28] M Nuske, L Broers, B Schulte, G Jotzu, SA Sato, A Cavalleri, A Rubio, JW McIver, and L Mathey. Floquet dynamics in light-driven solids. *Physical Review Research*, 2(4):043408, December 2020. doi:10.1103/PhysRevResearch.2.043408. [Cited on page 2.]

[29] André Eckardt. Atomic quantum gases in periodically driven optical lattices. *Reviews of Modern Physics*, 89(1):011004, March 2017. doi:10.1103/RevModPhys.89.011004. [Cited on page 2.]

[30] Mark S. Rudner and Netanel H. Lindner. The Floquet Engineer's Handbook. Preprint, June 2020. arXiv:2003.08252v2 [cond-mat, physics:quant-ph]. [Cited on pages 3, 9, and 14.]

[31] Konstantin L. Ivanov, Kaustubh R. Mote, Matthias Ernst, Asif Equbal, and Perunthiruthy K. Madhu. Floquet theory in magnetic resonance: Formalism and applications. *Progress in Nuclear Magnetic Resonance Spectroscopy*, 126-127:17–58, 2021. doi:10.1016/j.pnmrs.2021.05.002. [Cited on pages 3, 9, and 14.]

[32] Gonçalo Bastos Ventura. *Nonlinear optical response of two-dimensional crystals*. PhD thesis, University of Porto, 2021. [Cited on pages 5, 6, and 7.]

[33] Martin Holthaus. Floquet engineering with quasienergy bands of periodically driven optical lattices. *Journal of Physics B: Atomic, Molecular and Optical Physics*, 49(1):013001, November 2015. doi:10.1088/0953-4075/49/1/013001. [Cited on pages 9 and 15.]

[34] J. M. B. Lopes dos Santos. Floquet formalism notes. Personal Notes, 2021. [Cited on pages 9 and 24.]

[35] Marin Bukov, Luca D'Alessio, and Anatoli Polkovnikov. Universal High-Frequency Behavior of Periodically Driven Systems: from Dynamical Stabilization to Floquet Engineering. *Advances in Physics*, 64(2), March 2015. doi:10z.1080/00018732.2015.1055918. [Cited on page 9.]

[36] André Eckardt and Egidijus Anisimovas. High-frequency approximation for periodically driven quantum systems from a floquet-space perspective. *New journal of physics*, 17(9):093039, 2015. doi:10.1088/1367-2630/17/9/093039. [Cited on pages 9 and 14.]

[37] Saar Rahav, Ido Gilary, and Shmuel Fishman. Effective Hamiltonians for periodically driven systems. *Physical Review A*, 68(1):013820, July 2003. doi:10.1103/PhysRevA.68.013820. [Cited on page 9.]

[38] Naoto Tsuji. Floquet States. In *Encyclopedia of Condensed Matter Physics (Second Edition)*, pages 967–980. Academic Press, 2024. ISBN 978-0-323-91408-6. [Cited on page 9.]

[39] Jun John Sakurai and Jim Napolitano. *Modern quantum mechanics*. Cambridge University Press, 2020. ISBN 978-0-8053-8291-4. [Cited on pages 15 and 31.]

[40] J. M. B. Lopes dos Santos. 1D band optical response. Personal Notes, 2024. [Cited on page 32.]

[41] D. Colton and R. Kress. *Inverse Acoustic and Electromagnetic Scattering Theory*. Applied Mathematical Sciences. Springer Berlin Heidelberg, 1997. ISBN 978-3-540-62838-5. [Cited on page 42.]

[42] Neil W. Ashcroft and N. David Mermin. *Solid State Physics*. Harcourt College Publisher, 1976. ISBN 0-03-08993-9. [Cited on page 63.]

[43] Nico M Temme. *Special functions: An introduction to the classical functions of mathematical physics*. John Wiley & Sons, 2011. ISBN 0471113131. [Cited on page 64.]